The Roles of Necroptosis in the Pathogenesis of *Staphylococcus aureus* Infection

Kipyegon Kitur

Submitted in partial fulfillment of the requirements
for the degree of
Doctor of Philosophy
in the Graduate School of Arts and Sciences

COLUMBIA UNIVERSITY

2016

ABSTRACT

The Roles of Necroptosis in the Pathogenesis of *Staphylococcus aureus* Infection

Kipyegon Kitur

Staphylococcus aureus, particularly the epidemic methicillin-resistant *S. aureus* (MRSA) USA300 strain, is a major cause of severe necrotizing lung, skin and systemic infection. Although these infections are generally attributed to the pathogen's multiple toxins, exactly how *S. aureus* cause disease is not clearly defined. In this research, we sought to establish the role of necroptosis, a programmed form of necrosis, in the pathophysiology of *S. aureus* pneumonia, skin infection and sepsis. *S. aureus*, mainly through its multiple toxins, induced RIPK1/RIPK3/MLKL-mediated necroptosis in multiple host cells including human cell lines, freshly obtained alveolar macrophages, peripheral blood macrophages and epithelial cells. *S. aureus* toxin-associated pore-formation was essential for necroptosis, as cell death was blocked by exogenous K^+ or dextran as well as by MLKL inhibition. To understand the role of necroptosis in *S. aureus* pneumonia, we used *Ripk3*$^{-/-}$ mice and mice treated with necrostatin-1s (Nec-1s), a potent inhibitor of RIPK1. Inhibition of necroptosis in a mouse model of pneumonia led to significantly improved outcome from *S. aureus* infection marked by increased bacterial clearance, preserved lung architecture, decreased inflammatory markers in the airway and retention of an anti-inflammatory macrophage population.

In contrast, inhibiting necroptosis in vivo during skin infection led to worse outcome as determined by bacterial clearance and lesion sizes, which occurred in spite of the presence of

neutrophils, macrophages and γδ T cells. Nec-1s-treated mice and *Mlkl*$^{-/-}$ mice had significantly larger lesions, increased cytokine response and more *S. aureus* recovered from the infected areas compared to control groups. We observed a similar outcome in *Casp1/4*$^{-/-}$ mice, which have limited ability to process IL-1β. Unlike *Mlkl*$^{-/-}$ mice, *Ripk3*$^{-/-}$ mice had improved outcome with increased bacterial clearance and decreased inflammation because of the effects of RIPK3 in activating the NLRP3 inflammasome and apoptosis during *S. aureus* skin infection. *Casp1/4*$^{-/-}$ immune cells showed a significant defect in their ability to kill *S. aureus,* whereas *Mlkl*$^{-/-}$ peritoneal exudate cells and bone marrow-derived macrophages did not. These results show that caspase-1 is essential for bacterial killing whereas necroptosis is necessary for regulating excessive inflammation.

Similar to our findings in skin infection, inhibition of the executioner of necroptosis (using *Mlkl*$^{-/-}$ mice) or pyroptosis (using *Casp1/4*$^{-/-}$ mice) decreased survival in a mouse model of *S. aureus* sepsis. *Ripk3*$^{-/-}$ and wild type mice were equally resistant to *S. aureus* sepsis. Overall, these findings provide new insights into the complex roles of necrosome components in different tissues during *S. aureus* infection and may provide potential therapeutic targets to combat these infections.

Table of Contents

List of figures

Acknowledgements

I am extremely grateful to my mentor, Alice Prince, for giving me the opportunity to work in her laboratory and for providing me amazing guidance during the course of my research. In the same vein, I want to thank my thesis committee members – Richard Robinson, Lloyd Greene, Jahar Battacharya and Victor Torres. Their incisive questions, comments and general guidance were incredibly helpful during the past four years of my thesis work. I must also thank Robert Kass, Richard Robinson, Neil Harrison and Karen Allis at the Department of Pharmacology for providing me a nurturing environment for learning and research.

The current and past laboratory members of Prince Laboratory made my experience very enjoyable. And for that I am thankful. I specifically want to thank Dane Parker, Danielle Ahn and Taylor Cohen for teaching me many laboratory techniques. I am also grateful to several members of Prince Laboratory including Sarah Wachtel, Sebastian Riequelme, Hernan Penaloza, Matthew Wickersham, Pamela Nieto, Karen Acker, Grace Soong, Armand Brown and Franklin Paulino for their help with my research and for making my laboratory experience pleasant.

I wish to give special thanks to my family and friends. Specifically, I want to thank my parents, my siblings and friends in Kenya for their support. I am also grateful to my friends in the U.S. including Harivony Rakotoarivelo and many others at Columbia University who have made my stay really feel like home away from home.

I am also thankful to John Silke (WEHI) and Douglas R. Green (St. Jude Children's Research Hospital) for providing us with *Mlkl*$^{-/-}$ mice and Vishva Dixit (Genentech Inc.) for *Ripk3*$^{-/-}$ mice. I also thank Emily DiMango and Newell Robinson (Columbia University) for providing us with human bronchoalveolar lavages.

Finally, I want to thank the institutes that provided funding for my research. This work could not have been done without the generous support of the HHMI Med-into-Grad Fellowship to me and the National Institute of Health (NIH) grant 5R01HL079395 and 5R01AI103854 to Alice Prince.

Dedication

I dedicate this thesis to my parents – Kibochabas S. Babai and Cherogony G. Babai – who are the true heroes in my journey. They had no formal schooling, but they understood the value of education.

Chapter 1: Introduction

Background on *Staphylococcus aureus*

Staphylococcus aureus is a formidable bacteria capable of causing widespread types of infections ranging from skin and soft tissue disease to severe invasive infections with significant morbidity and mortality (1-5). Even though there are effective antibiotics to combat this pathogen, there is a growing resistance to current antibiotics. This medical concern along with the ability of *S. aureus* to infect healthy individuals and exacerbate comorbidity in various patients, begs for better understanding of this pathogen's host interaction with the aim of coming up with improved therapies.

The success of *S. aureus* lies in its ability to persist within its host and produce multiple virulence factors including adhesins, coagulases and toxins. *S. aureus* toxins target diverse types of host cells, contributing to immune evasion and promoting infection. These toxins fall into three categories: pore-forming toxins, "receptor interfering but not plasma membrane-damaging toxins," and "secreted enzymes" that interfere with host defense mechanisms (6). *S. aureus* produces two forms of pore forming toxins, namely α-hemolysin (also known as Hla or α-toxin) and bi-component cytotoxins such as Leukocidin AB/GH (LukAB/LukGH), LukSF (also known as Panton-Valentine Leukocidin, PVL), LukED and γ-hemolysin (HlgAB/LukAC) (7). At high concentrations, these toxins form pores on the host cell leading to loss of ions. At low concentrations, they interact with their receptors and stimulate a molecular signaling cascade leading to several outcomes including cell death and autophagy (7, 8). Some of these toxins such

as LukAB and PVL are specifically adapted to lyse human cells, while others like Hla can target a wide range of cells in multiple species.

Hla is an important *S. aureus* toxin that has been shown to exacerbate several infections including lung, bone, systemic and skin infection (9). Upon binding to its receptor ADAM10, Hla forms an heptameric pore leading to loss of monovalent ions (such as K^+) and loss of ATP from the host cell (10). Deletion of Hla or sequestration of Hla using antibodies significantly improve outcome during *S. aureus* skin and lung infections (11). Hla activates cellular signaling leading to cell death and production of pro-inflammatory cytokines such as IL-1β, IL-8 and IL-6 (12-14). Thus, Hla is a critical toxin not only because it can lyse multiple host cells including immune, endothelial and epithelial cells but also because of its ability to induce a diverse pro-inflammatory signaling in a host.

Mouse models

Most of the current understanding on the pathogenesis of *S. aureus* infections is derived from studies done using mouse models. These models have been invaluable, but they have significant limitations. First, *S. aureus* is better adapted to infect humans than mice. This pathogen produces many toxins that have higher tropism to human cells than to mouse cells. Panton-Valentine Leukocidin (PVL, which targets C5aR and C5L2 receptors) (15); Leukocidin A/B (LukAB, which targets the CD11b subunit of Mac-1 integrin) (16); γ-hemolysin AB (HlgAB, which targets the chemokine receptors CXCR1, CXCR2 and CCR2), HlgCB (which targets the complement receptors C5aR and C5L2) (17) show higher binding affinity to human receptors than to mouse receptors.

Second, in several *S. aureus* mouse models, supra-physiological inoculum has to be used to establish infection. For example, in our mouse models of pneumonia, we use approximately 10^7 CFU/mouse. However, humans are highly susceptible to *S. aureus* pneumonia even at doses that would not cause any serious infection in mice, especially during influenza pandemics.

Third, many vaccines developed in mouse models have failed to translate their efficacy to humans (18). The failure is potentially because humans have completely different immune system from mice and mice poorly recapitulate human inflammatory responses (19, 20) and that *S. aureus* produces numerous human-specific toxins that limited vaccine studies in mice (7).

These limitations can potentially be mitigated in two ways. The first way is to use primary human cells or human tissues grafted on mice. Human skin grafted on *scid* mice has already proved useful in studies of *S. aureus* skin infection (8). The second way, and which has more potential applications, is the use of "humanized" mouse models (21). "Humanized" mice have proven important in studying pathogens with human tropism such as HIV and *Salmonella enterica* serovar (22, 23). In a peritonitis model and skin model of *S. aureus* infection, humanized mice models illuminated our understanding of the human specific *S. aureus* pathogen PVL (24, 25). In our studies here, we use combinations of primary human cells and human skin grafts on mice. Future projects may use humanized mouse models.

Host cells

Epithelial cells are the first line of defense during *S. aureus* infection. Keratinocytes and lung epithelial cells, for example, provide a barrier to prevent *S. aureus* from invading deeper tissues and causing systemic infection. They secrete antimicrobial peptides such as cathelicidin and defensins (e.g. human β-defensin 2 and human β-defensin 3) that have the ability to kill *S. aureus*

(26, 27). Epithelial cells recognize foreign substances such as pathogen-associated molecular patterns (PAMPs), which are associated with microbial organisms, and danger-associated molecular pattern (DAMPs), which are associated with cell damage or death, through Toll-like receptors (TLRs) and Nod-like receptors (NLRs). Activation of these receptors leads to production of key cytokines such as IL-1β, KC and MIP-1β to recruit immune cells (specifically neutrophils and macrophages) to clear the invading microorganisms.

Neutrophils

Neutrophils play a critical role in immune defense. During *S. aureus* pneumonia for example, lack of neutrophils contributes to poor bacterial clearance and worse outcome (28). IL-1- and IL-17-mediated immune signaling are essential for recruitment of neutrophils and formation of neutrophil abscess and eventual clearance of pathogens in a mouse model of subcutaneous infection (26). Mice that cannot produce active IL-1β (*Il1b*$^{-/-}$) or that cannot respond to this cytokine (*Il1r*$^{-/-}$) develop bigger lesions and have poor bacterial clearance in *S. aureus* model of skin infection (26). A defect in the machinery that produces IL-1β (for example, a lack of Myd88, a key adaptor to TLR signaling; or inhibition of ASC-Caspase-1 pathway, which is essential for the processing of pro-IL1β to active form) leads to an impaired response to *S. aureus* in the skin. Thus, the recruitment of neutrophils to clear pathogens is essential for survival.

Once recruited to the site of infection, neutrophils immobilize and ingest microorganisms. They release neutrophil extracellular traps (NETs), a composition of chromatin and serine proteases, to arrest particles and invading organism so they can be phagocytosed by macrophages (29). NETs are an effective immune defense mechanism. However, some microbes

have evolved ways to evade them. *S. aureus*, for example, produces nuclease and adenosine synthase that converts NETs to deoxyadenosine, a product that is cytotoxic to immune cells (30). Other than NETs, neutrophils have other defense mechanisms including "respiratory busts" and degranulation. Respiratory busts is mediated by NADPH oxidases that produce superoxide, reactive oxygen species (ROS), which can then be converted to hydrogen peroxide and hypochlorous acid to kill ingested organisms. This NADPH pathway is so critical to immune defense that any defect in the pathway, for example in patients with chronic granulomatous disease (CGD), predisposes one to chronic infections (31). Aside from producing ROS, neutrophils can also undergo a process called degranulation that leads to the release of antimicrobial peptides such as lactoferrin and defensins and other enzymes such as gelatinases, elastases, collagenases, lysozymes and cathepsins (32). Thus, neutrophils are an essential part of immune defense against invading microorganisms.

Although a neutrophil response is essential for bacterial clearance, an excessive recruitment of neutrophils can be counterproductive. Neutrophil enzymes such as gelatinases, elastases, collagenases and lysozymes can destroy local tissues. This destruction is particularly problematic in the lung, where extensive damage can lead to serious edema. Even in skin, excessive neutrophil-mediated inflammation can cause damage and impair bacterial clearance. This point can be best illustrated by two examples. First, treatment of MRSA with β-lactams causes poor crosslinking of peptidoglycan that leads to a robust activation of the inflammasome, an excessive neutrophil response and a subsequent worse outcome in skin infection (33). Second, CXC chemokines, which recruit immune cells including neutrophils and $CD4^+$ T cells, mediate serious inflammation that causes tissue damage and poor *S. aureus* clearance (34). These

findings show that a balance between optimal neutrophil recruitment and regulation of inflammation is essential for bacterial clearance while minimizing immunopathology.

Macrophages

Macrophages have two critical functions. First, they participate in immunoregulation. Local tissue macrophages such as alveolar macrophages and kupffer cells produce chemokines that recruit other immune cells including neutrophils to clear foreign objects including pathogens. Macrophages limit the amount of tissue damage that dead cells can induce by clearing dead or dying cells through a process called efferocytosis (35). Once the source of insult has been removed and dead cells cleared, macrophages secrete cytokines to dampen inflammation, contributing to immune resolution and a return to tissue homeostasis.

The second essential function of macrophages is bacterial clearance. Several groups including our laboratory have previously shown the role of macrophages during *S. aureus* pneumonia (28, 36). Depletion of macrophages using clodronate-loaded liposomes worsens outcome in *S. aureus* pneumonia. Like neutrophils, macrophages are efficient phagocytes and thus are essential for bacterial clearance. Alveolar macrophages are adept in taking up *S. aureus* and killing them through reactive oxygen species (ROS) production and acidification of phagosomes. In response to *S. aureus*, resident macrophages produce chemokines such as *Cxcl1, Cxcl2, Ccl2, Ccl3* and *Ccl4* to recruit other immune cells including neutrophils to the site of infection (37).

S. aureus has evolved ways to eliminate macrophages as an immune evasion strategy. Using multiphoton intravital microscopy, Wenigner and colleagues have shown that *S. aureus*, through Hla, targets and kills perivascular macrophages leading to decreased neutrophil

attraction and transmigration. An *hla* null *S. aureus* strain was cleared better than wild type strain because *hla* was able to induce a robust chemokine release, which led to an influx of neutrophils and eventual clearance of the pathogen (37).

Macrophages in inflammation

Macrophages broadly fall in two categories – classically activated M1 macrophages and alternatively activated M2 macrophages (38, 39). M1 macrophages are inflammatory and phagocytic, whereas M2 macrophages have anti-inflammatory and wound healing capabilities. M1 macrophages express IFN-regulatory factor 5 (IRF5) and their surface markers include CD86 and CD80 (39, 40). On the other hand, M2 macrophages express YM1 and FIZZ1 proteins with MARCO, CD200R and CD206 as their surface markers. M1 and M2 macrophages have different cytokine profiles, with M1 producing pro-inflammatory cytokines such as TNF and IL-6 whereas M2 produce anti-inflammatory ones such as IL-10 and TGF-beta.

Importantly, however, these characteristics are not static since macrophages are plastic. Macrophages can adopt different states at different times and they can express both of the markers of M1-like and M2-like macrophages at the same time in response to the constantly changing needs of their microenvironment (39). This plasticity affords them the ability to induce inflammation in response to an insult and to resolve inflammation as the tissue returns to homeostasis in the local environment.

Mechanisms of cell death

In the lifespan of an organism, cells can die either accidentally or deliberately. Accidental death occurs in the presence of an extreme physical or chemical insult and involves the release of

intracellular organelles. Deliberate death is physiologically regulated and is often less detrimental to an organism than accidental death (41). There are several types of physiologically regulated forms of cell death, but the most understood ones are apoptosis, pyroptosis and necroptosis (**Figure 1.1**). The reason why cells evolved to die through multiple programmed ways is not fully known. Some of these forms of death serve redundant roles, but each has some unique functions. Whereas apoptosis is the only type of death that is known so far to be essential for natural development, three types of death participate in response to pathogens. However, they can have similar, unique or even opposing roles during infection. What is clear though is that an excessive or insufficient amount of any of these forms of death is detrimental to an organism, and thus the cell has to regulate them carefully.

Apoptosis

Apoptosis is a well-studied programmed mechanism of cell death. It is an essential part of development and tissue homeostasis (by eliminating unwanted cells) and part of immune defense (by removing infected cells). It is activated either through an extrinsic or intrinsic pathway (42) (**Figure 1.1**). The extrinsic pathway involves the stimulation of a death receptor (most of which belong to the TNF superfamily) including FasR and TNFR1. These receptors recruit cysteine-dependent aspartate-directed protease (caspase)-8, which then processes the executioners of apoptosis, caspase-3 and 7. The intrinsic pathway, on the other hand, involves the release of cytochrome c from the mitochondria leading to the formation of Apaf-1 complex that activates caspase-9, which in turn activates the executioner caspase-3. Apoptosis is generally accepted to be non-inflammatory, since it is a programmed part of development (required for pruning of

excessive or defective cells such as during thymocyte selection) and it involves generation of apoptotic cells that (before they release intracellular products) can be rapidly cleared by phagocytes. However, apoptosis, as a response to inflammatory stimuli or external assault (such as a response to cancer therapy or infection), is immunogenic (43).

When normal cells detach and lose contact from their epithelial cells and extracellular matrix (ECM), they lose critical survival signals from their "home" tissues and therefore undergo *anoikis*, a programmed form of cell death (44). Anoikis is a special type of apoptosis that happens to cells that have lost contact with their ECM. It is mediated by caspase-3 and other signaling complexes associated with apoptosis. Little is known about the role of anoikis in infections. Its role in tumorigenesis is well appreciated, as cancer cells evolve different strategies to subvert anoikis enabling them to metastasize (45).

Pyroptosis

Pyroptosis is a caspase-dependent form of cell death that is mediated by caspase-1 (**Figure 1.1**). Caspase-11 in mice (or its human equivalent, caspase-4) can also trigger pyroptosis (46). Other caspases that may participate in pyroptosis, but that are less well understood, are caspase-5 and -12. Caspase-1 is processed in a supramolecular complex called the inflammasome, which senses a wide variety of agonists through their Nod-like receptors (NLRs). The NLRP3 is activated by several compounds including crystals, pore-forming toxins, reactive oxygen species, K^+ efflux, extracellular ATP; NLRC4 is activated by flagellin; and NLRP1 is activated by anthrax lethal toxin. Another inflammasome complex is AIM2, which detects dsDNA (46). These inflammasome complexes process pro-caspase-1 to active caspase-1 (made up of p20 and p10

fragment). It was recently shown that caspase-1 cleaves gasdemin D, which executes pyroptotic cell death (47).

Pyroptosis and inflammasome activation play an important role in inflammation. Pryoptosis leads to loss of plasma membrane and a release of inflammatory products such as HMGB1 and IL-1α (48). Aside from cell death, the inflammasome processes two important inflammatory cytokines, pro-IL-1β and pro-IL-18. These cytokines have several roles including attracting immune cells such as neutrophils and macrophages, inducing production of other inflammatory cytokines such as TNF and IL-6, and contributing to wound healing (48).

Apoptosis and pyroptosis are well studied in the context of *S. aureus* infection. Apoptosis has been shown to participate *S. aureus* clearance (49). Pyroptosis, which can be mediated by *S. aureus* pore forming toxins such as Hla and PVL, has a complex role – it exacerbates pneumonia, while limiting skin infection (12, 50, 51).

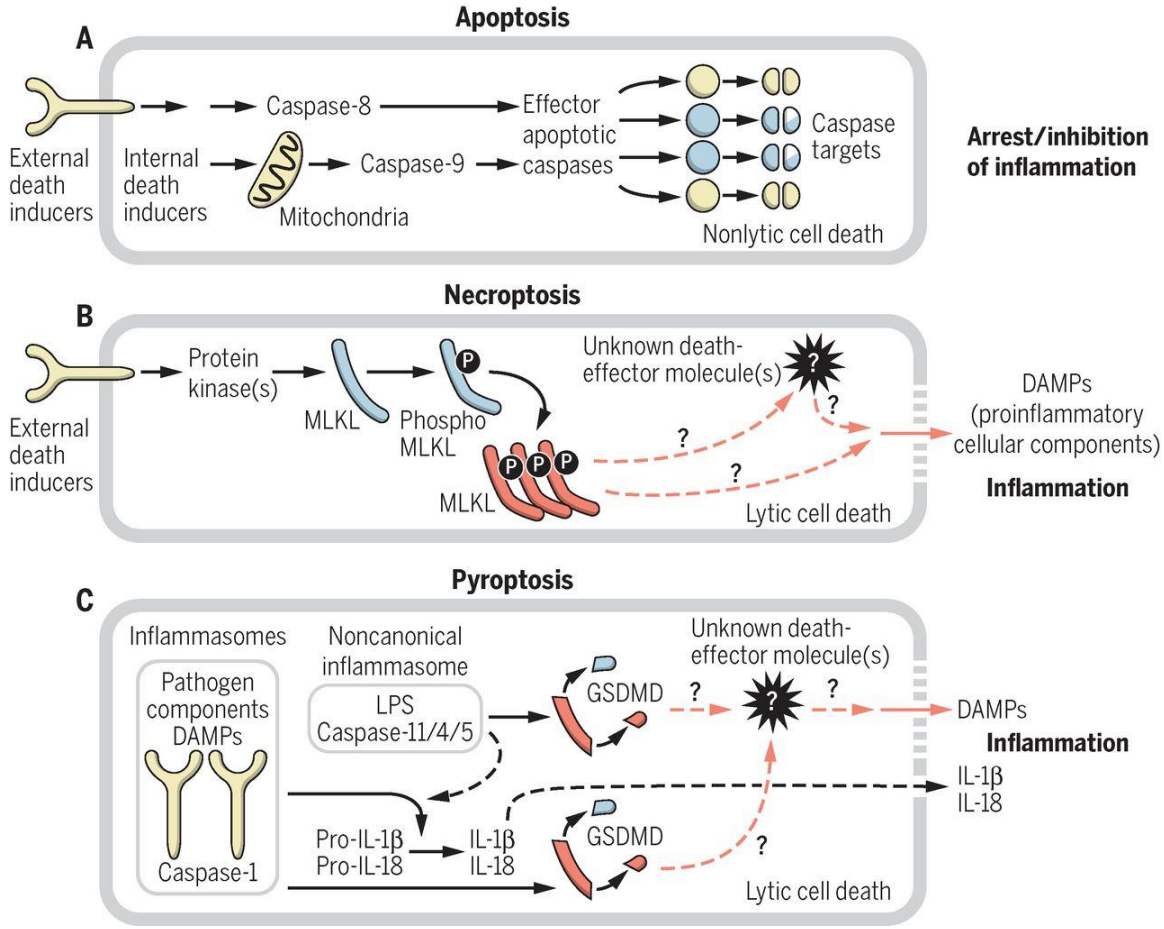

Figure 1.1: Major cell death pathways
(**A**) Apoptosis is activated either through an extrinsic or intrinsic pathway. The extrinsic pathway requires caspase-8 and the intrinsic one requires caspase-9. Caspase-8 and -9 activate executioner caspases that mediate cell death. Apoptosis is less inflammatory since it generates apoptotic cells that can be rapidly cleared by phagocytes.
(**B**) Necroptosis is activated by RIPK1 and RIPK3 and is executed by mixed lineage kinase domain-like (MLKL) protein.
(C) Pyroptosis is mediated by caspase-1/11/4/5, which process the inflammatory cytokines IL-1β and IL-18.

Necroptosis

Necroptosis is a caspase-independent programmed form of cell death that requires receptor-interacting serine/threonine protein kinase (RIPK)1 and RIPK3 and is executed by mixed lineage

kinase domain-like (MLKL) protein (43, 53) (**Figure 1.1**). Necroptosis can be triggered by stimulation of several receptors such as the death receptors (TNFR, TRAIL and FAS), Toll-like receptors (specifically TLR3 and TLR4), or the T cell receptor (TCR) in the absence of active caspase-8 (**Figure 1.2**). Necroptosis is well studied in the context of the pleotropic cytokine TNF. Activation of TNF receptor (TNFR1) leads to the recruitment of RIPK1 through its death domain (DD). RIPK1 can then recruit RIPK3 through RIP homotypic interaction motifs (RHIM) (54). Other receptors that have RHIM and can recruit RIPK1 are TLR3, TLR4 and IFNAR. DNA and type 1 interferon (IFNs) can also activate necroptosis through DAI and IFNAR1 respectively (55) (**Figure 1.2**). When caspase-8 is blocked (such as in the presence of pan-caspase inhibitor, Z-VAD), RIPK1 recruits RIPK3 via RHIM, and the two kinases auto-phosphorylate. Activated RIPK3 then phosphorylates its substrate, the pseudokinase MLKL, leading to necroptosis.

Exactly how MLKL executes cell death is unresolved. Phosphorylated MLKL translocates to the plasma membrane and oligomerizes to form a pore leading to a loss of essential ions in the cell, and eventually cell death.(56) The exact ions that contribute to necroptosis are controversial, with some groups suggesting Ca^{2+}, others proposing Na^{+}, and recent groups showing Mg^{2+} (57-59).

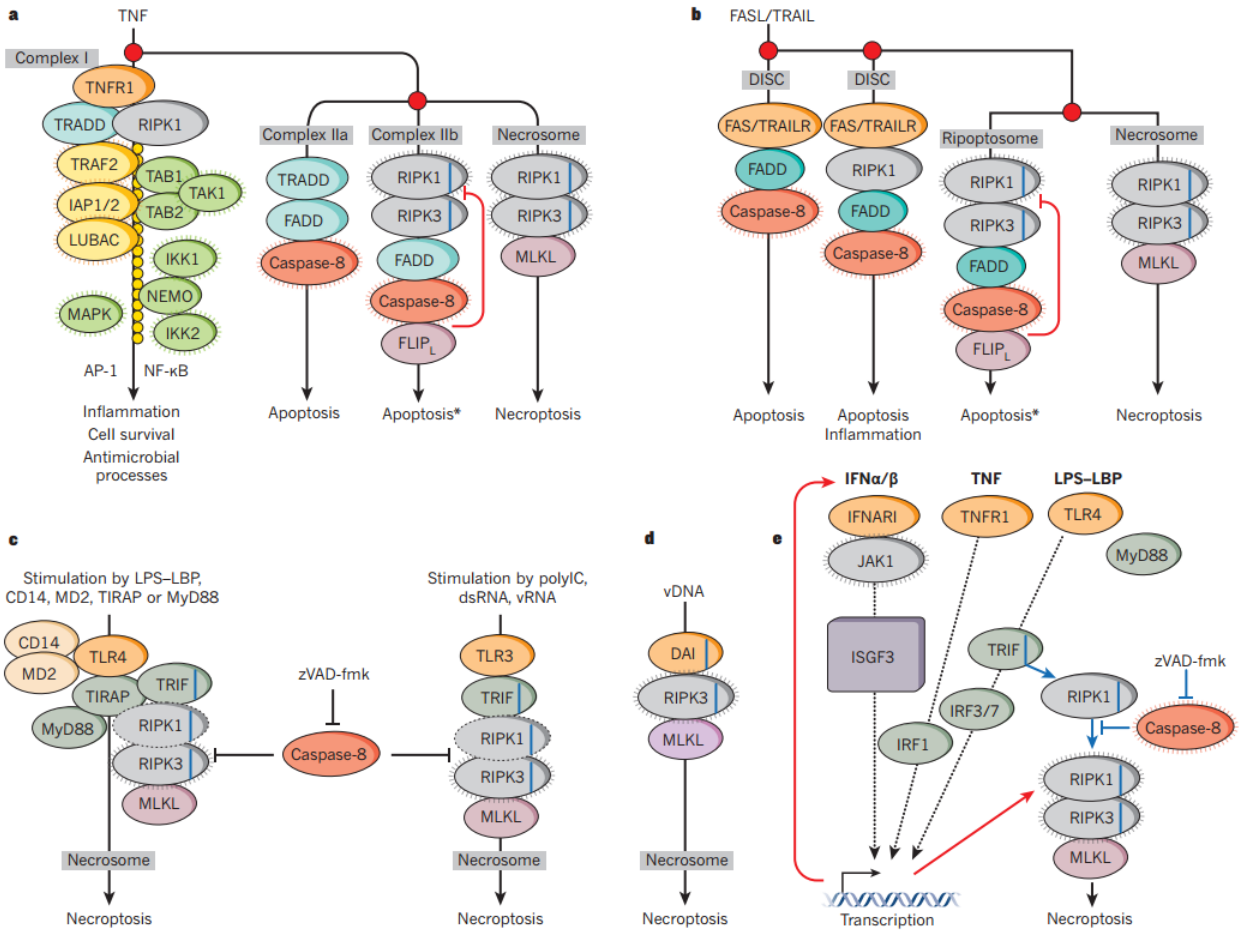

Figure 1.2: Necroptosis is activated by a diverse upstream signaling
(**A**) TNFR stimulation can lead to several signaling cascades. Complex I (which is composed of TRADD, RIPK1, TRAF2, IAP1, IAP2 and LUBAC) activates AP-1 and NF-kB, leading to production of inflammatory cytokines and promotion of cell survival. Complex IIa (composed of TRADD, FADD and caspase-8) is the canonical extrinsic apoptosis pathway; it is activated when complex I is destabilized for example by a cytotoxic agent such as cycloheximide. Complex IIb is also apoptosis, but differs from complex I by its dependence on RIPK1-RIPK3 scaffolding functions, which leads to activation of caspase-8. Necrosome complex (RIPK1-RIPK3-MLKL) triggers necroptosis in the absence of active caspase-8. Necroptosis requires both the scaffolding and kinase activities of RIPK1 and RIPK3, which phosphorylate MLKL to induce necroptosis.
(**B**) FASL induces a similar signaling to TNF, except that it cannot activate NF-κB or AP-1 cascade.
(**C**) TLR3 and TLR4-induced necroptosis is mediated by the RHIM-containing adapter TRIF, which recruits RIPK1 and RIPK3 complex.
(**D**) Viral double-stranded DNA (vDNA) stimulates DNA-dependent activator of IFN regulatory factors (DAI), which recruits RIPK3 through its RHIM domain to induce RIPK1-independent necroptosis.
(**E**) IFNAR1 induces transcriptional production of necrosome components that are assembled in the presence of TNR1 and TLR4 stimulus.

Mouse models have shed light into the complex functions of necroptosis-mediating proteins. For instance, *Ripk1*$^{-/-}$ mice die soon after birth, whereas *Ripk3*$^{-/-}$ and *Mlkl*$^{-/-}$ mice are viable and healthy (60). The function of RIPK1 in necroptosis is context dependent. RIPK1's kinase function, which can be inhibited by necrostatin-1 and its analogs, triggers necroptosis. On the other hand, RIPK1's scaffolding function inhibits necroptosis and regulates other cell survival activities including NF-κB activation (61).

Necroptosis in response to microbial pathogens

Similar to other forms of cell death such as apoptosis and pyroptosis, necroptosis is a critical part of cellular response to microbial pathogens. Several pathogens have evolved ways to modulate this pathway to their advantage (62). Necroptosis generally leads to a release of intracellular pathogens such as viruses and bacteria. This release can promote local inflammation, which helps clear the viruses. Excessive inflammation, however, can be damaging and needs to be regulated.

Vaccinia virus (VV), murine cytomegalovirus (MCMV) and influenza A virus best exemplify the complex role of necroptosis during viral infection. VV, a large double-stranded DNA virus, produces B13R, a potent caspase inhibitor (63). Caspase-8 inhibition by B13R promotes activation of TNFR-mediated necroptosis and eventual clearance of VV by mouse fibroblasts (64). During VV infection, *Ripk3*$^{-/-}$ and *Tnfr2*$^{-/-}$ mice showed reduced necrotic damage, but impaired VV clearance and eventually succumbed to infection (65). Similarly, MCMV activates necroptosis through DNA-dependent activator of interferon regulatory factors (DAI/ZBP1), promoting clearance. However, this virus has evolved vIRA, a RHIM-containing protein that sequesters RIPK3, subverting cell death and promoting its survival (66). Necroptosis

during influenza A virus pneumonia, however, is detrimental not because it impairs viral clearance but because it perturbs pulmonary homeostasis and leads to damaging inflammation in the airways (67).

As in viral infections, necroptosis as a response to bacterial infection plays diverse functions. *Salmonella enterica* serovar Typhimurium (*S.* Typhimurium) targets and kills macrophages through necroptosis, which is mediated by type 1 interferons. *Ifnar*$^{-/-}$ and *Ripk3*$^{-/-}$ mice have increased clearance and survival during *S.* Typhimurium infection (68). Necrosome components during *Mycobacterium tuberculosis* (MTB) play a complex role. ROS, which is upstream of cell death, helps with MTB clearance. However, if cell lysis is allowed to proceed, it leads to release and dissemination of MTB. Thus, inhibitors that target cyclophilin D or acid sphingomyelinase, which are downstream of ROS, but upstream of cell death protects from infection in a zebrafish model (69). Caspase-8 and RIPK3 mediate clearance of *Yersinia pestis* through their activation of the inflammasome. Deletions of both CASP8 and RIPK3 (but not RIPK3 alone) lead to reduced activation of caspase-1 and production of pro-inflammatory cytokines, which increases susceptibility to infection (70, 71). These examples illustrate the complex role of necroptosis in controlling or exacerbating infections.

Necroptosis in host defense

Necrosome components can drive inflammation through cell death or by activating the inflammasome. Necroptosis is seen as proinflammatory because it leads to the release of intracellular components such as HMGB1 and DNA, which are potent activators of inflammation. The indirect way in which the necrosome components can activate inflammation is by activating the inflammasome. RIPK3 and MLKL are often linked to inflammation and there

are data suggesting that these components can activate NLRP3 inflammasome. Depletion of IAPs in dendritic cells leads to activation of the NLRP3 inflammasome in a RIPK3-dependent manner (72). TLR signaling promotes inflammasome activation when caspase-8 and IAPs are blocked (73). In the context of disease, RNA viruses activate the inflammasome through RIPK1-RIPK3-Drp1- NLRP3 pathway leading to viral clearance (74). RIPK3 leads to exuberant IL-1β production promoting injury in a dextran sodium sulfate (DSS) colitis model (75). Thus, the necrosome components and inflammation are intertwined and both are critical in the pathogenesis of many diseases.

The consequences of necroptosis are not necessarily proinflammatory. Although necroptosis results in the release of inflammatory intracellular components, it may decrease inflammation by eliminating the cells that produce cytokines and inflammatory products (76, 77). Additionally, cell death releases viable intracellular pathogens, which can then be effectively cleared by bactericidal neutrophils and thus removing the source of inflammatory stimuli (77). Therefore, the consequences of necroptosis are complex and likely dependent upon the nature of the pathogen and site of infection.

Necroptosis in *S. aureus* infection

Necroptosis plays a role in releasing intracellular pathogens including viruses and some bacteria such as *S.* Typhimurium. *S. aureus* is both an intracellular and extracellular organism that causes serious infections accompanied by cell death, inflammation and tissue necrosis. The mechanism by which *S. aureus* causes inflammation and tissue damage is not well understood. We wanted to define the consequences of necroptosis in *S. aureus* infection, specifically its role in bacterial clearance and inflammation. Does necroptosis impede bacterial clearance by removing critical

cells or does it participate in clearance by releasing intracellular *S. aureus* so that they can be taken up by cells that are more bactericidal? Does necroptosis participate in immunoregulation by eliminating inflammatory cells or does it add to inflammation by releasing inflammatory products?

In the following chapters, we address the complex roles of necroptosis in *S. aureus* infection in two parts. In the first section, we define the contribution of necroptosis in a mouse model of pneumonia. We show that *S. aureus* toxins induce lung damage through necroptosis. In the second section, we demonstrate the complex role of necroptosis in dampening inflammation and improving outcome during *S. aureus* skin and systemic infection. Ultimately, this research has identified the specific roles of necroptosis during three common types of *S. aureus* infection.

Chapter 2: *Staphylococcus aureus* toxins induce lung damage through necroptosis

Introduction

Staphylococcus aureus is a major cause of pneumonia, particularly ventilator-associated and community-acquired pneumonia, and is a significant cause of morbidity and mortality during influenza epidemics (78-80). *S. aureus* pneumonia is often accompanied by excessive inflammation. During pneumonia, some level of inflammation – marked by the presence of neutrophils, monocytes, macrophages and inflammatory cytokines – is necessary for bacterial clearance. However, excessive inflammation in the lung, where clear airways are required for proper aeration, is damaging. Thus, a tight regulation of inflammation is essential.

Alveolar macrophages, the most abundant immune cells in the normal airway, contribute to pathogen clearance and immune regulation (81). Aside from actively clearing foreign objects in the lung, alveolar macrophages produce inflammatory cytokines and antimicrobial peptides to kill pathogens. Macrophages are avid phagocytes, but *S. aureus* has evolved ways to evade them. *S. aureus* produces numerous virulence factors including pore-forming toxins that can lyse macrophages, thwarting their functions. The mechanism by which *S. aureus* kills macrophages and the implication of macrophage death in pneumonia are not fully understood.

This chapter focuses on understanding *S. aureus*-macrophage interaction and the role of macrophages in regulating inflammation during pneumonia. We tested the hypothesis that *S. aureus* kills macrophages through necroptosis, contributing to lung damage. We show that *S. aureus*, mainly through its toxins, targets and kills macrophages through necroptosis leading to acute inflammation and severe pneumonia. Inhibition of necroptosis rescued macrophages

resulting in increased bacterial clearance, better resolution of inflammation and significantly improved outcome in a mouse model of *S. aureus* pneumonia.

Results

***S. aureus* induces necrosis in macrophages –** USA300 *S. aureus* expresses multiple toxins that can induce leukocyte death through multiple mechanisms. To document the efficiency at which *S. aureus* kills macrophages, we measured cytotoxicity using lactate dehydrogenase (LDH) assay in THP-1 cells, a macrophage-like cell line, infected with wild type (WT) or *hla* null *S. aureus* strain. Although the rate of cytotoxicity over the first 2 hours was greatest in THP-1 cells exposed to WT as compared to those exposed to *hla* null strain, cytotoxicity was similar in cells infected with any of the USA300 strains by 3 hours (**Figure 2.1A**). These results show that macrophages are highly susceptible to *S. aureus* killing.

We next wanted to understand the mechanism by which *S. aureus* was killing macrophages. To determine if macrophage death were mediated by caspases, we pretreated THP-1 cells with the pan-caspase inhibitor, Z-VAD, and infected the cells with *S. aureus* for 2 hours. Z-VAD significantly decreased *S. aureus*-induced cytotoxicity in THP-1 cells (**Figure 2.1B**). THP-1 cells treated with Z-VAD released reduced amounts of IL-1β (**Figure 2.1C**), suggesting a possible contribution of pyroptosis to macrophage death. These results confirm previous findings that toxin production by *S. aureus* induces a caspase-mediated cell death, accompanied by the release of mature IL-1β in several model systems (12, 50).

We measured the relative contribution of apoptosis – a programmed form of cell death that is executed by caspase 3/7 (42) – in the killing of THP-1 cells by *S. aureus*. Incubation of THP-1 cells with *S. aureus* for 2 hours did not result in an apoptotic phenotype of the cells in

contrast to a staurosporine-treated control (**Figure 2.1D**). Although we observed *S. aureus*-induced caspases 3/7 activation (**Figure 2.1E)**, inhibition of these caspases did not prevent *S. aureus*-induced THP-1 cytotoxicity (**Figure 2.1F**). Thus, despite that *S. aureus* activates caspase 3/7, apoptosis seems not to be the dominant pathway through which *S. aureus* kills immune cells.

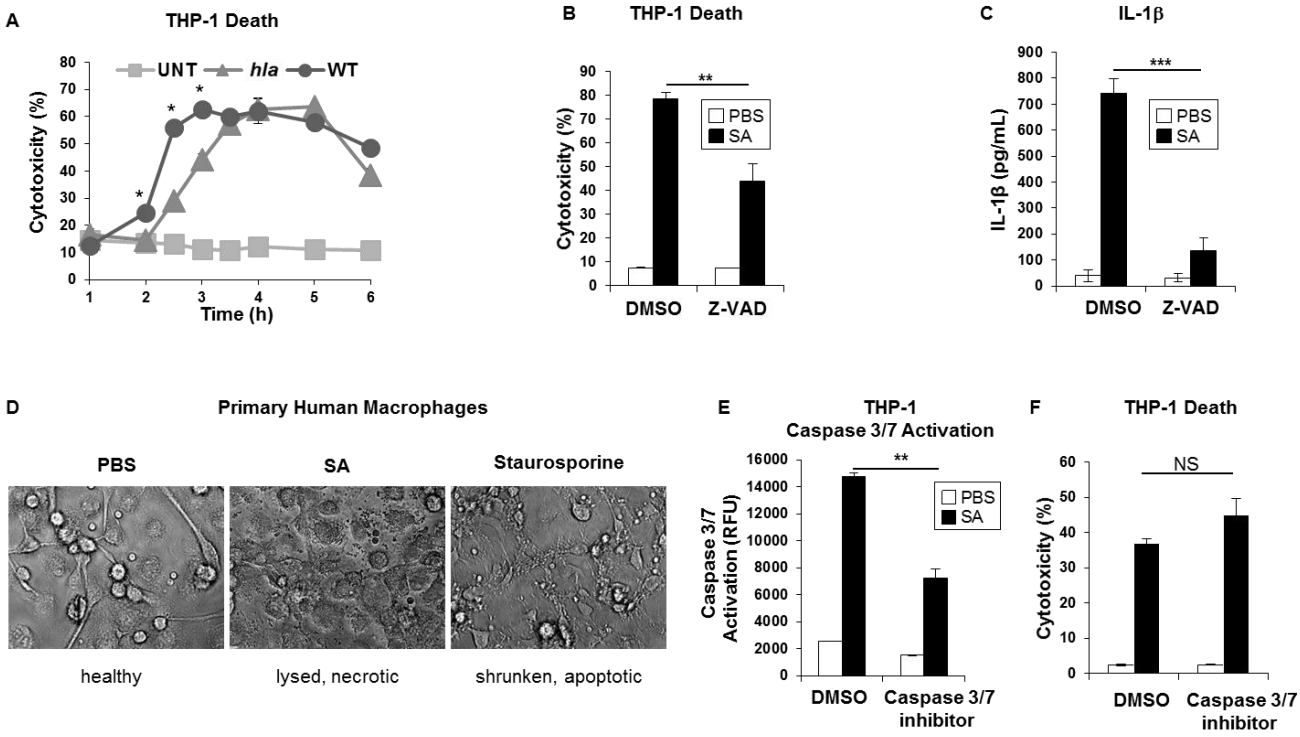

Figure 2.1: *S. aureus* induces necrosis in macrophages
(**A**) Cytotoxicity in THP-1 cells treated with *S. aureus* USA300 (WT) or its α-hemolysin *(hla*) mutants at MOI of 10 for the duration indicated.
(**B**) Cytotoxicity in THP-1 cells pretreated with 20 μM Z-VAD or DMSO for 1 hour and stimulated with *S. aureus* for 2 hours.
(**C**) Secreted IL-1β levels as measured by ELISA in THP-1 cells from "B".
(**D**) Images of primary human macrophages stimulated with PBS, WT USA300 (SA) or staurosporine for 2 hours (magnification x400).
(**E**) Caspase 3/7 activation in THP-1 cells pretreated with 20 μM caspase 3/7 inhibitor or DMSO for 1 hour and stimulated with *S. aureus* for 2 hours.
(**F**) Cytotoxicity in THP-1 cells from "E."
Data are represented as mean ± SD of three or more technical replicates and are a representative of two to four independent experiments. * $p < 0.05$, ** $p < 0.01$, *** $p < 0.001$, and NS stands for "not significant."

***S. aureus* kills macrophages through necroptosis –** Necroptosis is a caspase-independent programmed form of necrosis mediated by RIPK3 (and in some instances RIPK1) and MLKL,

which disrupts the integrity of the plasma membrane when activated (53). To determine if *S. aureus* induces necroptosis, we infected THP-1 cells with USA300 and measured the level of phosphorylated MLKL (pMLKL). We observed pMLKL in THP-1 cells after 2 hours of infection (**Figure 2.2A**). We determined whether biochemical inhibitors of necroptosis – necrostatin-1, which targets (RIPK1); and necrosulfonamide (NSA), which inhibits MLKL – could rescue macrophages from death. A dose-dependent inhibition of *S. aureus*-induced THP-1 cytotoxicity in the presence of necrostatin-1 (Nec-1) was observed (**Figure 2.2B**). The MLKL inhibitor NSA, as well as necrostatin-1s (Nec-1s), a more stable and potent analog of Nec-1, also protected human THP-1 cells from death as well as human peripheral-derived macrophages (**Figures 2.2C and 2.2D**). NSA also protected freshly harvested human alveolar macrophages from *S. aureus* induced cytotoxicity (**Figure 2.2E**). To confirm the results we obtained using biochemical inhibitors, we used genetic means to block necroptosis. We observed that gene silencing using siRNA targeting RIPK3 or MLKL in THP-1 cells decreased *S. aureus*-induced cytotoxicity (**Figures 2.2F and 2.2G**). *Ripk3*$^{-/-}$ mouse alveolar macrophages showed decreased cytotoxicity compared to WT macrophages (**Figure 2.2H).** Thus, *S. aureus* induces necroptosis in both human and mouse macrophages.

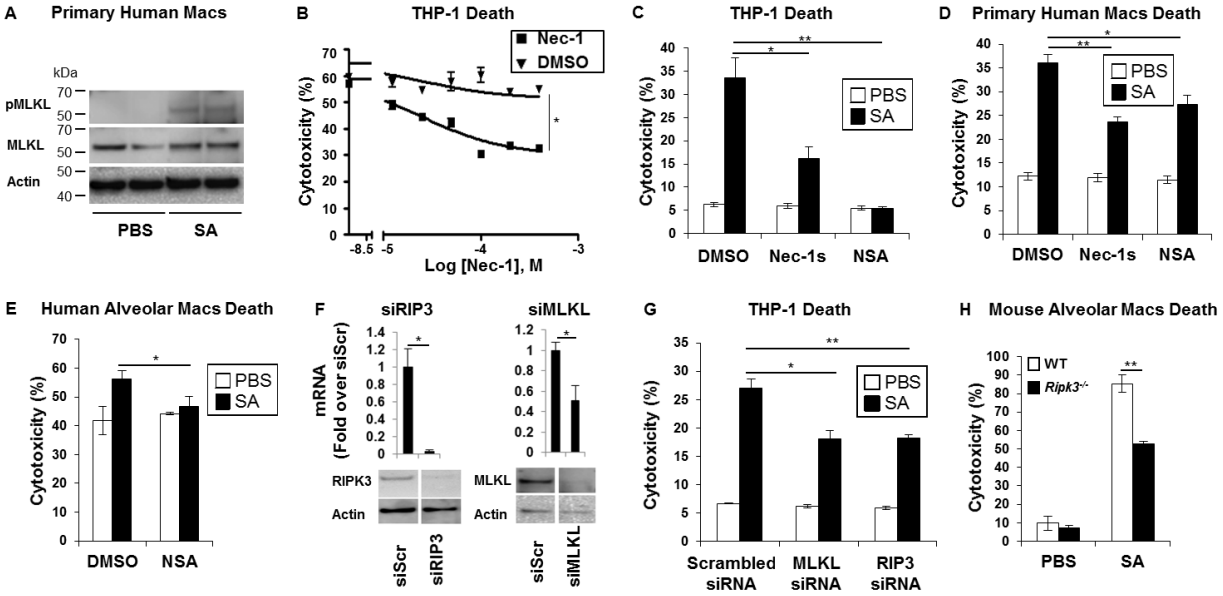

Figure 2.2. *S. aureus* induces necroptosis in macrophages
(**A**) Western blot showing primary human macrophages that were stimulated for 2 hours with *S. aureus* (SA) or PBS and blotted with antibodies against phosphorylated MLKL (pMLKL), MLKL and actin.
(**B**) Cytotoxicity in THP-1 cells pretreated with increasing concentrations of necrostatin-1 stable (Nec-1s) and incubated with *S. aureus* or PBS for 2 hours.
(**C**) Cytotoxicity in THP-1 cells pretreated for 1 hour with 200 µM necrostatin-1 stable (Nec-1s), 10 µM necrosulfonamide (NSA) or DMSO and incubated with *S. aureus* or PBS for 2 hours determined by LDH assay.
(**D**) Cytotoxicity in primary human macrophages pretreated with 10 µM NSA, 200 µM Nec-1s or DMSO.
(**E**) Cytotoxicity in freshly obtained human alveolar macrophages pretreated with 10 µM NSA or DMSO).
(**F**) THP-1 cells were transfected for 72 hours with RIPK3, MLKL small interfering RNA (siRNA) or siRNA scrambled control (siScr). mRNA and protein levels of RIPK3 and MLKL was measured by quantitative real time PCR and western blot.
(**G**) Cytotoxicity in THP-1 cells with depleted RIPK3 or MLKL and infected with *S. aureus* for 2 hours.
(**H**) Cytotoxicity in primary alveolar macrophages from WT and *Ripk3*$^{-/-}$ mice incubated with USA300 MOI of 100 for 2 hours.
Data are a representative of two to four independent experiments. Data are represented as mean ± SD of three or more technical replicates. * $p < 0.05$, ** $p < 0.01$, *** $p < 0.001$

***S. aureus* toxins contribute to macrophage necroptosis –** We next hypothesized that *S. aureus* virulence factors, specifically pore-forming toxins, are the activators of necroptosis in macrophages. *S. aureus* produces multiple toxins that are adept in killing human and murine leukocytes. The *agr* locus is a global regulator of multiple *S. aureus* virulence factors including toxins such as Hla, PVL, LukAB, and PSMs. To test the hypothesis that *S. aureus* toxins contribute to necroptosis, we used live WT USA300, *agr*, *hla*, *psm* (*psmα/β/hld*), *lukAB*,

lukSF (*pvl*) mutants and their supernatants. Live WT and *pvl* null mutants and their supernatants killed THP-1 cells effectively, whereas live mutants and supernatants from *agr*, *hla*, *psm* (*psmα/β/hld*), *lukAB* showed attenuated killing of THP-1 cells (**Figures 2.3A and 2.3B**). *pvl* and WT had the same level of killing despite a robust expression of *pvl* by the WT strain (**Figures 2.3A, 2.3B and 2.3C**). NSA effectively decreased the cytotoxicity induced by these *S. aureus* strains and their supernatants (**Figures 2.3A and 2.3B**). Thus, cytotoxicity was not dependent upon the expression of any one specific toxin since NSA protected cytotoxicity associated with WT and toxin-null USA300 strains

Hla is one of the most important *S. aureus* toxins, which has been shown to lyse both epithelial and immune cells leading to necrotizing pneumonia. We showed that purified Hla killed THP-1 cells in a dose-dependent manner and NSA could significantly decrease the Hla-induced cell death (**Figure 2.3D**). We sought to show that the effect that we observed was due to Hla-toxin activity and its ability to induce a signaling cascade (possibility through its interaction with its receptor, ADAM10). We stimulated cells with *hla* and *hla* complemented with Hla H35L plasmid (*hla*H35L), which produces Hla that can interact with ADAM10 but that cannot assemble to form a pore on the host cell (14), a p*hla* (an *hla* strain complemented with Hla-producing plasmid) in the presence of NSA or DMSO. We observed that *hla* null and *hla*H35L strains had limited killing ability compared with p*hla* and WT strains (**Figures 2.3E and 2.3F**). NSA significantly decreased cytotoxicity induced by these strains (**Figure 2.3F**). Thus, *S. aureus* toxins are efficient at killing macrophages and a necroptosis inhibitor can significantly decrease their cytotoxicity.

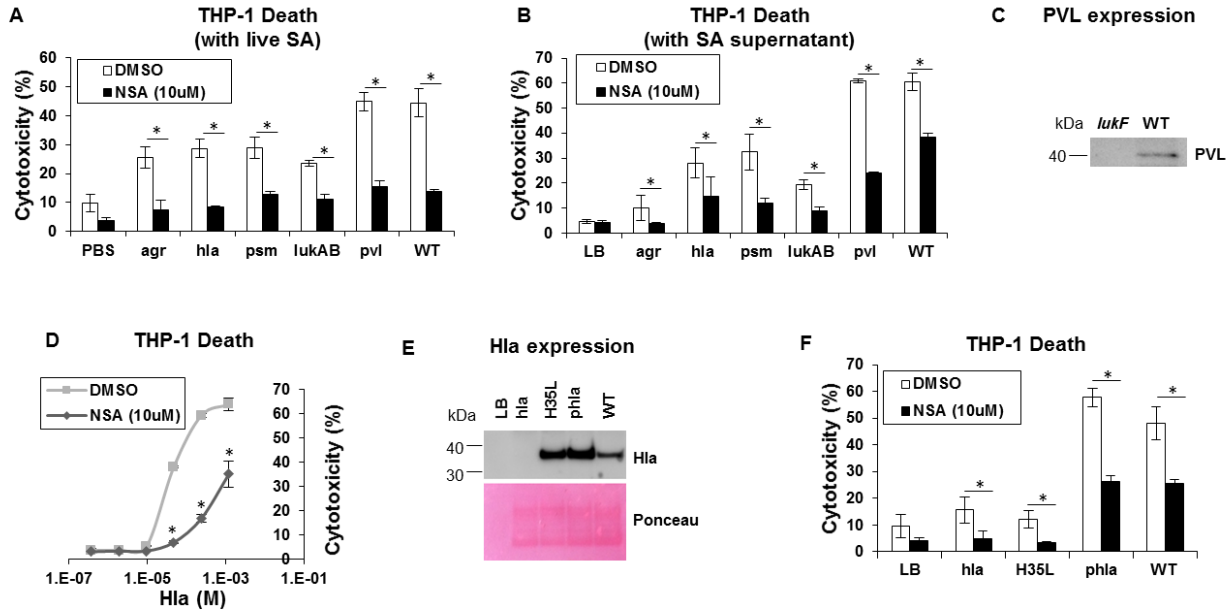

Figure 2.3. Necroptosis inhibitors can inhibit *S. aureus* toxin-induced cell death
(**A**) Cytotoxicity in THP-1 cells pretreated with 10 µM NSA or DMSO and infected with *agr, hla*, *psm* (*Δα/β/hld*), *lukAB*, *pvl* and wild type (WT) USA300 *S. aureus* mutants for 2 hours (*$p < 0.005$).
(**B**) Cytotoxicity in THP-1 cells pretreated with NSA or DMSO and exposed to supernatant harvested from mutants in "A." (*$p < 0.0001$).
(**C**) Western blot showing the expression of PVL in supernatants from *pvl* and WT USA300 strains.
(**D**) Cytotoxicity in THP-1 cells pretreated with NSA or DMSO and exposed to purified Hla for 2 hours (*$p < 0.05$).
(**E**) Western blot showing the expression of Hla in supernatant harvested from *hla* mutant, *hla* mutant complemented with *hla*H35L or *hla* plasmid and WT.
(**F**) Cytotoxicity in THP-1 cells pretreated with NSA or DMSO and exposed to supernatant harvested from *hla*, *hla*H35L, p*hla* plasmid and WT (*$p < 0.05$).
Data are a representative of two to four independent experiments. Data are represented as mean ± SD of three or more technical replicates. * $p < 0.05$

The necrosome complex and the inflammasome share components – It has previously been shown that the necrosome components (particularly RIPK3) can influence the activation of the NLRP3 inflammasome (72). It is also known that *S. aureus* Hla can activate the NLRP3 inflammasome through K^+ efflux (82). We tested the hypothesis that the necrosome components modulate the inflammasome during *S. aureus* infection. To test this hypothesis, we infected THP-1 cells with WT and *hla* null strains in the presence of a necroptosis inhibitor. We observed that WT and p*hla S. aureus* strains activated the inflammasome, as measured by caspase-1 cleavage

and production of IL-1β (**Figures 2.4A and 2.4B**). NSA significantly inhibited inflammasome activation, almost to the extent induced by the *hla* null *S. aureus* strain (**Figures 2.4A-C**). Similar to NSA, extracellular K^+ decreased cell death and IL-1β production further showing a link between necroptosis and the inflammasome (**Figures 2.4D and 2.4E**). However, production of ROS, which has previously been shown to mediate RIPK3's activation of NLRP3 (74), was not involved since N-acetyl-cysteine (NAC) did not decrease IL-1β production or cell death (**Figures 2.4E and 2.4F**). Dextran, an osmoprotectant, prevented THP-1 death and IL-1β release (**Figures 2.4G and 2.4H**). Thus, the necrosome and the inflammasome components are intertwined and both potentially determine outcome during *S. aureus* infection.

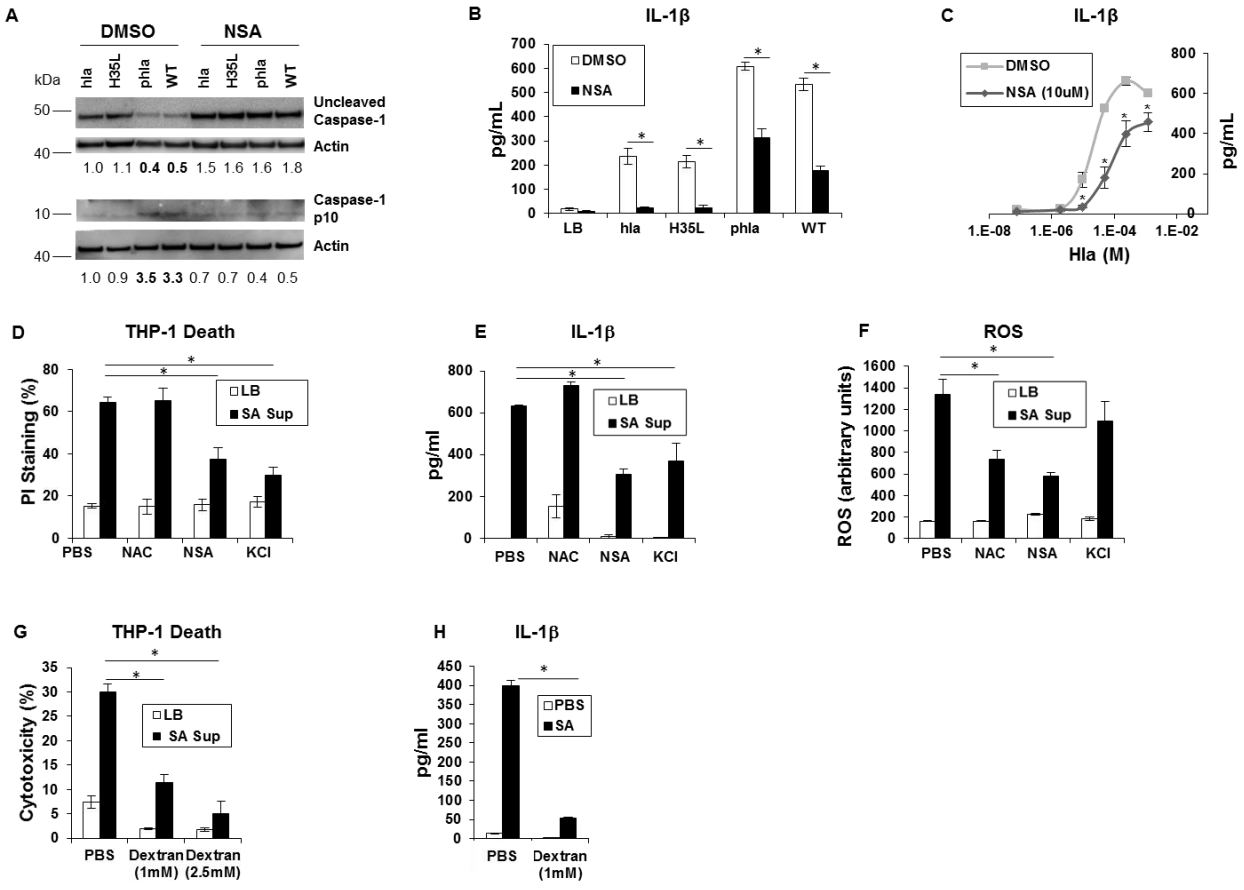

Figure 2.4. The necrosome and the inflammasome components are intertwined
(**A**) Caspase-1 western blot of THP-1 cells pretreated with NSA or DMSO and exposed to SA supernatant for 2 hours.
(**B**) Levels of IL-1β as quantified by ELISA in THP-1 cells pretreated with NSA or DMSO and exposed to SA supernatant for 2 hours (*$p < 0.05$).
(**C**) Levels of IL-1β as quantified by ELISA in THP-1 cells pretreated with NSA or DMSO and exposed to increasing concentrations of purified Hla for 2 hours (*$p < 0.05$).
(**D**) Cytotoxicity as measured by PI staining in THP-1 cells pretreated with 1 mM N-acetylcysteine (NAC), 10 μM NSA, 60 mM KCl or PBS and exposed to SA supernatant for 2 hours (*$p < 0.005$).
(**E**) IL-1β in samples in "D".
(**F**) ROS levels in samples in "D".
(**G**) Cytotoxicity as measured by LDH assay in THP-1 cells pretreated with 1 mM, 2.5 mM dextran or PBS and exposed to SA supernatant for 2 hours.
(**H**) IL-1β in samples in "G".
Data are a representative of two independent experiments with three technical replicates (mean and SD). * $p < 0.05$, ** $p < 0.01$, *** $p < 0.001$.

Pharmacological inhibition of necroptosis improves outcome in *S. aureus* pneumonia – After documenting that *S. aureus* kills macrophages through necroptosis, we hypothesized that the loss of this critical immune cell population contributes to poor bacterial clearance and damaging inflammation typical of *S. aureus* pneumonia. To test this hypothesis, we characterized the effects of a pharmacological inhibition of necroptosis on bacterial clearance and immune cell recruitment in a mouse model of *S. aureus* pneumonia. Necrostatin-1s-treated mice had significantly improved clearance of bacteria from airway fluid (**Figure 2.5A**). Macrophage numbers in the lung were slightly increased and neutrophil numbers were significantly increased in both airway (BAL) and lung of Nec-1s-treated mice compared to DMSO-treated group (**Figures 2.5B and 2.5C**). Other immune cells such as $CD4^+$ T cells and NK cells were increased after infection, but were not affected by Nec-1s-treatment at the baseline and after infection (**Figures 2.5D and 2.5E**). Nec-1s-treatment resulted in decreased *Kc*, *Il6* and *Tnf* as compared to the control group in the mRNA but not in the protein level (**Figure 2.5F and 2.5G**). Thus, even though Nec-1s has a short half-life and modest potency (83), it improved outcome during acute *S. aureus* pneumonia.

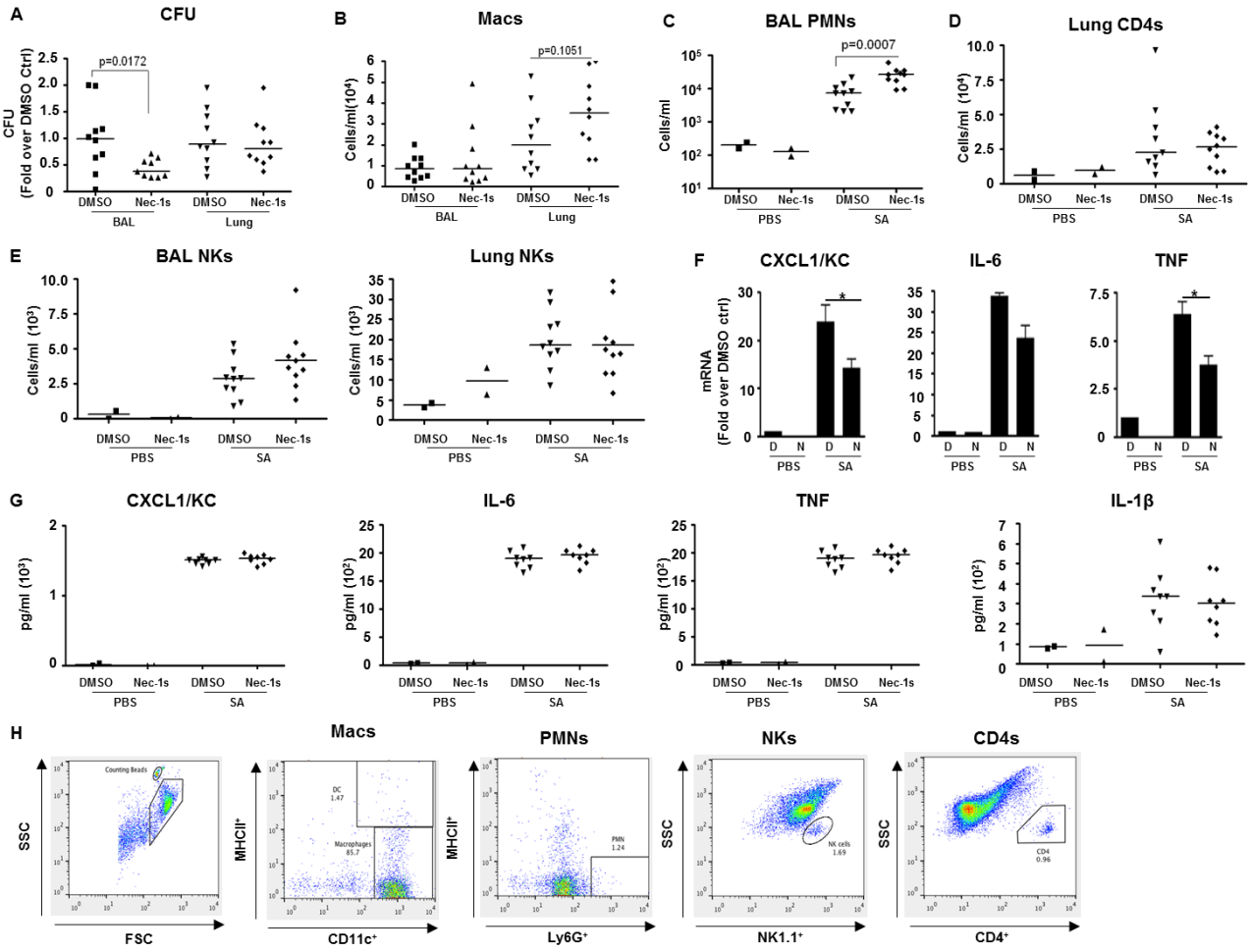

Figure 2.5. Pharmacological blockade of necroptosis improves outcome in *S. aureus* pneumonia
(**A**) C57BL/6J mice were treated with necrostatin-1 stable (Nec-1s) or DMSO and infected with USA300 (SA). *S. aureus* colony forming units (CFU) recovered from BAL and lung were quantified and normalized to DMSO controls (ctrl).
(**B and C**) Macrophages (Macs) in BAL and lung and neutrophils (PMNs) in BAL.
(**D**) CD4+ T cells (CD4s) in lung.
(**E**) Natural killer cells (NKs) in BAL and lung.
(**F**) *Cxcl1/Kc*, *Il6* and *Tnf* expression in the lung homogenate quantified by real time PCR compared to control (ctrl).
(**G**) CXCL/KC, IL-6, TNF and IL-1β levels in the BAL of Nec-1s-treated mice after *S. aureus* infection.
(**H**) FACS blots showing gating strategies for immune cells.
Data are pooled from two independent experiments. Each point represents a mouse. Lines show median values. * $p < 0.05$, ** $p < 0.01$, *** $p < 0.001$

Genetic inhibition of necroptosis improves outcome in *S. aureus* pneumonia – To confirm the results that we obtained with the pharmacological inhibitor of necroptosis, we used *Ripk3*$^{-/-}$ (also known as *Rip3*$^{-/-}$) mice to prove that preventing macrophage necroptosis improves outcome from

S. aureus infection. We compared the ability of WT C57BL/6J and *Ripk3*$^{-/-}$ mice to clear *S. aureus* infection (**Figure 2.6**). One day after infection, *Ripk3*$^{-/-}$ mice exhibited significantly increased *S. aureus* clearance from both the bronchial alveolar lavage fluid and lung as compared to WT mice (**Figure 2.6A**). The improved staphylococcal clearance correlated with better epithelial barrier function, as assessed by protein leakage into the BAL fluid and better preservation of normal lung architecture (**Figures 2.6B and 2.6C**). We also observed significant decreases in several proinflammatory cytokines/chemokines including IL-6, CXCL1/KC, IL-1β and IL-1α (**Figures 2.6D and 2.6E**). Together, these results show that necroptosis mediates damage during *S. aureus* pneumonia.

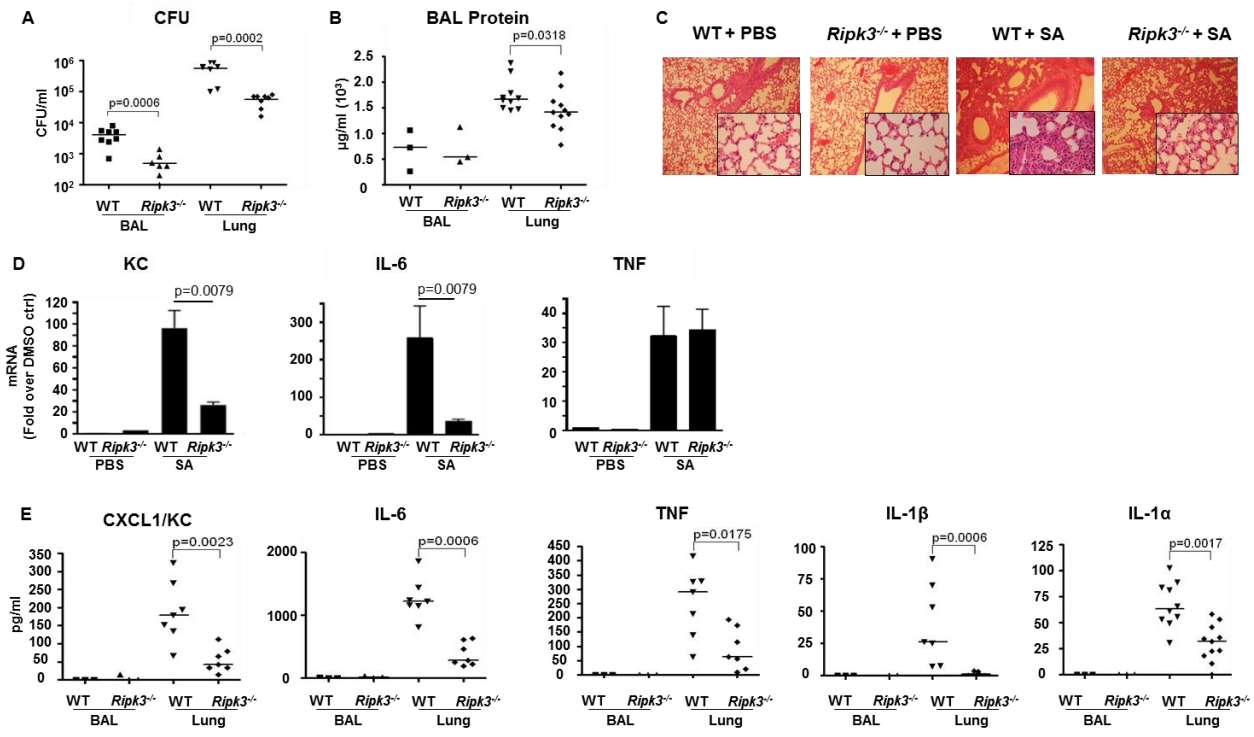

Figure 2.6. *Ripk3*$^{-/-}$ mice have increased *S. aureus* clearance
(**A**) CFU recovered in BAL and lung of *Ripk3*$^{-/-}$ or WT mice infected with USA300 (SA) for 18 hours.
(**B**) Protein in the BAL fluid of WT and *Ripk3*$^{-/-}$ mice.
(**C**) Hematoxylin and eosin stain (H&E) staining of WT and *Ripk3*$^{-/-}$ mice lungs (magnification of 100x; insert, magnification of 400x).

(**D**) *Cxcl1/Kc*, *Il6* and *Tnf* levels in lung as measured by quantitative RT-PCR
(**E**) CXCL1/KC, IL-6, TNF, IL-1β and IL-1α levels in the BAL fluid as measured by ELISA.
Data are pooled from three independent experiments. Each point represents a mouse. Lines show median values.

To determine the mechanism by which *S. aureus* mediated necroptosis, we infected WT and *Ripk3*$^{-/-}$ mice with WT and *agr* null USA300 strains. WT mice cleared both strains poorly in both BAL and lung as compared to *Ripk3*$^{-/-}$ mice (**Figures 2.7A and 2.7B**). WT mice exhibited increased clearance of *agr* null strain and preserved lung architecture after *agr* infection compared to after WT USA300 infection, whereas *Ripk3*$^{-/-}$ mice did not show any phenotype in the lung (**Figures 2.7A and 2.7B**). These results show that *agr*-regulated toxins activate necroptosis leading to impaired bacterial clearance.

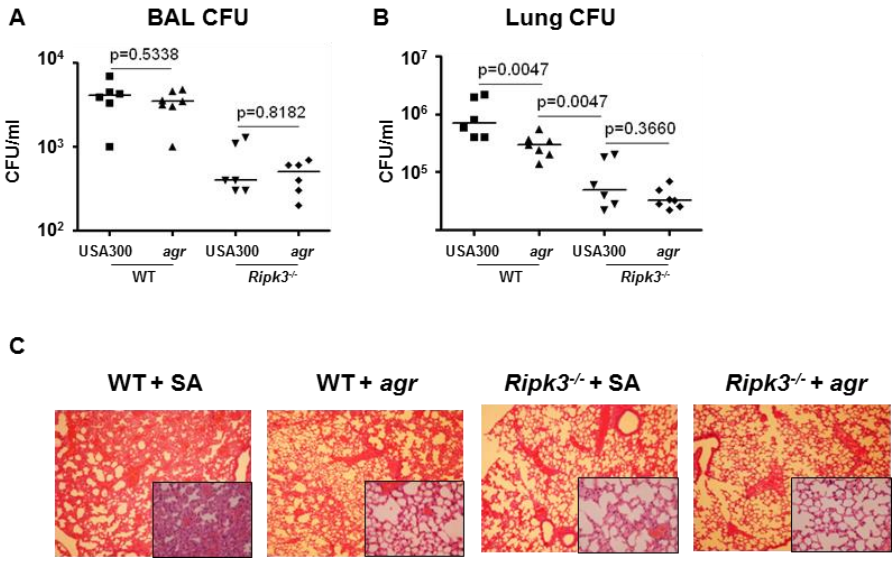

Figure 2.7. *S. aureus* toxins induce necroptosis leading to poor outcome during pneumonia
(**A**) CFU recovered in BAL and lung of *Ripk3*$^{-/-}$ or WT mice infected with WT USA300 or *agr* strain.
(**B**) Hematoxylin and eosin stain (H&E) staining of WT and *Ripk3*$^{-/-}$ mice lungs (magnification of 100x; insert, magnification of 400x) infected with WT USA300 or *agr* strain.
Data are pooled from three independent experiments. Each point represents a mouse. Lines show median values.

***S. aureus*-induced necroptosis targets macrophages in a mouse model of pneumonia –** We next hypothesized that *S. aureus* targets resident macrophages through necroptosis and these cells may not be easily replenished from the bone marrow or local stores. To test this hypothesis, we quantified the different types of immune cells recruited into the BAL and lung following *S. aureus* infection. PMNs were quickly recruited into the lungs within 4 h and they predominated the lung and BAL after 24 h of infection (**Figures 2.8A and 2.8B**). The predominance of alveolar macrophages in the airway in the uninfected mice was maintained at 4 hours post inoculation, but by 24 hours PMNs were the dominant immune cells in the infected lung (**Figure 2.8C**). NK cells, DCs and $CD4^+$ T cells were readily detected after infection, with NK cells increasing in number in BAL after infection (**Figures 2.8D-G**). Considering that epithelial and immune cells produce neutrophil and macrophage chemokine production in response to infection, there was actually a net decrease in the absolute number of macrophages in the lung at 24 hours following infection (**Figure 2.8H**), suggesting that the local reservoir was depleted.

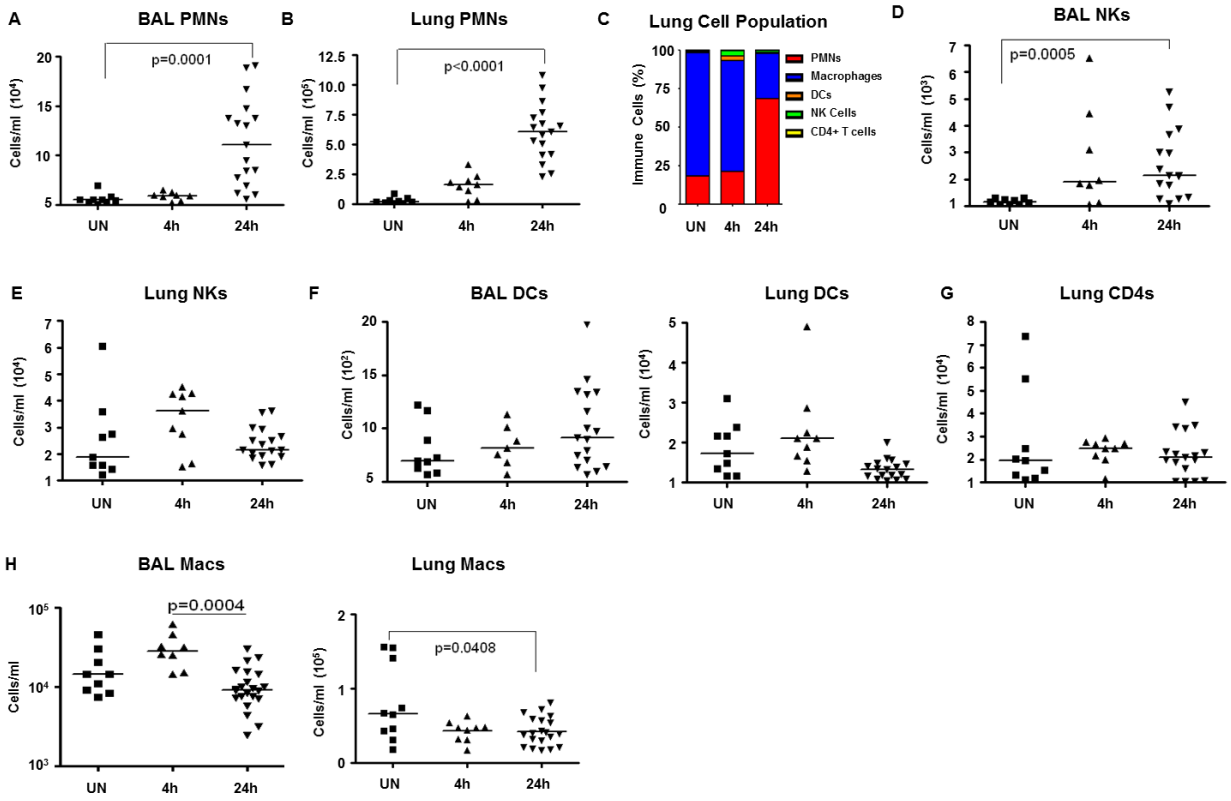

Figure 2.8. Macrophage expansion is limited during *S. aureus* pneumonia
(**A**) Number of neutrophils (PMNs) in BAL and lung of mice infected intranasally with *S. aureus* for 24 h.
(**C**) Percentages of immune cell populations at 4 and 24 hours as compared to uninfected controls (UN) determined.
(**D and E**) Natural killer cells (NKs) in BAL (D) and lung (E).
(**F**) Dendritic cells (DCs) in BAL and lung.
(**G**) $CD4^+$ T cells in lung.
(**F**) Macrophages (Macs) in BAL and lung.
Data are pooled from three independent experiments. Each point represents a mouse. Lines show median values

To confirm that the relative lack of alveolar macrophages was due to *S. aureus*-induced necroptosis, we measured the number of macrophages in *Ripk3*$^{-/-}$ mice after *S. aureus* pneumonia. *Ripk3*$^{-/-}$ mice had significantly more macrophages persisting in the BAL and lung after infection than WT mice (**Figures 2.9A and 2.9B**). No statistically significant differences in other immune cell populations including PMNs, DCs and NKs were observed (**Figures 2.9C-F**). We next stained BAL macrophages in WT and *Ripk3*$^{-/-}$ mice with propidium iodide, a dead cell stain. We

recovered more dead macrophages in BAL of WT mice compared to *Ripk3*$^{-/-}$ mice (**Figures 2.9G and 2.9H**), confirming that the macrophages were dying through necroptosis. Thus, necroptosis is a key way in which *S. aureus* depletes macrophages in vivo, worsening outcome during pneumonia.

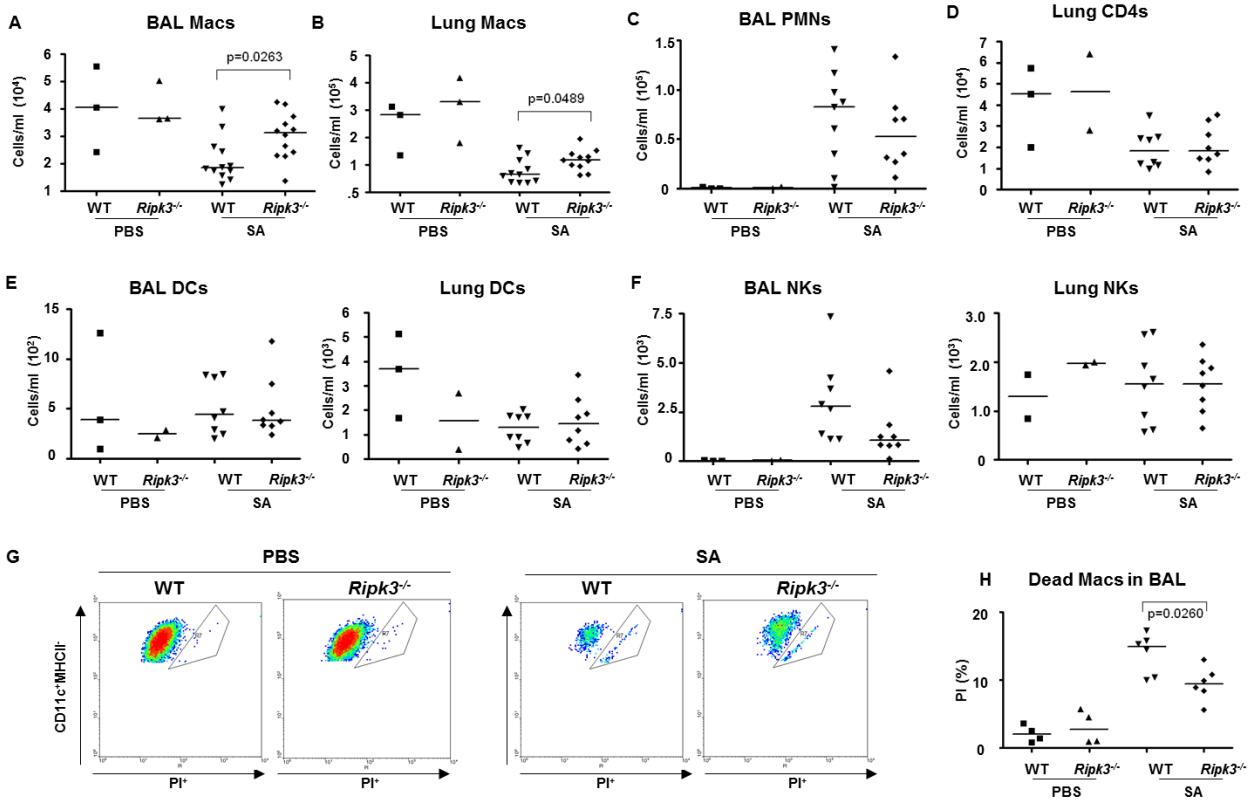

Figure 2.9. *S. aureus*-induced necroptosis targets macrophages in vivo
(**A**) Number of macrophages (Macs) in *Ripk3*$^{-/-}$ and WT mice infected with *S. aureus*.
(**B**) Neutrophils in BAL of *Ripk3*$^{-/-}$ and WT mice.
(**C**) Macs in BAL and lung of *Ripk3*$^{-/-}$ and WT mice.
(**D**) CD4^{+} T cells in lung of *Ripk3*$^{-/-}$ and WT mice.
(**E**) Dendritic cells in BAL and lung of *Ripk3*$^{-/-}$ and WT mice.
(**F**) NK^{+} T cells in BAL and lung of *Ripk3*$^{-/-}$ and WT mice.
(**G**) Representative FACS blots of propidium iodide positive (PI^{+}) macrophages in the BAL of WT and *Ripk3*$^{-/-}$ mice.
(**H**) Quantification of PI^{+} macrophages in the BAL of WT and *Ripk3*$^{-/-}$ mice.
Data are pooled from three independent experiments. Each point represents a mouse. Lines show median values.

Alveolar macrophages from *Ripk3*$^{-/-}$ have an anti-inflammatory phenotype in the setting of *S. aureus* pneumonia – We tested the hypothesis that the reason *Ripk3*$^{-/-}$ mice had improved bacterial clearance and decreased inflammation in the lung was that *Ripk3*$^{-/-}$ macrophages were more anti-inflammatory compared to WT macrophages. To test this hypothesis, we examined the abundance of specific markers on the pulmonary macrophages recovered from WT and *Ripk3*$^{-/-}$ mice (**Figure 2.10**). We first looked at the level of macrophage activation, which happens in the presence of pathogen, using CD54^{+} (ICAM^{+}) marker. Compared with control mice, *Ripk3*$^{-/-}$ mice expressed more CD54^{+} macrophages in both BAL and lung (**Figure 2.10A**) showing their increased level of activation. CD86 expression, a pro-inflammatory macrophage marker, was not changed in WT and *Ripk3*$^{-/-}$ mice BAL and lung (**Figure 2.10B),** whereas the number of CD206, an anti-inflammatory marker was significantly increased in *Ripk3*$^{-/-}$ mice macrophages harvested from the lung (**Figure 2.10C**). Similarly, the other major anti-inflammatory receptor CD200R was significantly increased in the macrophage populations isolated from both BAL and lung (**Figure 2.10D**). The increase in anti-inflammatory macrophages corresponded to the decrease in proinflammatory cytokines (KC, IL-6, CXCL1/KC, IL-1β and IL-1α) noted in the *Ripk3*$^{-/-}$ mice (**Figure 2.6D and 2.6E**). Thus, *Ripk3*$^{-/-}$ mice, which are protected from macrophage loss through necroptosis, have increased number of macrophages with an anti-inflammatory phenotype and a corresponding decrease in production of major proinflammatory cytokines. These observations suggest that the critical function of alveolar macrophages in the setting of *S. aureus* infection is to regulate the inflammatory response, and that the loss of macrophages through necroptosis is a major contributor to the hyperinflammatory milieu characteristic of *S. aureus* pneumonia.

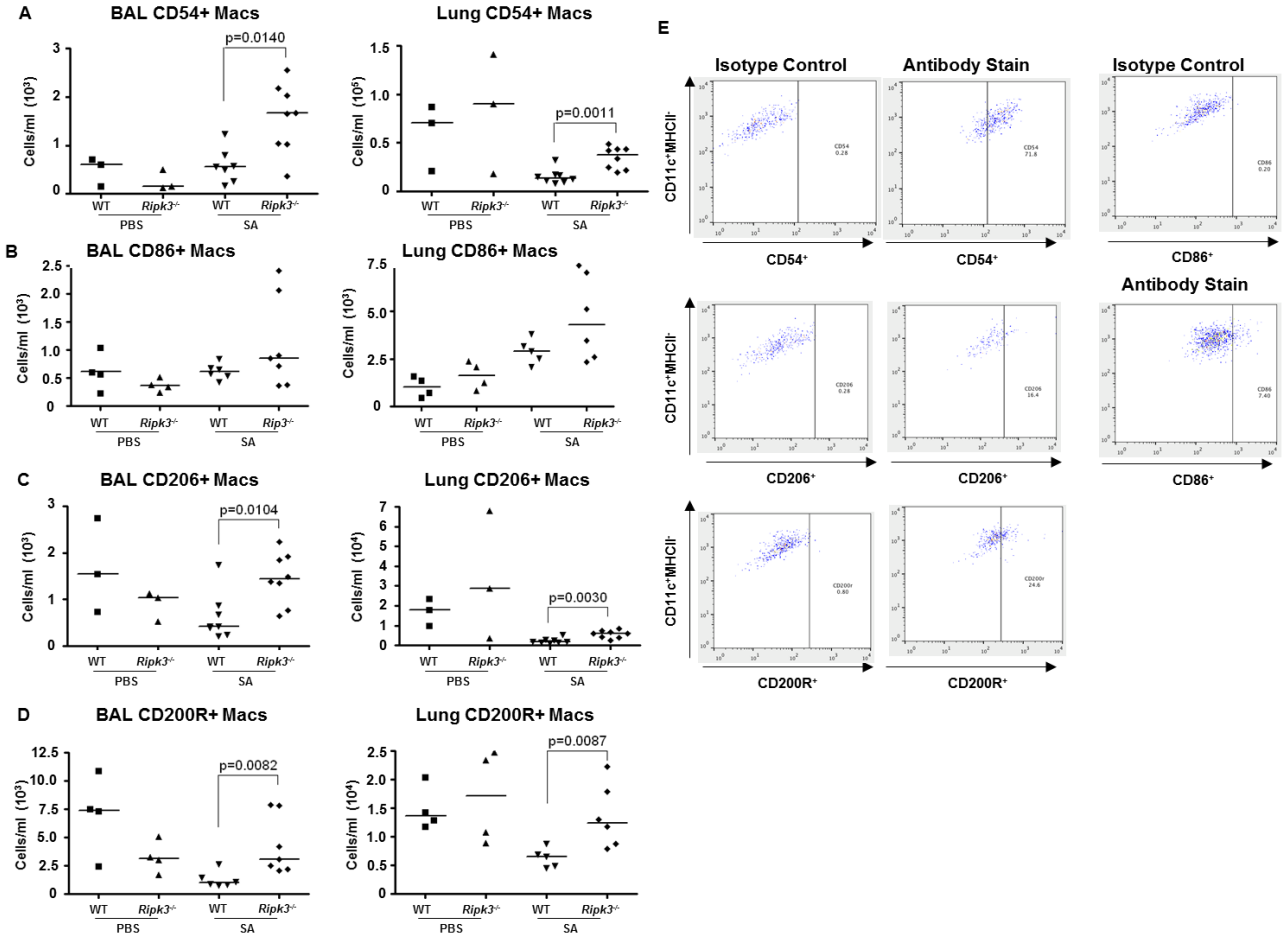

Figure 2.10. Pulmonary macrophages from *Ripk3*$^{-/-}$ mice have an anti-inflammatory phenotype
(**A**) Absolute number of CD54^{+} macrophages (Macs) in BAL and lung of *Ripk3*$^{-/-}$ and WT mice.
(**B**) CD86^{+} macrophages in BAL and lung.
(**C**) CD206^{+} macrophages in BAL and lung.
(**D**) CD200 receptor positive (CD200R^{+}) macrophages in BAL and lung.
(**E**) Gating strategies for macrophage markers**.**
Data are pooled from two independent experiments. Each point represents a mouse. Lines show median values.

Macrophage depletion leads to poor outcome during *S. aureus* pneumonia – To confirm further the contribution of macrophages, which are lost through necroptosis during *S. aureus* pneumonia, to the overall clearance of *S. aureus* from the lung, we treated mice with either PBS- or clodronate-loaded liposomes (**Figure 2.11**). Clodronate-loaded liposome depleted 95.4% and 91.6% of macrophages in the BAL and lung respectively in uninfected group and the significant decrease in clodronate-liposome-treated mice was noticeable in infected group (**Figure 2.11A**).

The consequences of macrophage depletion were evident in the significantly increased staphylococcal load recovered from both the BAL and lungs of the clodronate-treated mice (**Figure 2.11B**). We observed no significant difference in the number of neutrophils in either the airway or the lung (**Figures 2.11C and 2.11D**). However, macrophage-depleted mice had significantly greater ratio of staphylococci to neutrophil numbers at 24 hours post infection (**Figure 2.11E**). These results suggest that despite the presence of neutrophils, macrophages are essential for *S. aureus* clearance during pneumonia.

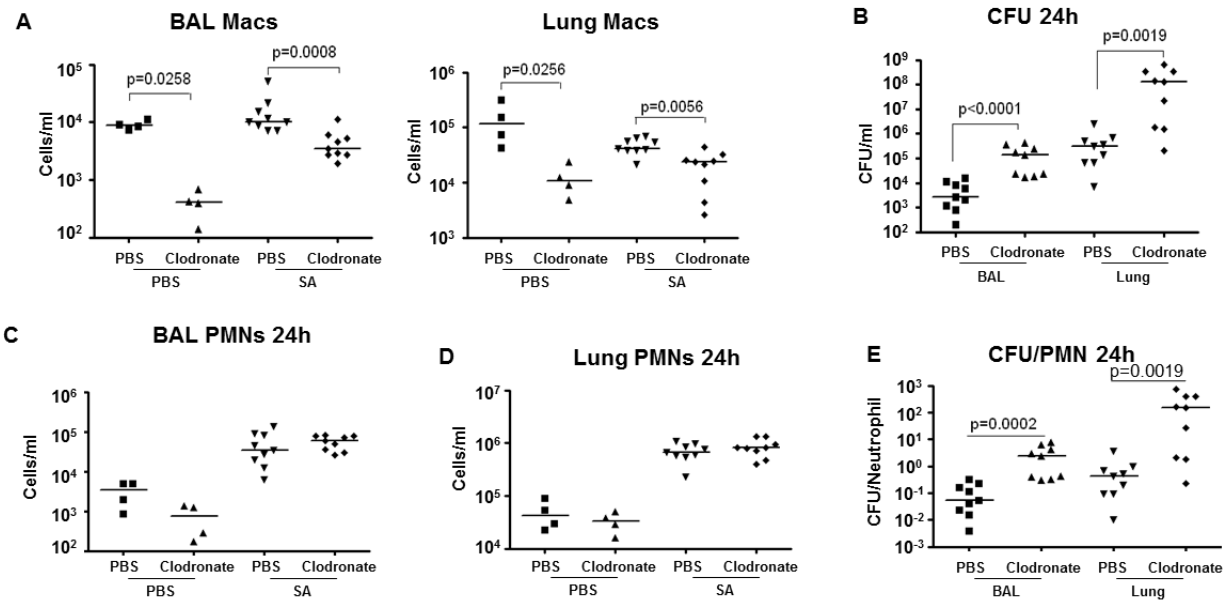

Figure 2.11. Depletion of pulmonary macrophages impairs *S. aureus* clearance
(**A**) Number of macrophages in BAL and lung of mice treated with clodronate- or PBS-loaded liposomes and infected intranasally with *S. aureus*.
(**B**) CFU recovered from BAL and lung from macrophage depleted mice.
(**C, D**) PMNs in BAL and lung 24 hours post-infection.
(**E**) Ratios of CFU to PMNs in BAL and lung.
Data are pooled from three independent experiments. Each point represents a mouse. Lines show median values.

We next quantified the recruitment of other types of immune cells into the lungs and airways to see if there were changes in other immune cell numbers to compensate for the lack of

alveolar macrophages. We observed that clodronate-treatment led to a decrease in the number of DCs in the BAL at 4 hours post infection, but the number of DCs at 24 hours was significantly increased in the clodronate-treated group as well as in the lung (**Figure 2.12A)**. The population of NK cells in the BAL by 4 hours post infection was not different but it was significantly increased in the lung at 4 hours in the clodronate-treated mice (**Figure 2.12B**). The number of NK cells changed after 24 hours, with more of them in BAL and no difference in lung in clodronate-treated mice (**Figure 2.12B**). Macrophage depletion did not affect the $CD4^+$ T cell population (**Figure 2.12C**).

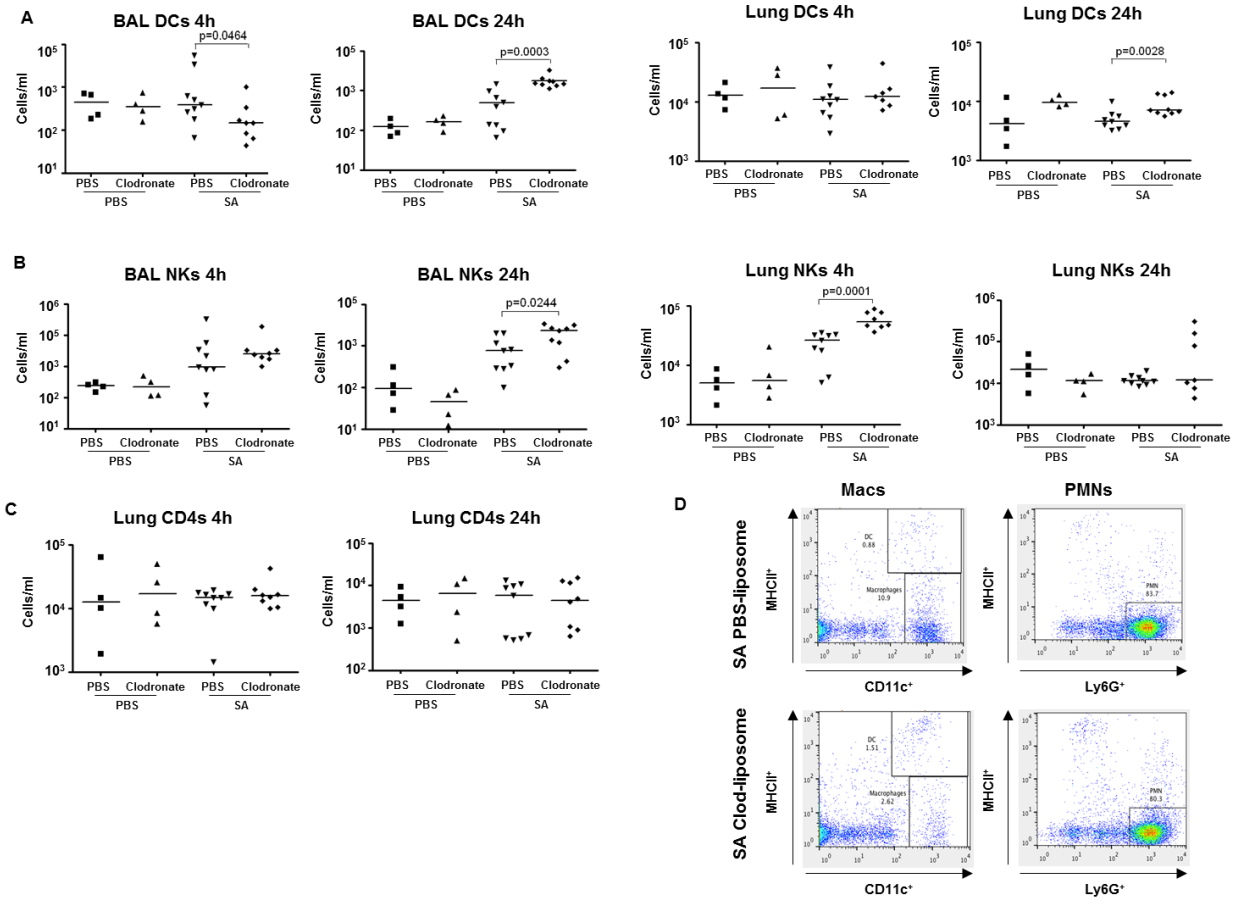

Figure 2.12. Immune cells in macrophage-depleted mice
(**A**) DCs in BAL and lung 4 h and 24 h post-infection in macrophage-depleted mice.

(**B**) NKs in BAL and lung 4 h and 24 h post-infection.
(**C**) CD4 T cells in lung 4 h and 24 h post-infection.
(**D**) Representative FACS blots showing depleted Macs and unchanged PMNs after clodronate-treatment.
Data are pooled from three independent experiments. Each point represents a mouse. Lines show median values.

Macrophage-depleted mice had increased lung damage marked by worse histopathology and significantly increased loss of lung architecture after *S. aureus* infection (**Fig 2.13A and 2.13B**). These results demonstrate that the regulatory functions of alveolar macrophages are critical in dampening inflammation and minimizing damage during acute staphylococcal pneumonia.

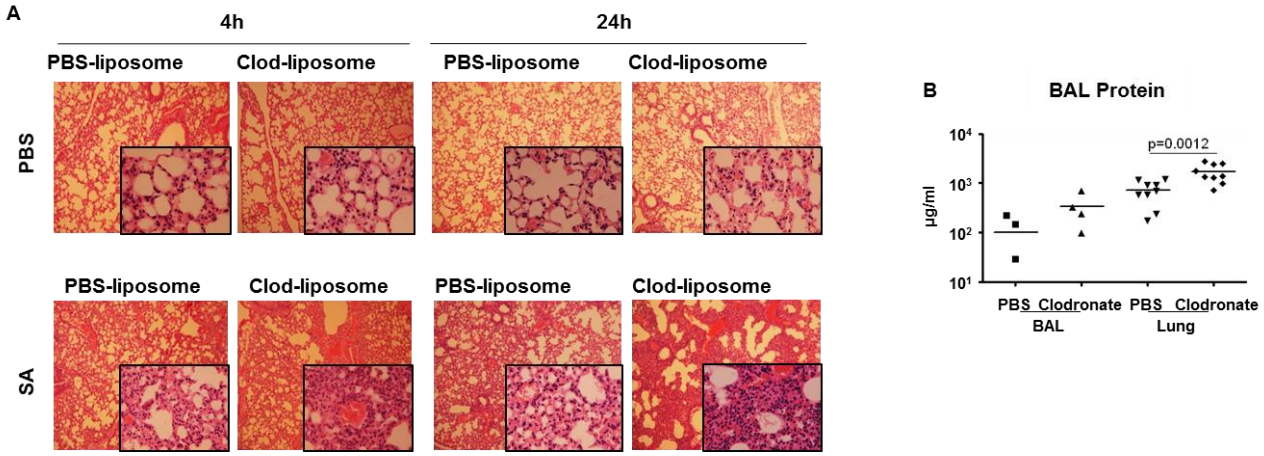

Figure 2.13. Macrophages regulate inflammation in *S. aureus* pneumonia
(**A**) Representative hematoxylin and eosin (H&E) stained imaged of mouse lung depleted of macrophages and infected with *S. aureus* (magnification 100x; insert, magnification 400x)
(**B**) Protein in the BAL fluid in macrophage-depleted mice lung post *S. aureus* infection.
Data are pooled from three independent experiments. Each point represents a mouse. Lines show median values.

Compensation for macrophage depletion during *S. aureus* pneumonia – We wanted to understand if the reason the *Ripk3*$^{-/-}$ mice did well after *S. aureus* was solely due to macrophage necroptosis. Several mammalian cells can undergo necroptosis with the right stimulation, and neutrophils in particular have been shown to die through necroptosis during *S. aureus* infection

(84). Using clodronate-loaded liposomes, we depleted macrophages in *Ripk3*$^{-/-}$ and WT mice and infected them with *S. aureus* for 24 hours (**Figure 2.14A**). As previously shown, depleting macrophages in WT mice worsens their outcome during *S. aureus* infection (**Figure 2.14B and 2.14C**). However, depleting macrophages in *Ripk3*$^{-/-}$ mice did not affect outcome as they still had significantly improved *S. aureus* clearance as compared with WT mice and significantly decreased expression of proinflammatory cytokines (**Figures 2.14B-D**). These *Ripk3*$^{-/-}$ mice had significantly increased neutrophil numbers and a trending increase in the number of DCs, which likely contributed to their ability to clear infection (**Figure 2.14E and 2.14F**). The *Ripk3*$^{-/-}$ mice lacking macrophages have increased epithelial damage as evidenced by significantly increased levels of protein in BAL fluid, as compared with PBS controls **(Figure 2.14G**). Thus, even though *S. aureus* can target multiple cells and that other immune cells can compensate for the lack of macrophages, lung macrophages play a key role in regulating inflammation and their death through necroptosis significantly contributes to lung damage.

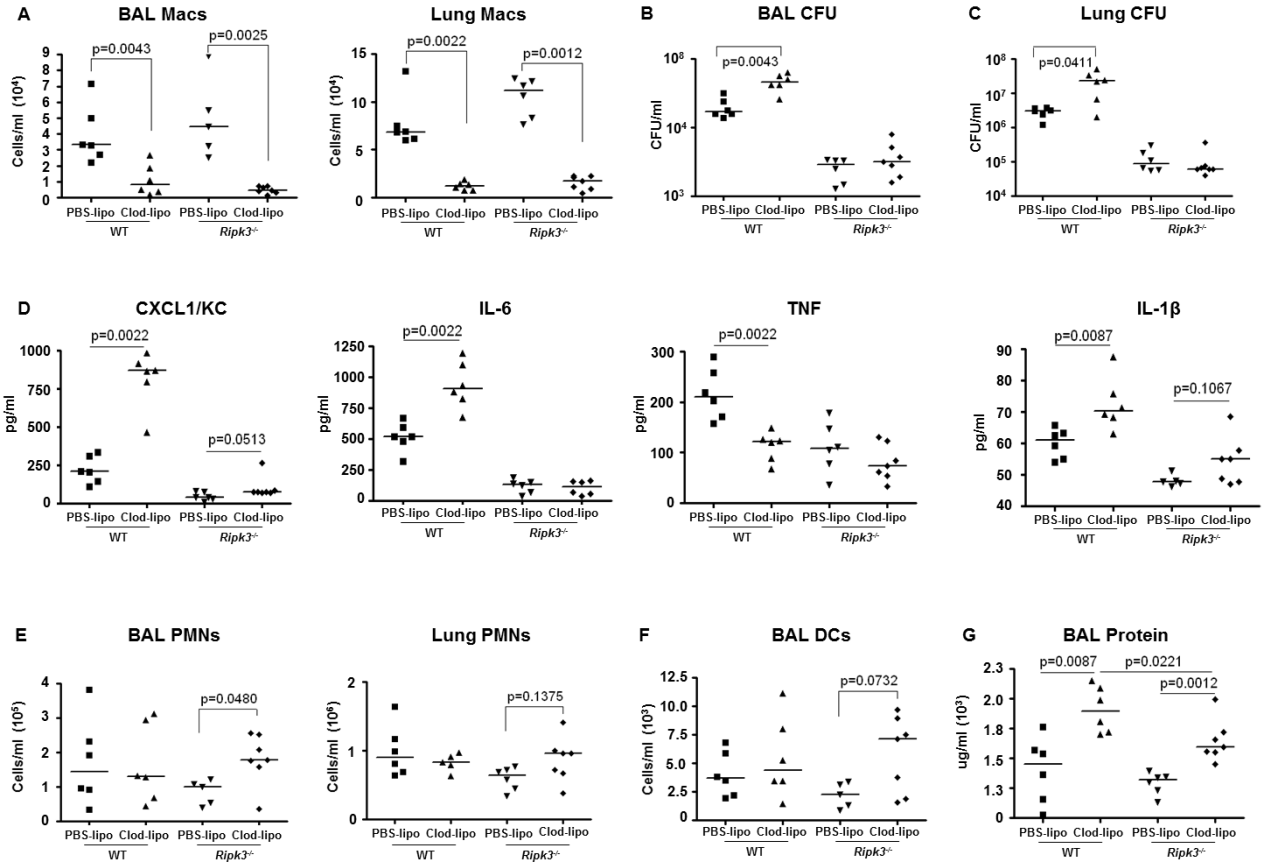

Figure 2.14. Depletion of pulmonary macrophages impairs *S. aureus* clearance
(**A**) Number of macrophages in BAL and lung of *Ripk3*$^{-/-}$ and WT mice treated with clodronate- or PBS-loaded liposomes and infected intranasally with *S. aureus*.
(**B and C**) CFU recovered from BAL and lung from macrophage depleted *Ripk3*$^{-/-}$ and WT mice.
(**D**) CXCL1/KC, IL-6, TNF and IL-1β levels in the BAL fluid of *Ripk3*$^{-/-}$ and WT mice.
(**E**) Number of neutrophils in BAL and lung of *Ripk3*$^{-/-}$ and WT mice.
(**F**) Number of DCs in BAL and lung of *Ripk3*$^{-/-}$ and WT mice.
(**G**) Protein in the BAL fluid of WT and *Ripk3*$^{-/-}$ mice.
Data are pooled from three independent experiments. Each point represents a mouse. Lines show median values.

Discussion

In this chapter, we show that *S. aureus*-induced macrophage necroptosis contributes to a defect in bacterial clearance and resolution of inflammation. Inhibition of necroptosis using either Nec-1, which blocks RIPK1, or NSA, which inhibits MLKL, resulted in decreased macrophage death

as did RIPK3 and MLKL knockdown by siRNA in vitro. NSA significantly reduced macrophage cytotoxicity induced by purified supernatant from WT *S. aureus*, suggesting that *S. aureus* toxins induce necroptosis.

In a murine model of pneumonia, *S. aureus* toxin-induced necroptosis killed macrophages in the lung leading to acute inflammation. Nec-1s-treatment led to increased bacterial clearance. Compared to wild type C57BL/6 mice, *Ripk3*$^{-/-}$ mice had significantly improved outcome from *S. aureus* pneumonia. Pulmonary macrophages of *Ripk3*$^{-/-}$ mice were resistant to death and upregulated anti-inflammatory markers, CD200R and CD206. Improved macrophage survival in *Ripk3*$^{-/-}$ mice was associated with improved lung architecture and decreased inflammation as marked by protein leakage and inflammatory cytokines in the airways. Therefore, inhibition of necroptosis preserves macrophage population that helps clear pathogens and minimizes potentially damaging inflammation.

We could not identify a single *S. aureus* pore-forming toxin that mediated necroptosis in vivo. In a mouse model of pneumonia, WT mice cleared the *agr* mutant better, but not to the same level as *Ripk3*$^{-/-}$ mice. Since *agr* is a "master" regulator of *S. aureus* virulence factors and yet *agr*-infected WT mice showed a dramatic clearance phenotype as *Ripk3*$^{-/-}$ mice, we did not expect a major phenotype with a single toxin. Understanding the "single" *S. aureus* toxin that "matters the most" in a mouse model of pneumonia is also difficult since some *S. aureus* toxins are human specific and others are differentially expressed in vivo. PVL, for example, is a human specific toxin and we did not expect to see a major effect with this toxin in mice (85-91).

S. aureus can induce necroptosis in multiple host cells. It has been shown that *S. aureus* kills neutrophils through necroptosis (84) and we show in the next chapter the implications of *S. aureus*-induced necroptosis in epithelial cells during skin infection. We saw here that, unlike in

WT mice, depleting macrophages in *Ripk3*$^{-/-}$ mice did not alter bacterial clearance phenotype in *S. aureus* pneumonia. This effect was possibly due to the compensation of macrophage roles by DCs and PMNs, which were increased in numbers in macrophage-depleted *Ripk3*$^{-/-}$ mice, potentially because these cells were also resistant to *S. aureus*-induced necroptosis. However, despite these compensatory effects, macrophage-depleted *Ripk3*$^{-/-}$ mice had poor preservation of lung architecture compared to *Ripk3*$^{-/-}$ mice with intact macrophages. Thus, even though macrophage bacterial clearance phenotype may be compensated by other immune cells, their anti-inflammatory phenotype may not be easily replaceable.

In sum, this chapter has increased scientific understanding of the immunoregulatory role of macrophages. It also showed how *S. aureus* targets and kills this critical population leading to lung damage and demonstrated the therapeutic potential of specifically preserving macrophages and enhancing macrophage numbers during *S. aureus* pneumonia. Targeting the host response rather than developing new antimicrobial agents will potentially usher in a new and much needed generation of targeted therapies to protect critical immune cells from inflammatory death and improve outcome during *S. aureus* pneumonia.

Chapter 3: Necroptosis dampens inflammation leading to improved outcome during *Staphylococcus aureus* skin and systemic infection

Introduction

In the previous chapter, we showed that *S. aureus* kills macrophages, a cell population that is critical for bacterial clearance and regulation of inflammation, through necroptosis and thus leading to lung damage. In this chapter, we continue our quest to understand the role of necroptosis in the pathogenesis of two other common *S. aureus* diseases – skin and systemic infections.

Necroptosis in *Staphylococcus aureus* skin infection

Methicillin-resistant *S. aureus* strain (MRSA) USA300 is a leading cause of skin and soft tissue infection (92). It causes a wide-ranging form of skin infections extending from superficial infections to serious deep tissue infection. During *S. aureus* skin infection, a balance between a brisk inflammatory response to clear the pathogen and severe inflammation that may contribute to pathology is essential. Skin inflammation after *S. aureus* infection is often marked by the presence of abundant pro-inflammatory cytokines such as KC, IL-1β, TNF and IL-6 and an increase in the number of inflammatory cells such as neutrophils, monocytes, and macrophages. Abrogation of this inflammatory milieu, either by genetic mutation (such as using *Myd88*$^{-/-}$, *Il1r*$^{-/-}$, *Il1b*$^{-/-}$ or *Il17*$^{-/-}$ mice) or by neutrophil depletion, leads to worse outcome during *S. aureus* infection (26). On the other hand, excessive inflammation at the site of infection causes skin damage and decreased bacterial clearance (33, 34).

Keratinocytes can undergo apoptosis (as part of the natural differentiation process) or necroptosis (such as during infection or autoimmune disease), and the balance between the two is tightly regulated by RIPK3 and caspase-8 (61). As keratinocytes mature from the basal layer, which is made up of continuously dividing cells, to the corneal layer, which is made of corneocytes, they lose their organelles and die through a caspase-8-mediated non-inflammatory process (27). In the absence of caspase-8, necroptosis in the skin ensues (93). Similarly, deletion of *Ripk1* in mice skin leads to a fulminant inflammation mediated by RIPK3-dependent necroptosis (61). Thus, necroptosis in skin can be inflammatory as it involves production of DAMPs such as DNA, HMGB1 and several cytokines including IL-1α and IL-33.

Even though necroptosis leads to the release of inflammatory products, it also eliminates cells responsible for generating these products, an effect that may decrease inflammation over time. Necroptosis in cells suppresses excessive production of NF-kB-dependent inflammatory cytokines such as TNF and KC (76). Cell death also releases intracellular pathogens, which can then be phagocytosed and cleared by more competent immune cells such as neutrophils, eventually decreasing inflammation by removing the source of inflammatory stimuli (77). Thus, the role of cell death in regulating inflammation and the effects of inflammation during microbial infection is complex. Little is known about the role of necroptosis in *S. aureus* skin and systemic infection.

Regulated inflammation accompanied by sufficient and efficient bacterial clearance determines outcome during *S. aureus* infection. We tested the hypothesis that necroptosis lessens inflammation and contributes to better outcome in *S. aureus* sepsis and skin infection. This chapter shows that inhibition of necroptosis leads to worse outcome as shown by decreased bacterial clearance and increased lesion sizes along with amplified inflammation in a

subcutaneous model of *S. aureus* infection. We confirmed these observations in a systemic model of *S. aureus* infection.

Results

***S. aureus* induces necroptosis in skin –** To understand the importance of necroptosis during *S. aureus* skin infection, human skin grafted on SCID mice was infected with *S. aureus* for 3 days and the skin biopsies stained for phosphorylated MLKL (pMLKL), a marker of necroptosis. Confocal images of the grafts showed upregulation of MLKL and pMLKL in *S. aureus* infected skin (**Figure 3.1A**). pMLKL was present in most layers of the skin with strong prominence on the epidermis. *S. aureus* induced cytotoxicity in keratinocyte cell line (HaCaT) and primary skin cells (HEKn) and this form of cell death could be significantly decreased by RIPK1 inhibitor, Nec-1s; by RIPK3 inhibitor, GSK'872; and by MLKL inhibitor, NSA (**Figures 3.1B-D**). We observed a similar protection by NSA in primary keratinocytes (HEKn cells) (**Figure 3.1E**). Knockdown of *MLKL* by siRNA also decreased *S. aureus* induced death in HaCaT cells (**Figures 3.1F and 3.1G**). Together, these results show that *S. aureus* induces necroptosis in keratinocytes.

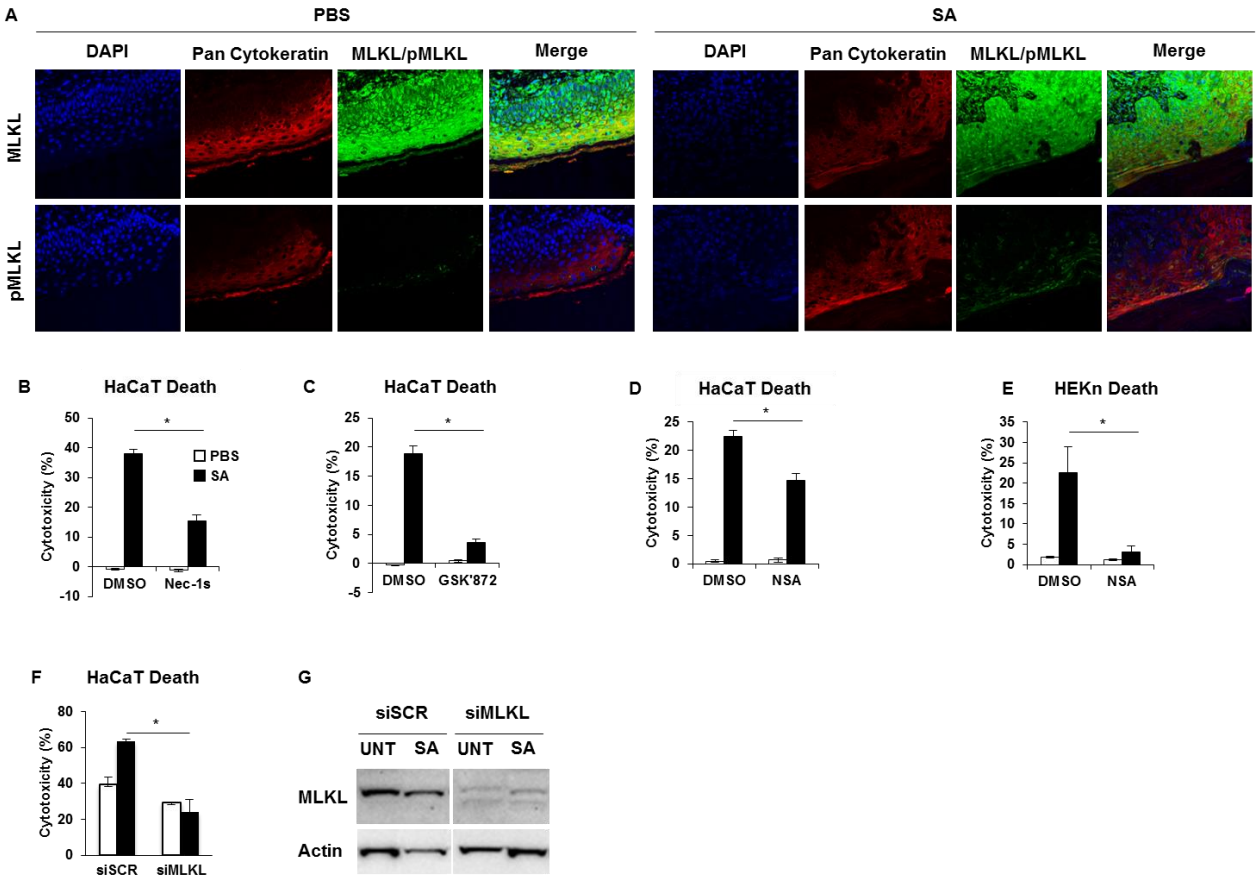

Figure 3.1. *S. aureus* induces necroptosis in skin cells
(**A**) Representative images of sections obtained from *S. aureus*-infected human skin grafts on SCID mice and stained for DAPI (blue), pan cytokeratin (red) and MLKL or phospho-MLKL (Green). Magnification of 200x.
(**B**) Cytotoxicity in keratinocyte cell line (HaCaT) pretreated with 200 µM necrostatin-1 stable (Nec-1s) and infected with *S. aureus* MOI of 10 for 4 h.
(**C**) Cytotoxicity in HaCaT cells pretreated with 10 µM GSK'872.
(**D** and **E**) Cytotoxicity in HaCaT cells (**C**) or primary keratinocytes (HEKn) (**D**) pretreated with 10 µM necrosulfonamide (NSA).
(**F**) Cytotoxicity in HaCaT cells with *MLKL* knocked down with siRNA.
(**G**) Western blot of HaCaT cells showing knockdown of *MLKL* by siRNA or scrambled control.
Data are represented as bar graphs with mean ± SEM. **p*<0.05, ***p*<0.01.

Pharmacological inhibition of necroptosis leads to poor outcome in *S. aureus* skin infection

– To understand the role of necroptosis during *S. aureus* skin infection, mice were infected subcutaneously with 2 x 10^6 CFU/mouse of *S. aureus* and treated with necrostatin-1s (Nec-1s) or

DMSO control for 5 days. We observed that Nec-1s-treated mice had more CFU and bigger lesions compared to DMSO group (**Figures 3.2A-C**). Since immune cells, particularly neutrophils (PMNs), gamma-delta (γδ) T cells and macrophages (Macs), have been previously shown to be essential for *S. aureus* clearance, we looked at their numbers in Nec-1s and DMSO treated mice. Nec-1s treated mice had more PMNs, γδ T cells, and Macs (**Figures 3.2D-F**). The increased number of immune cells was accompanied by increased levels of inflammatory cytokines in Nec-1s treated mice (**Figures 3.2G and 2H**). The histopathology of Nec-1s-treated mice exhibited increased adiposity and necrosis and increased TUNEL staining after infection (**Figures 3.2I and 3.2J**). The poor outcome experienced by Nec-1s-treated mice occurred in spite of the presence of large number of immune cells suggesting that either immune cells contribute to damaging inflammation and/or that necroptosis contributes to bacterial killing.

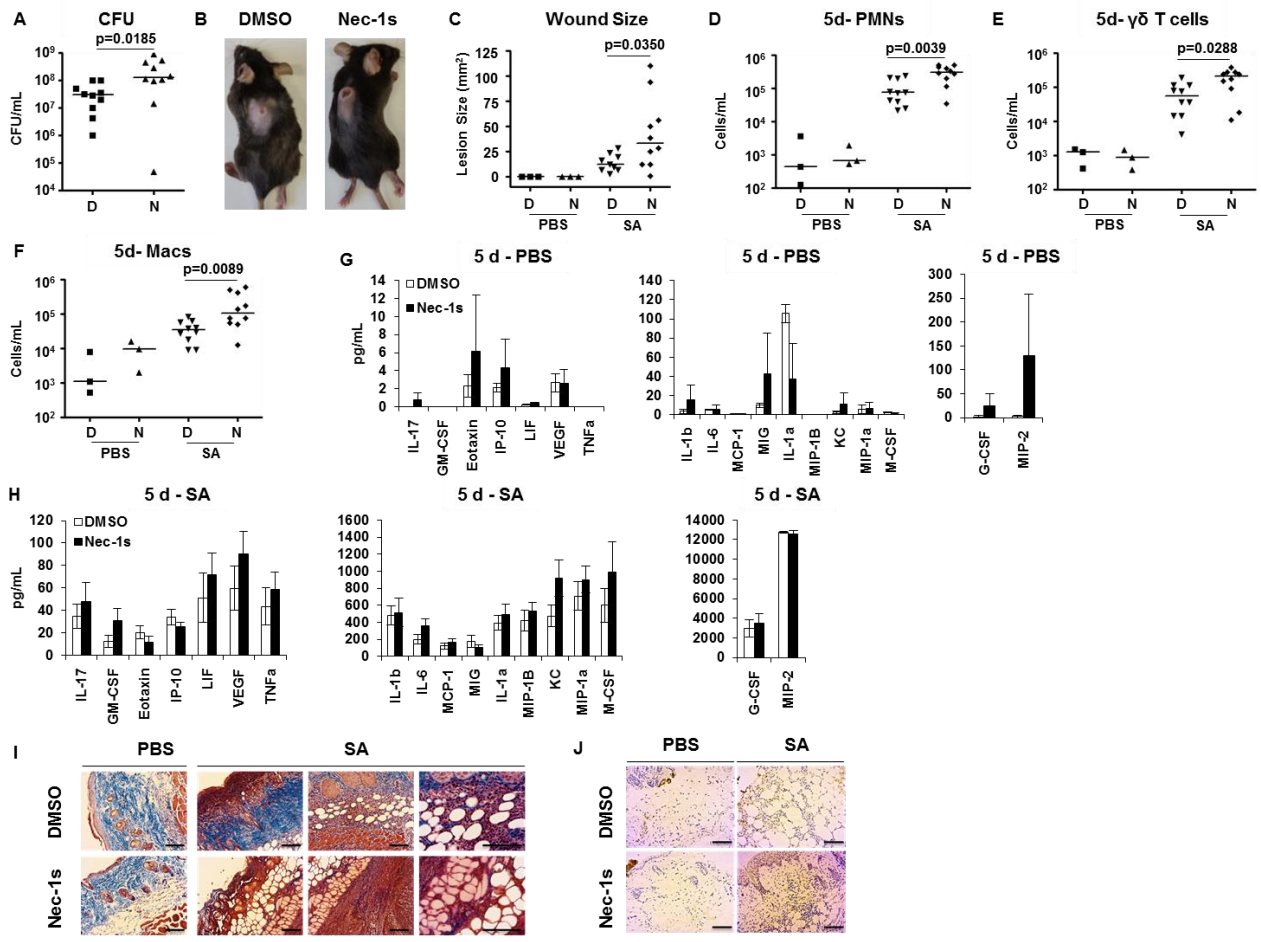

Figure 3.2. Pharmacological inhibition of necroptosis leads to worse outcome in *S. aureus* skin infection

(**A**) *S. aureus* CFU recovered on day 5 from mice were infected subcutaneously with *S. aureus* (SA) and treated with 10mg/kg necrostatin-1 stable (N) or DMSO control (D) for 5 days.

(**B**) Representative images of mice showing lesions 5 days after infection.

(C) Quantification of lesion sizes on day 5.

(**D-F**) Number of neutrophils (PMNs) (**D**), gamma-delta (γδ) T cells (**E**), and macrophages (Macs) (**F**) on infected mice.

(**G**) Cytokines from Nec-1s or DMSO treated mice and infected with PBS control.

(**H**) Cytokines from Nec-1s or DMSO treated mice and infected with *S. aureus*.

(**I** and **J**) Representative images of trichrome stain (**I**) or TUNEL stain (**J**) on skin biopsies of infected mice. Scale bars, 100 μm.

Each point represents a mouse and lines show median values. Data are represented as bar graphs with mean ± SEM. Results shown are pooled from at least two independent experiments. **p*<0.05, ***p*<0.01.

Necroptosis and pyroptosis are essential during *S. aureus* skin infection – To confirm the results we obtained by pharmacological inhibition of necroptosis, we subcutaneously infected *Mlkl*$^{-/-}$ mice, which lack the protein essential for execution of necroptosis, with *S. aureus* for 5

days. Like Nec-1s-treated mice, *Mlkl*$^{-/-}$ mice had reduced bacteria clearance and displayed bigger lesion sizes than WT controls after *S. aureus* infection (**Figures 3.3A-C**). Trichrome and TUNEL staining also revealed extensive inflammation and damage in *S. aureus* infected *Mlkl*$^{-/-}$ and *Casp1/4*$^{-/-}$ mice with increased adiposity, TUNEL positive cells and overall inflammation in mutant mice (**Figure 3.3D**). Strikingly, *Mlkl*$^{-/-}$ mice had increased active caspase-1 (p20) at baseline and after infection (**Figure 3.3E**), potentially caspase-1 was compensating for the lack of *Mlkl*.

We next wanted to determine the contribution of caspase-1 during *S. aureus* skin infection. Previous research has shown that IL-1β, which is processed by caspase-1, is essential for neutrophil recruitment and bacterial clearance in skin (26), but the exact role of pyroptosis during *S. aureus* skin infection has not been studied. To establish the role of pyroptosis during skin infection, we infected *Casp1/4*$^{-/-}$ mice with *S. aureus* for 5 days. On day 5, we obtained similar phenotypes in *Casp1/4*$^{-/-}$ mice to those in mice lacking *Mlkl* (**Figures 3.3A-D**). Together, these results show that the executioners of both necroptosis and pyroptosis participate in controlling *S. aureus* skin infection.

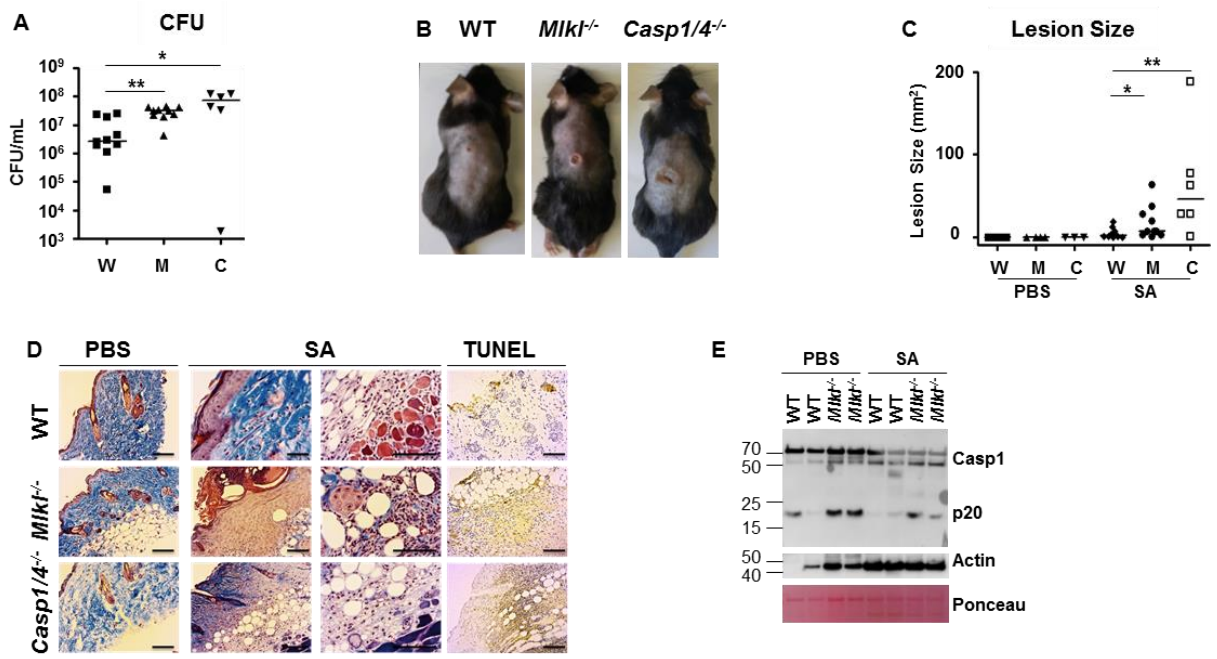

Figure 3.3. *Mlkl*$^{-/-}$ *and Casp1/4*$^{-/-}$ mice have worse outcome during *S. aureus* skin infection
(**A**) *S. aureus* CFU recovered from *Mlkl*$^{-/-}$, *Casp1/4*$^{-/-}$ and wild type (WT) mice infected subcutaneously with 2 x 10^6 CFU/mouse of *S. aureus* (SA) for 5 days
(**B**) Representative images of lesions on infected mice.
(C) Quantification of lesion sizes from (**B**).
(**D**) Representative images of trichrome stain and TUNEL stain on skin biopsies of *S. aureus*-infected mice. Scale bars, 100 μm.
(**E**) Immunoblot showing cleaved caspase-1 (p20), full-length caspase-1, actin and ponceau on skin homogenate of infected WT and *Mlkl*$^{-/-}$ mice.
Each point represents a mouse and lines show median values. Results shown are pooled from at least two independent experiments. *p<0.05, **p<0.01.

Necroptosis limits excessive inflammatory response in *S. aureus* skin infection – We tested the hypothesis that necroptosis reduces inflammation – marked by decreased cytokine production and recruitment of immune cells – and results in decreased damage during *S. aureus* skin infection. To test this hypothesis, we measured key inflammatory cytokines in *Mlkl*$^{-/-}$ mice after 1 and 5 days of *S. aureus* infection. Compared to WT mice, *Mlkl*$^{-/-}$ and *Casp1/4*$^{-/-}$ mice showed no defect in killing *S. aureus* and recruiting immune cells including PMNs, gamma-delta T cells and macrophages after 1 day of infection (**Figure 3.4A-C).** At this earlier time point in infection, *Mlkl*$^{-/-}$ mice had significantly upregulated T cell chemokines including RANTES (CCL5), IP10

(CXCL10), MCP1 and MIG (CXCL9) (**Figures 3.4D-F**), cytokines that have previously been shown to mediate inflammatory damage in *S. aureus* skin infection. Most other cytokines including IL-1β and MCSF were trending lower (**Figures 3.4D-F**).

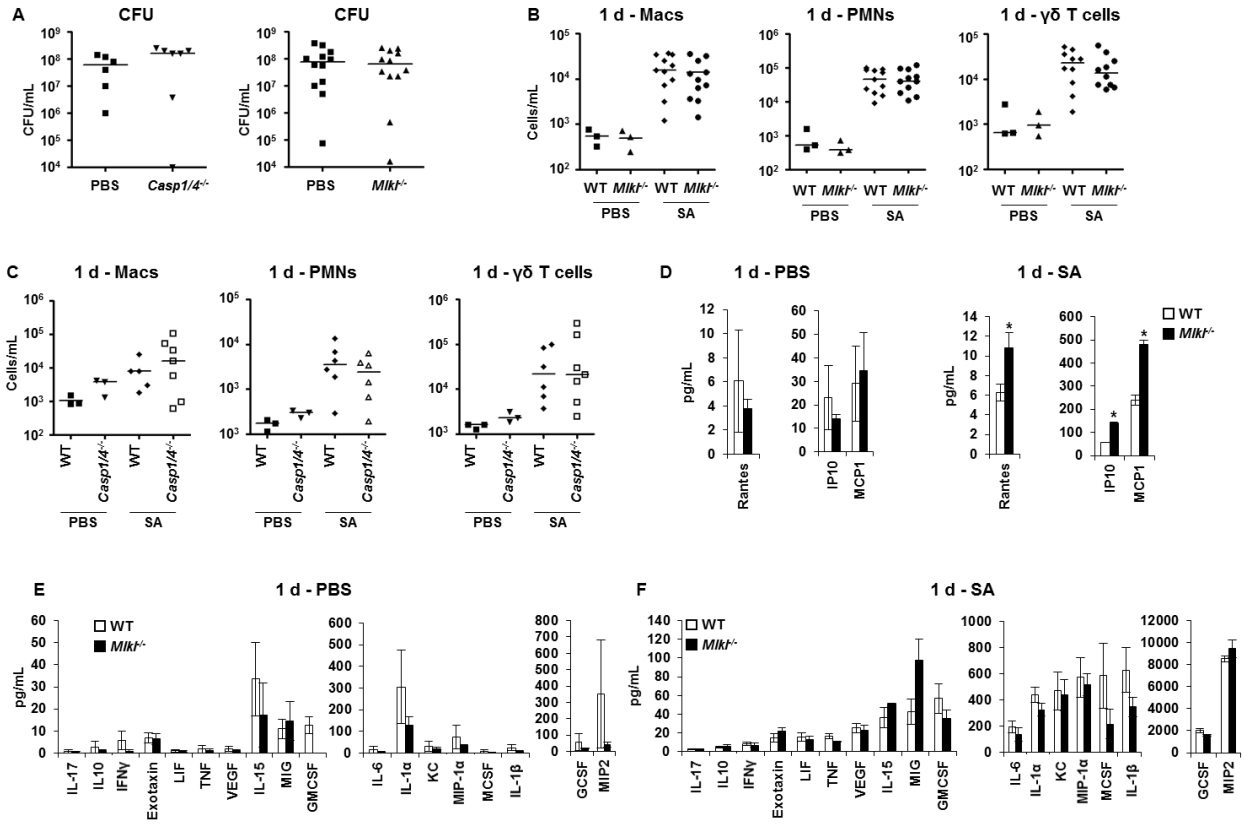

Figure 3.4. Response of wild type, *Mlkl*$^{-/-}$ and *Casp1/4*$^{-/-}$ mice after 1 day of *S. aureus* skin infection
(**A**) *S. aureus* CFU recovered from *Mlkl*$^{-/-}$, *Casp1/4*$^{-/-}$ and wild type (WT) mice were infected subcutaneously with 2 x 10^6 CFU/mouse *S. aureus* USA300 (SA) for 1 day.
(**B** and **C**) Numbers of neutrophils (PMNs), gamma-delta (γδ) T cells, and macrophages (Macs) in *Mlkl*$^{-/-}$ mice (**B**), *Casp1/4*$^{-/-}$ mice (**C**) and compared to WT mice.
(**D-F**) Cytokines from WT and *Mlkl*$^{-/-}$ mice infected with *S. aureus* or PBS for 1 day.
Each point represents a mouse and lines show median values. Data are represented as bar graphs with mean ± SEM. Results shown are pooled from at least two independent experiments. *p<0.05.

Five days after infection, *Mlkl*$^{-/-}$ and *Casp1/4*$^{-/-}$ had more immune cells (**Figures 3.5A-C**). Most of the important inflammatory cytokines including IL-1β, KC, MCSF, TNF, IL-1α, MCP1, IL-6 and MIP1β were significantly upregulated in *Mlkl*$^{-/-}$ compared to WT controls (**Figures**

3.5D and 3.5E). *Casp1/4*$^{-/-}$ mice did not show equally remarkable increase in inflammatory cytokines as *Mlkl*$^{-/-}$ mice did after infection (**Figures 3.5F and 3.5G**). These results suggest that the reason *Mlkl*$^{-/-}$ mice had poor outcome after *S. aureus* infection is not due to a defect in immune cell response, but rather due to excessive inflammation that impaired bacterial clearance and cause skin damage.

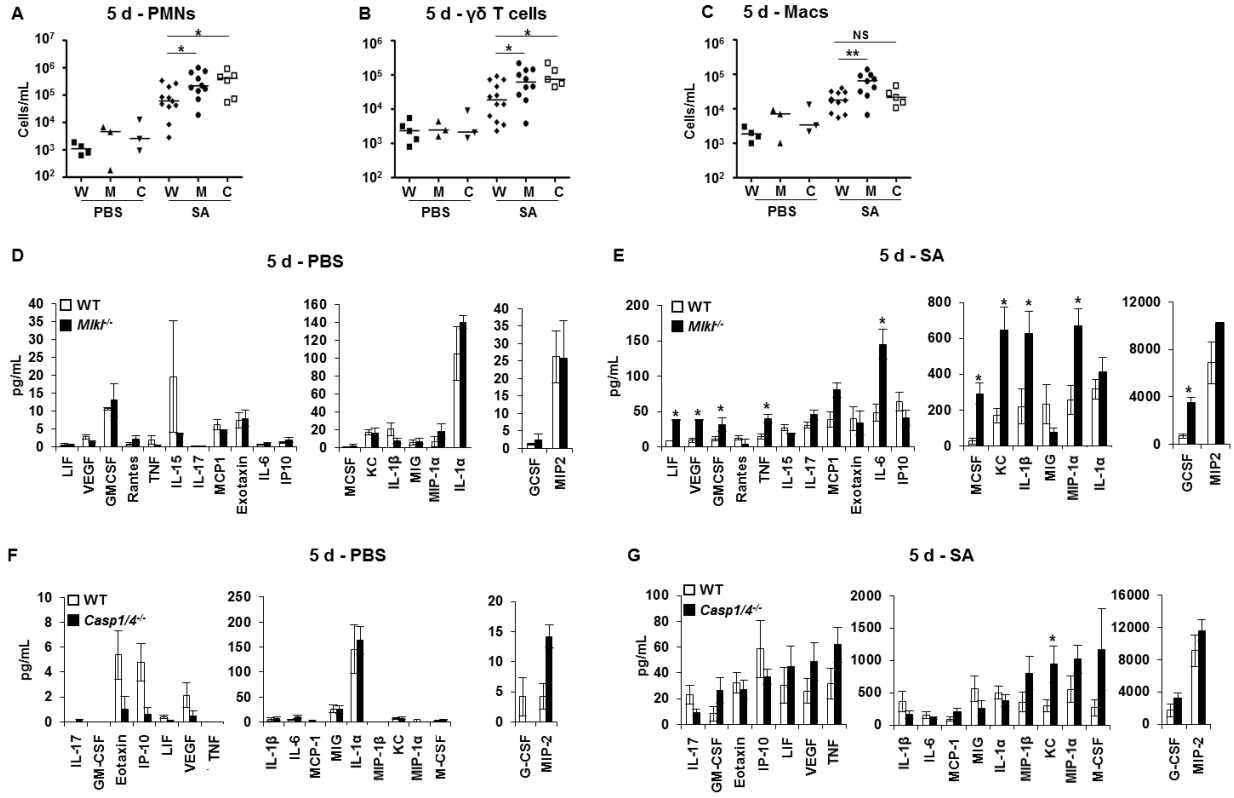

Figure 3.5. *Mlkl*$^{-/-}$ mice have heightened inflammatory response to *S. aureus* skin infection
(**A-C**) Number of neutrophils (PMNs) (**A**), gamma-delta (γδ) T cells (**B**), and macrophages (Macs) (**C**) in *Mlkl*$^{-/-}$, *Casp1/4*$^{-/-}$ and WT mice infected subcutaneously with 2 x 10^6 CFU/mouse *S. aureus* USA300 (SA) for 5 days.
(**D**) Baseline cytokines from PBS-treated WT and *Mlkl*$^{-/-}$ mice.
(**E**) Cytokines from *S. aureus* infected WT and *Mlkl*$^{-/-}$ mice.
(**F**) Baseline cytokines from PBS-treated WT and *Casp1/4*$^{-/-}$ mice.
(**G**) Cytokines from *S. aureus* infected WT and *Casp1/4*$^{-/-}$ mice.
Each point represents a mouse and lines show median values. Data are represented as bar graphs with mean ± SEM. Results shown are pooled from at least two independent experiments. *p<0.05, **p<0.01.

***Ripk3*$^{-/-}$ mice exhibited increased *S. aureus* clearance during skin infection –** To characterize further the role of necroptosis in *S. aureus* host defense, we evaluated the response of *Ripk3*$^{-/-}$ mice to infection (**Figure 3.6**). RIPK3 is a target of RIPK1 and a major effector of necroptosis (94, 95). However, RIPK3 can regulate several other pathways that can influence inflammation, including NF-κB, apoptosis and NLRP3 inflammasome pathway (43). In contrast to the *Mlkl*$^{-/-}$ mice or Nec-1s-treated mice, we noted significantly improved outcome in the *Ripk3*$^{-/-}$ mice marked by decreased staphylococcal burden, despite no change in lesion sizes (**Figures 3.6A-C**). *Ripk3*$^{-/-}$ mice had slightly improved skin architecture compared to WT mice following infection (**Figure 3.6B**).

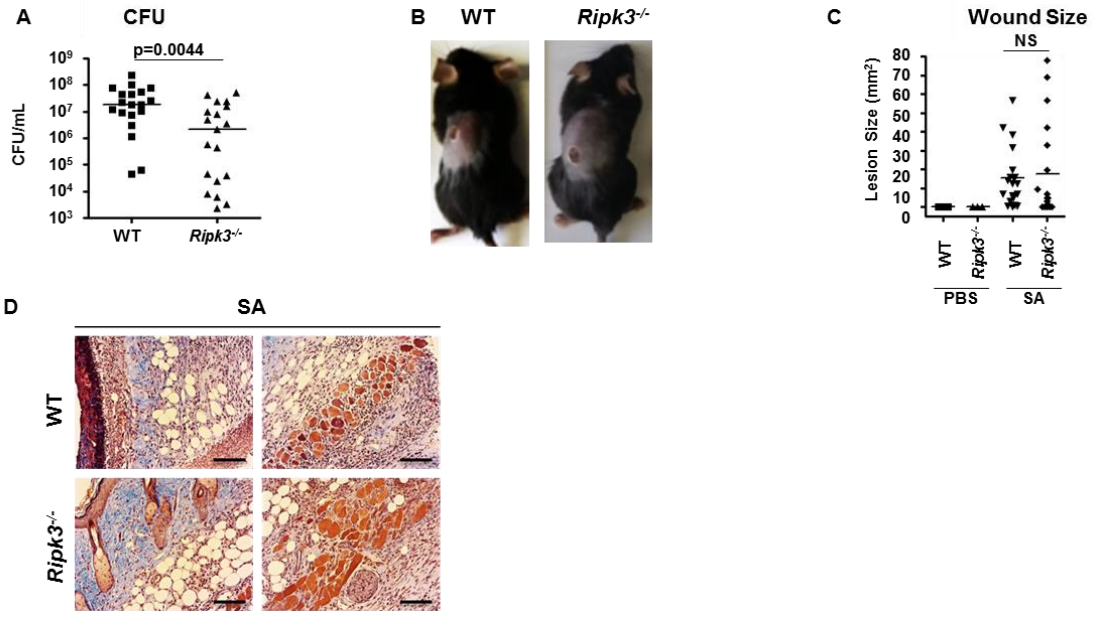

Figure 3.6. *Ripk3*$^{-/-}$ mice exhibit increased *S. aureus* clearance during skin infection
(**A**) *S. aureus* CFU recovered on day 5 on day of infection on *Ripk3*$^{-/-}$ and wild type (WT) mice infected subcutaneously with *S. aureus* (SA) for 5 days.
(**B**) Representative images of mice showing lesions on day 5 of skin infection.
(C) Quantification of lesion sizes on day 5.
(**D**) Representative images of trichrome stain on skin biopsies of *S. aureus*-infected mice. Scale bars, 100 μm.
Each point represents a mouse and lines show median values. Results shown are pooled from at least two independent experiments.

To understand if the improved phenotype we observed in *Ripk3*$^{-/-}$ mice was due to their ability to regulate inflammation, we analyzed their inflammatory response to *S. aureus*. We observed a diminished inflammatory cell recruitment and a reduced cytokine production (including significantly less IL-1β and G-CSF) following infection in *Ripk3*$^{-/-}$ mice, but no differences in baseline cytokine activity between the knockout and WT mice (**Figures 3.7A-E**).

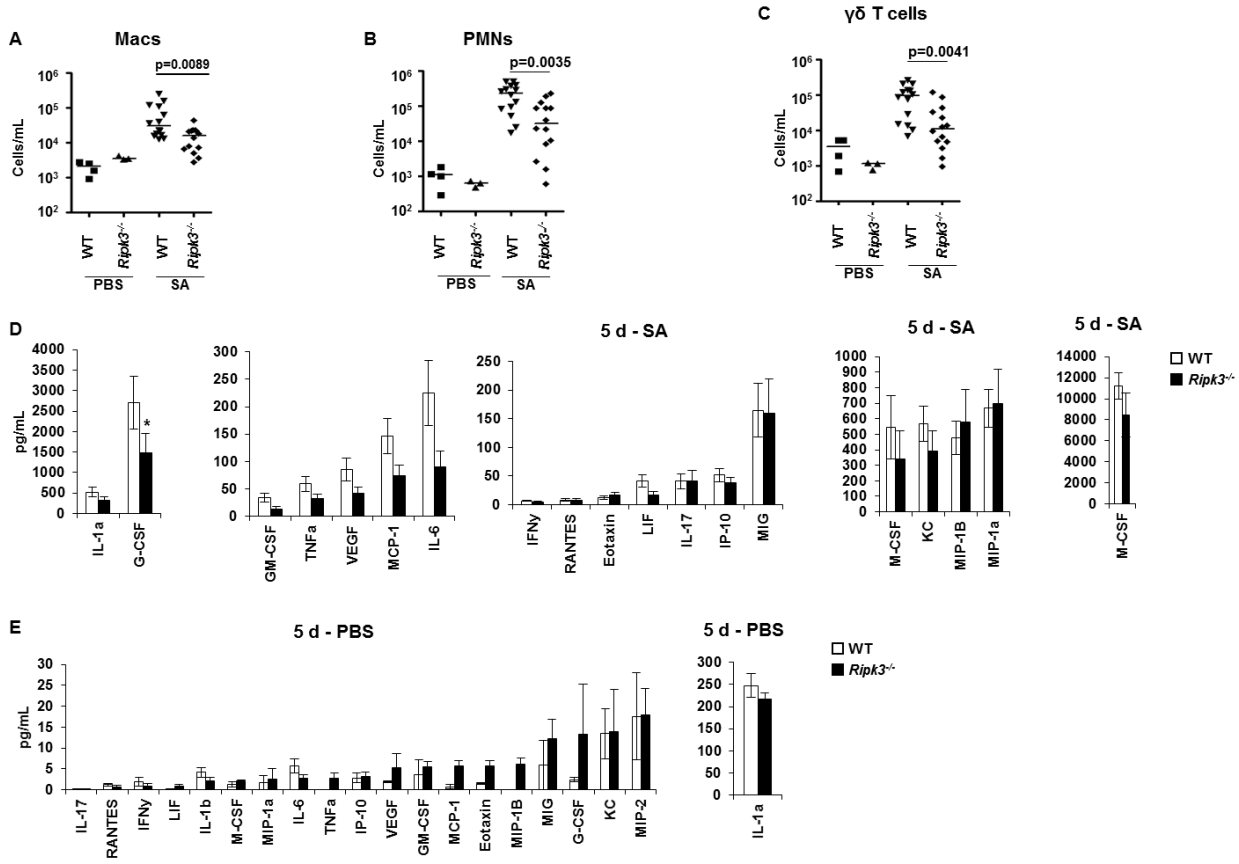

Figure 3.7. *Ripk3*$^{-/-}$ mice exhibit decreased inflammatory response during *S. aureus* skin infection
(**A-C**) Number of macrophages (Macs) (**A**) neutrophils (PMNs) (**B**) and gamma-delta (γδ) T cells (**C**) in infected area.
(**D and E**) Cytokines after 5 days of infection with *S. aureus* (**A**) or PBS control (**B**).
Each point represents a mouse and lines show median values. Data are represented as bar graphs with mean ± SEM. Results shown are pooled from at least two independent experiments. *p<0.05.

We postulated that the disparity in the results obtained in *Ripk3*$^{-/-}$ and *Mlkl*$^{-/-}$ mice were likely due to the additional roles of RIPK3, which are independent of its effects on its substrate MLKL, such as its ability to activate NLRP3 inflammasome (73), to induce NF-κB (96), to activate CaMKII-dependent necrosis (97) and to induce apoptosis in multiple cell types (98-102). In the absence of RIPK3, we observed decreased inflammasome activation, as marked by decreased production of IL-1β (**Figure 3.8A**). We also observed less cell death due to apoptosis, as shown by decreased Annexin V^{+} in all cells and immune cells and by decreased TUNEL staining in skin biopsies of infected *Ripk3*$^{-/-}$ mice (**Figures 3.8B and 3.8C**). Thus, deletion of *Ripk3* resulted in diminished IL-1β production and decreased apoptosis, resulting in increased eradication of infection and reduced inflammation-induced damage.

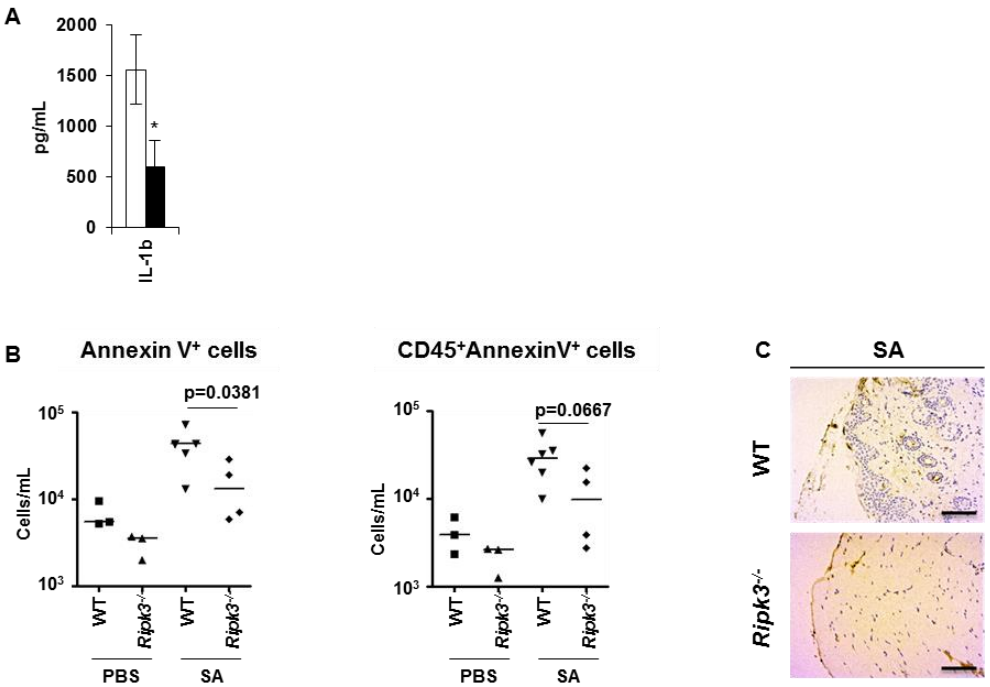

Figure 3.8. *Ripk3*$^{-/-}$ mice have decreased apoptosis activation and IL-1β production

(**A**) IL-1β produced by *Ripk3*$^{-/-}$ and WT mice after 5 days of *S. aureus* skin infection
(**B**) Number of total Annexin V^{+} cells and number of Annexin V^{+} immune cells (CD54^{+}) after 5 days of infection.
(**C**) Representative images of trichrome stain (**H**) or TUNEL (**I**) on skin biopsies of *S. aureus*-infected mice. Scale bars, 100 μm.
Each point represents a mouse and lines show median values. Data are represented as bar graphs with mean ± SEM. Results shown are pooled from at least two independent experiments. *p<0.05.

Inflammasome is necessary for *S. aureus* killing – After showing that the lack of *Mlkl* or *Casp1/4* contributes to poor outcome, marked by excessive inflammation during *S. aureus* skin infection, we wanted to tease out the exact roles of necroptosis and pyroptosis in bacterial clearance. We measured bacterial killing capacity of primary keratinocytes (HEKn), peritoneal exudate cells (PECs) and bone marrow-derived macrophages (BMDMs) when necroptosis is inhibited. *Ripk3*$^{-/-}$, *Mlkl*$^{-/-}$, *Casp1/4*$^{-/-}$ and WT PECs and BMDMs did not have any differences in taking up *S. aureus* (**Figures 3.9A and 3.9B**). 24 hours after infection, we recovered more *S. aureus* in *Casp1/4*$^{-/-}$ than in WT PECs and BMDMs (**Figures 3.9C and 3.9D**). *Ripk3*$^{-/-}$ and *Mlkl*$^{-/-}$ immune cells exhibited no defect in bacterial killing abilities (**Figures 3.9C and 3.9D**). The defect in *S. aureus* clearance by *Casp1/4*$^{-/-}$ BMDMs correlated with decreased production of IL-1β (**Figure 3.9E**). A similar impairment of *S. aureus* killing ability was observed in HEKn when caspases were inhibited (using ZVAD) but not when necroptosis was blocked (using NSA) (**Figure 3.9F**). These data suggest that the necrosome complex decreases damage during *S. aureus* infection by limiting inflammation, whereas the inflammasome components are essential for bacterial killing, potentially through their effects on phagosomal PH (103).

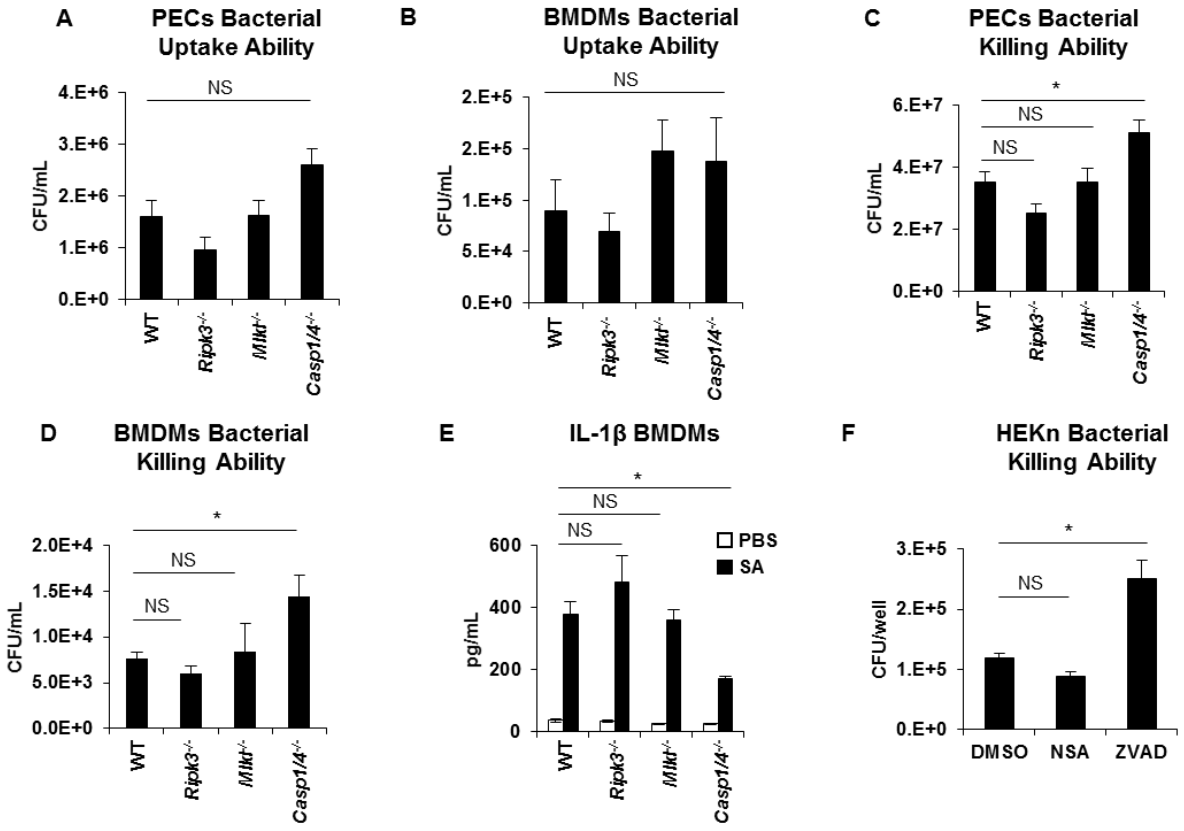

Figure 3.9. Caspase-1/4 but not the necrosome components are necessary for *S. aureus* killing
(**A and B**) *S. aureus* uptake by mouse peritoneal exudate cells (PECs) (**A**) and bone marrow-derived macrophages (BMDMs) (**B**) infected with *S. aureus* for 1 h.
(**C and D**) *S. aureus* killing by PECs (**C**) and BMDMs (**D**) infected with *S. aureus* for 24 h.
(**D**) *S. aureus* uptake by BMDMs from mice after 1 h infection.
(**E**) IL-1β released by BMDMs after 4 h stimulation with *S. aureus*.
(**F**) *S. aureus* killing by primary keratinocytes (HEKn cells) pretreated with 10 μM NSA or 50 μM ZVAD, infected with *S. aureus* for 2 h and treated with gentamicin for 4 h.
Each point represents a mouse and lines show median values. Data are represented as bar graphs with mean ± SEM. Results shown are pooled from at least two independent experiments. *p<0.05, **p<0.01.

Necroptosis contributes to improved outcome in *Staphylococcus aureus* sepsis

S. aureus is a major cause of sepsis, associated with higher morbidity and mortality than bacteremia caused by other pathogens (92). These infections are increasing in frequency as more patients undergo invasive procedures. *S. aureus s*ystemic infections are often accompanied by excessive inflammation and organ failure, which can be detrimental.

Since we observed previously that necroptosis contributed to better outcome by regulating excessive inflammation in skin *S. aureus* infection and not by participating directly in bacterial killing, we thought that a systemic model of *S. aureus* infection would further illuminate our understanding of the role of necroptosis in regulating inflammation particularly by immune cells. We hypothesized that necroptosis limits inflammation leading to a better outcome in *S. aureus* sepsis. To test this hypothesis, we infected mice retro-orbitally with 1 x 10^8 CFU/mouse of *S. aureus* and treated them with Nec-1s or DMSO. Nec-1s infected mice had more bacteria systemically 1 and 2 days after infection compared to DMSO controls (**Figure 3.10A)**.

To confirm the results that we obtained with the pharmacological inhibitor of necroptosis, we infected *Ripk3*$^{-/-}$, *Mlkl*$^{-/-}$, *Casp1/4*$^{-/-}$ and WT mice systemically with *S. aureus*. *Casp1/4*$^{-/-}$ mice and *Mlkl*$^{-/-}$ mice died at a faster rate compared to WT mice, even though *Casp1/4*$^{-/-}$ mice's phenotype was more severe (with median survival of 2 days) compared to *Mlkl*$^{-/-}$ (with median survival of 4 days) (**Figure 3.10B**). We did not observe any survival differences between *Ripk3*$^{-/-}$ and WT mice (**Figure 3.10B**). *Casp1/4*$^{-/-}$ did worse possibly because of the role of caspase-1/4 in killing bacteria, whereas *Mlkl*$^{-/-}$ possibly could not regulate inflammation. Together, these results show that *Mlkl*$^{-/-}$, like *Casp1/4*$^{-/-}$, is essential for controlling systemic *S. aureus* infection.

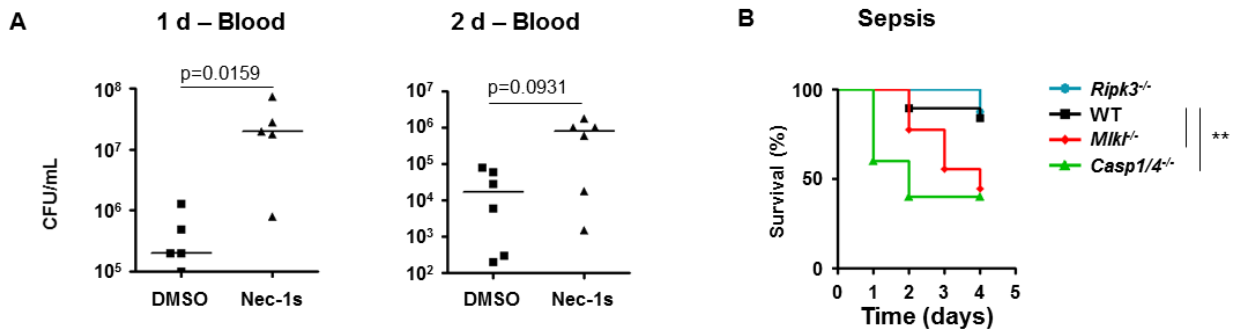

Figure 3.10. Caspase-1/4 and MLKL are essential in *S. aureus* sepsis
(**A**) CFU recovered from blood 1 or 2 days after infection of mice treated with Nec-1s and infected systemically with 1 x 10^8 CFU/mouse of *S. aureus* via retro-orbital route.
(**H**) Kaplan-Meier survival curves of WT (n=19), *Ripk3*$^{-/-}$ (n=8), *Mlkl*$^{-/-}$ (n=9) and *Casp1/4*$^{-/-}$ (n=5) mice after retro-orbital injection with 1 x 10^8 CFU/mouse of *S. aureus*.
Each point represents a mouse and lines show median values. Results shown are pooled from at least two independent experiments. ** p<0.01.

Discussion

In this chapter, we established that necroptosis regulates inflammation during *S. aureus* skin infection. Inhibition of necroptosis by pharmacological and genetic means led to worse outcome. *Mlkl*$^{-/-}$ or Nec-1s-treated mice had significantly larger lesion sizes and more CFU recovered from the infected tissues compared to control groups. A similar outcome was observed in *Casp1/4*$^{-/-}$ mice, which cannot undergo pyroptosis and have limited ability to process IL-1β. The poor outcome in *Casp1/4*$^{-/-}$ and *Mlkl*$^{-/-}$ mice occurred despite the abundance of immune cells including neutrophils, macrophages, and gamma-delta T cells. Unlike *Casp1/4*$^{-/-}$ immune cells, *Mlkl*$^{-/-}$ PECs and BMDMs had no defect in bacterial clearance showing that necroptosis-driven clearance is likely due to its ability to regulate inflammation.

Unlike *Mlkl*$^{-/-}$ mice, *Ripk3*$^{-/-}$ mice had improved outcome with better bacterial clearance and decreased inflammation after *S. aureus* skin infection. We attributed this difference in outcome of *Ripk3*$^{-/-}$ mice versus *Mlkl*$^{-/-}$ mice to the fact RIPK3 can regulate several inflammatory pathways independently of MLKL. *Ripk3*$^{-/-}$ mice had less production of inflammatory cytokines and displayed decreased apoptosis as marked by decreased expression of annexin V on their site of infection. These results are in line with previous findings showing that RIPK3 increases inflammation (independently of MLKL) by stimulating the NLRP3 inflammasome and IL-1β production (43, 73), in inducing NF-κB (96) and in activating apoptosis in multiple cell types

(98-102). Thus, unchecked inflammation can exacerbate the injury cause by *S. aureus* and that necroptosis helps limit this damage.

Adequate amount of inflammation tightly is necessary for bacterial clearance. In the early stages of infection, neutrophils have to be recruited briskly to the site of infection to clear the pathogens before they disseminate (26). Excessive inflammation, however, can be counterproductive – leading to enhanced tissue damage and impaired bacterial clearance (33). Thus, as described in the literature and as shown in this chapter, a balance between a quick immune response (to clear *S. aureus*) and excessive inflammation (that may be damaging) is essential. Necroptosis works in concert with inflammasome activation, which helps clear bacteria, to resolve subcutaneous and systemic *S. aureus* infection. Targeting the necroptosis pathway to curb excessive inflammation during infections is potentially an important therapeutic option.

Chapter 4: Conclusion

S. aureus is an important human pathogen that causes serious infections marked by cell death, inflammation, and tissue necrosis; and associated with significant morbidity and mortality. In this work, we defined for the first time the specific roles of RIPK1/RIPK3/MLKL-mediated necroptosis during the three common types of *S. aureus* infection – lung, skin and systemic infection. Our findings also added to the current literature on the contribution of apoptosis and pyroptosis during *S. aureus* infection. We showed that apoptosis was not a significant contributor to *S. aureus*-induced cell death. We showed that *S. aureus* activated pyroptosis, marked by the activation of caspase-1 and the release of IL-1β. Inhibition of caspase-1/4 impaired the bacterial killing capacity of both immune cells and keratinocytes. Mice lacking *Casp1/4* exhibited decreased bacterial clearance and increased lesion sizes during *S. aureus* skin infection and increased mortality during sepsis compared to their wild type controls.

The chief contribution of this work was to the understanding of the specific roles of necroptosis during the pathogenesis of *S. aureus* lung, skin and systemic infection. First, we showed through biochemical and genetic means that *S. aureus* induced necroptosis in multiple cell types, including immune and skin cells. Necroptosis in both human and murine cells was mediated by *S. aureus* through its pore-forming toxins. These results were recently confirmed by a separate research group, which documented that bacterial pore forming toxins induce necroptosis by damaging host mitochondria, depleting ATP and releasing reactive oxygen

species (104). Using both pharmacological inhibitors and knockout mice, we then teased out the roles of necroptosis in *S. aureus* pneumonia, skin infection, and sepsis.

The first section showed that *S. aureus* targets and kills macrophages through necroptosis, eliminating a cell population that is critical for bacterial clearance and inflammation resolution in pneumonia. Pharmacological and genetic inhibition of necroptosis led to increased bacterial clearance and decreased expression of inflammatory cytokines. This phenotype was mediated by pulmonary macrophages in *Ripk3*$^{-/-}$ mice, which were not only resistant to death, but also upregulated anti-inflammatory markers. The improved macrophage survival in *Ripk3*$^{-/-}$ mice corresponded to an improved lung architecture and decreased inflammation. These results need to be confirmed using *Mlkl*$^{-/-}$ mice or kinase-dead knockin *Rip3* (KDKI RIP3) mice to ensure that the observations that we made were not due to the scaffolding effects of RIPK3, which include activation of the inflammasome, induction of apoptosis, and activation of NF-κB (105).

In the second section, we demonstrated the complex roles of necroptosis in dampening inflammatory responses to *S. aureus* skin and systemic infections. Using a combination of knockout mice and biochemical inhibitors, we showed that mice that are unable to activate necroptosis have greater tissue damage, greater proinflammatory cytokine production and increased immune cell recruitment but significantly higher bacterial loads compared to control mice. Unlike *Mlkl*$^{-/-}$ or necrostatin-1s-treated mice, *Ripk3*$^{-/-}$ mice cleared *S. aureus* better and had decreased inflammation when compared to WT mice. This seemed inconsistent at first, since RIPK3 is a key mediator of necroptosis. However, we showed that the direct effects of RIPK3 in modulating inflammation – by directly activating IL-1β and apoptosis – played a more important role than necroptosis in controlling outcome to *S. aureus* skin infection (**Figure 4.1**).

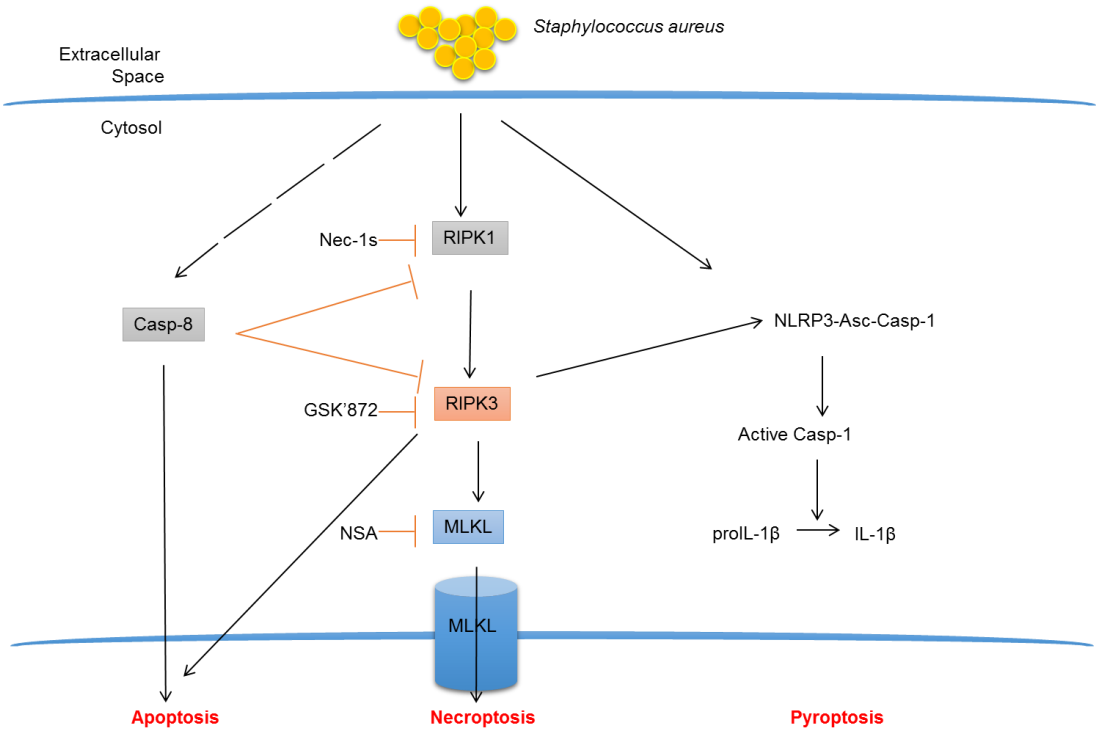

Figure 4.1. Pathways of *S. aureus*-induced cell death
S. aureus can activate apoptosis, necroptosis and pyroptosis through its virulence factors. *S. aureus* toxins can induce both necroptosis and pyroptosis. RIPK1/RIPK3/MLKL proteins mediate necroptosis. All these pathways are interlinked and they potentially occur concurrently in different infected cells.

Mlkl$^{-/-}$ and *Casp1/4*$^{-/-}$ mice had significantly greater mortality from staphylococcal sepsis than wild type and *Ripk3*$^{-/-}$ mice. *Casp1/4*$^{-/-}$ mice phenotype could possibly be due to the role of caspase-1/4 in mediating clearance of intracellular *S. aureus*. Inhibition of necroptosis led to defective bacterial clearance and increased mortality in a model of *S. aureus* sepsis, even though immune cells that were unable to undergo necroptosis had no bacterial killing defect. This phenotype could possibly be explained by the role of necroptosis in regulating inflammation, which in turn leads to better bacterial clearance and increased survival. Our observations are consistent with recent publications that show the complex role of necroptosis – particularly the role of necroptosis in limiting pathological inflammation by eliminating the source of inflammatory stimuli (77).

The contributions that we made on the roles of necroptosis seem to be inconsistent, with necroptosis being detrimental in *S. aureus* pneumonia, while being beneficial in skin and systemic infection. This disparity could potentially be because necroptosis-mediated inflammation in pneumonia leads to lung damage. Necroptosis in the skin and in the periphery, however, decreases excessive inflammation leading overall improved outcome.

The observed differences in the role of necroptosis between outcome in skin and lung *S. aureus* infection is similar to the dichotomy observed in the role of inflammasome in different tissues. *Nlrp3*$^{-/-}$ and *Casp1/4*$^{-/-}$ mice, as well as mice that cannot produce or respond to IL-1β, have less severe pneumonia compared to WT mice (50, 106). On the other hand, *Casp1/4*$^{-/-}$ and *Il1b*$^{-/-}$ mice have more severe *S. aureus* skin and systemic infection than WT mice (26, 107). These findings provide new insights into the opposing roles of different inflammatory pathway during *S. aureus* infection and suggest paying attention to the site of infection in designing immunomodulatory therapy to target these pathways.

It appears that pyroptosis, apoptosis and necroptosis are intertwined. Our finding that *Ripk3*$^{-/-}$ mice had decreased apoptosis and inflammasome activation during *S. aureus* skin infection adds to the growing body of literature showing the multiple roles of the kinase and scaffolding functions of RIPK3 (105). The connection between MLKL and the caspase-1 remains unresolved however. Inhibitors of MLKL blocked caspase-1 and IL-1β production in vitro. However, this finding was in conflict with our observations in vivo, where we showed that *Mlkl*$^{-/-}$ mice exhibited upregulated caspase-1 activity and increased IL-1β release after *S. aureus* skin infection. Therefore, exactly how *S. aureus* toxins activate the necrosome components and how the necrosome complex regulates the inflammasome remain important questions for future research. However, even though these cell death pathways may be interlinked, they are not

necessarily redundant. Specifically, caspase-1/4, and not any of the necrosome components (RIPK3 and MLKL), is required for killing of intracellular *S. aureus* killing by host cells.

These studies have expanded the current understanding on the role of necroptosis during *S. aureus* infection and have proffered some interesting applications. Since necroptosis has tissue specific roles, understanding the site of infection is essential for developing and administering beneficial necroptosis-modulating drugs. For instance, one could develop specific molecules to target and prevent *S. aureus*-induced necroptosis in pneumonia or compounds to activate necroptosis in *S. aureus* systemic and skin infection. Caution must be taken when developing drug targets for necroptosis and cell death pathways in general though. One big concern with blocking necroptosis is that it may allow development and propagation of tumorigenic cells. Bearing in mind the complex roles of necroptosis, targeting this pathway holds great therapeutic potential in *S. aureus* infection.

Finally, we have addressed the complex roles of necroptosis during *S. aureus* lung, skin and systemic infection. We showed that whereas necroptosis induced lung damage and contributed to poor outcome during *S. aureus* pneumonia, it dampened inflammation and improved outcome during *S. aureus* skin and systemic infection. Future projects may work on fully understanding how *S. aureus* products activate necroptosis and the role of necroptosis in infections using humanized mice. Ultimately, developing "druggable" targets and making targeted drugs for this pathway offer promising alternatives or complementary therapy to antibiotics and could improve healthcare outcomes and reduce morbidity, mortality and huge costs associated with *S aureus* infections.

Chapter 5: Materials and Methods

Bacteria. These are the *Staphylococcus aureus* strains used in this research: (a) Wild type USA300 LAC, α-hemolysin (*hla*), *pha*H35L and the complemented p*hla* mutants (obtained from Juliane Bubeck-Wardenburg, University of Chicago, IL). (b) Wild type USA300 LAC and Panton-Valentine leukocidin (*lukS-F/PV pvl; lukSF*) mutant (obtained from Frank DeLeo, National Institute of Allergy and Infectious Diseases, Rocky Mountain Laboratories, MT) and complemented mutant (Δ*pvl/pvl*$^{+}$; provided by Binh Diep, UCSF). (c) α, β and γ phenol-soluble modulins (*PSMα/β/hld*) triple mutant (obtained from Michael Otto, National Institute of Allergy and Infectious Diseases, MD). (d) *lukAB* (obtained from Victor Torres, NYU Langone Medical Center, NY) and (e) *agr* null strain.

WT *S. aureus* and mutant strains were grown overnight in Luria Broth (LB) at 37°C to a stationary phase. *The strains were* diluted to 1:100 in broth and grown to OD 1.000. *S. aureus* was spun down at 10,000 x *g* and suspended in phosphate buffered saline (PBS) to achieve the required density. To heat-kill the bacteria, we incubated the cultures at 65°C for 1.5 h. We obtained *S. aureus* supernatant by growing USA300 LAC and mutant strains overnight to stationary phase in LB and spinning down the bacteria at 10,000 *g* for 5 minutes. Supernatant from the cells were purified by passing it through a 20-μm pore size sterile filter (Millipore).

Mice. C57BL/6J (Jackson Laboratory), *Casp1/4*$^{-/-}$ (B6N.129S2-*Casp1*^{tm1Flv}/J, Jackson Laboratory) (108), *Ripk3*$^{-/-}$ (Vishva Dixit, Genentech) (109) and *Mlkl*$^{-/-}$ (John Silke, Walter and Eliza Hall Institute of Medical Research via Douglas R. Greene, St. Jude Children's Research Hospital) (110) were used in this research.

Infection models:

Mouse model of pneumonia. Six- to seven-week-old sex-matched wild type and *Ripk3*$^{-/-}$ mice were anesthetized with 100 mg/kg ketamine (Henry Schein) and 5 mg/kg xylazine (Henry Schein). Mice were inoculated intranasally with 10^7 CFU/mouse of WT *S. aureus* or *agr* null mutant in 50 µl of PBS. 18 to 20 hours after infection, mice were sacrificed, bronchoalveolar lavage fluid (BAL) obtained and lungs harvested. Recovered bacteria (CFU) were enumerated by serial dilutions on Luria Bertani (LB) agar plates and CHROMagar (Becton Dickinson) *S. aureus* plates and incubating the plates overnight at 37°C as previously described (106, 111).

Mouse cells were obtained and stained as described below and BAL protein content measured by Bradford assay (111). Lungs were fixed in 4% paraformaldehyde overnight and maintained in 70% ethanol before paraffin sectioning. Lung histology was done by the Columbia University Molecular Pathology Shared Resource (MPSR) core as previously described (36). Images were taken on an Olympus Cx41 microscope using a Canon Powershot S5IS camera.

To inhibit necroptosis by pharmacological means, C57BL/6J mice were treated with 300 µg RIPK1 Inhibitor II, 7-Cl-O-Nec-1 (Nec-1s, Calbiochem) or DMSO 18 hours before and at the time of infection. Treated mice were infected with 10^7 CFU/mouse *S. aureus* and sacrificed 4 hours after infection. We counted bacteria and stained cells as described above.

Mouse model of skin infection. Mice were anesthetized as described above, shaved on the back and inoculated subcutaneously with 2 x 10^6 CFU/mouse of *S. aureus* in 100 µl of PBS using $26G^{5/8}$ sterile needle (Becton Dickinson &Co.). Lesions sizes (mm^2) were monitored daily and mice were sacrificed 1 or 5 days after infection. For pharmacological inhibitor experiments, we

treated mice with 10mg/kg Nec-1s or DMSO control 24 hours before infection, during infection and daily for 4 days post-infection. Mice were sacrificed 5 days after infection and analysis done as described below.

Two three-millimeter punch biopsy (Premier Uni-Punch) skin specimens were obtained from the lesions of infected mice. The first biopsy tissue was fixed in 4% paraformaldehyde for 1 day and stored in 70% ethanol. The Columbia University Medical Center Histology Core performed Trichrome and TUNEL staining on the paraffin sections. Images were taken on Zeiss Axiocam MRc 5 microscope (Zeiss).

The second biopsy tissue was homogenized using a cell strainer to obtain a single cell suspension in PBS. We enumerated recovered bacteria (colony forming units, CFU) from the homogenate by serial dilutions on Luria Bertani (LB) agar plates at 37°C. We spun down host cells and used homogenate for ELISA and stained cells for FACS as described below.

We performed skin grafts on NOD-scid *IL2Rγ*null (NSG, Jackson Laboratory) (112) mice as previously described (8). After successful engraftment, we infected skin grafts for 3 days, excised the grafts, and fixed them for histopathological analysis (8).

Mouse model of sepsis. 1×10^8 CFU/mouse of *S. aureus* in 100 μl PBS was delivered intravenously through the retro-orbital injection route to six- to eight-week-old anesthetized mice. We monitored survival every day. For pharmacological inhibitor experiments, we treated mice with 10mg/kg Nec-1s or v/v DMSO control 24 hours before infection, during infection and 4 hours (for 24 h experiments) or 24 hours (for 48 hour experiments) post infection. We sacrificed mice 24 hours or 48 hours after infection and enumerated bacteria and analyzed cytokines in their blood.

Lung macrophage depletion. Lung macrophages in mice were depleted by intranasally administering 75 µl clodronate-loaded liposomes or PBS-loaded liposomes for control group (ClodronateLiposomes.org, Netherlands). Mice were infected with *S. aureus* and sacrificed 4 and 24 hours post-infection. Macrophage depletion in lung and BAL of the mice was confirmed by flow cytometry analysis.

Flow Cytometry:

Pneumonia. Bronchoalveolar lavage fluids (BAL) were obtained by instilling 3 × 1 ml of PBS into the trachea of euthanized mice. Lungs were harvested and passed through a cell strainer (Fisher Scientific) with 400 µl PBS to obtain single cell homogenate. BAL was centrifuged at 200x *g* for 10 minutes and lung homogenate at 400x *g* for 6 minutes. Red blood cells were lysed and the remaining cells washed with FACS buffer (10% fetal bovine serum and 0.1% sodium azide in PBS). Cells were suspended in 100 µl FACS buffer and stained for 30 minutes at 4°C in presence of counting beads (Bang Laboratories, Inc.).

Murine cells were stained with a combinations of fluorescein isothiocyanate-labelled (FITC) anti-Ly-6G (Gr-1; RB6-8C5; Biolegend), peridinin chlorophyll (PerCP)-Cy5.5-labelled anti-CD11c (N418; Biolegend), allophycocyanin (APC)-labelled anti-MHC II (I-A/I-E; Biolegend), phycoerythrin(PE)-labelled anti-NK 1.1 (NKR-P1C, Ly-55; Biolegend), FITC-CD200R (Biolegend), PE-CD86 (eBiosciences), FITC-CD54 (Biolegend), PE-CD206 (Biolegend) and propidium iodide (PI, Life Technologies). Neutrophils ($Ly6G^{+}/MHCII^{-}$), macrophages ($CD11C^{+}/MHCII^{low\text{-}mid}$) and dendritic cells ($CD11c^{+}/MHCII^{high}$) were analyzed using WinMIDI Version 2.9 and FlowJo vX.0.7 (FlowJo, LLC).

Skin infection. Homogenized skin cells were suspended in 100 µl FACS buffer and stained for 30 minutes at 4°C combinations of phycoerythrin (PE) anti-CD54 (YN1/1.7.4, Biolegend), fluorescein isothiocyanate-labelled (FITC) anti-Ly-6G (Gr-1; RB6-8C5; Biolegend), peridinin chlorophyll (PerCP)-Cy5.5-labelled anti-CD11c (N418; Biolegend), allophycocyanin (APC)-labelled anti-MHC II (I-A/I-E; Biolegend) and APC-labelled anti-TCR γδ T cells (γδ T cells) were used. Neutrophils (PMNs; $Ly6G^{+}/MHCII^{-}$), macrophages (Macs; $CD11C^{+}/MHCII^{low\text{-}mid}$) and γδ T cells were analyzed using FlowJo_V10 (FlowJo, LLC).

Cytokine analysis. Cytokine levels from BAL fluid were quantified using human IL-8 (BD Pharminogen), TNF (Biolegend), IL-6 (Biolegend) and IL-1β (R&D systems) and mouse CXCL1/KC (R&D Systems), TNF (Biolegend), IL-6 (Biolegend) and IL-1β (Biolegend), IL-1α (Biolegend) were quantified by ELISA according to manufacturer's instructions. Cytokine levels from THP-1 supernatants were quantified using human IL-1β (R&D Systems) ELISA.

Multiplex ELISA on skin homogenate was performed by Eve Technologies Corporation (Calgary, Canada) and analyzed using Microsoft Excel to determine mouse cytokine levels.

Cell Culture:

Immune cells.

THP-1 human monocytic cells (THP-1 cells, ATCC) were grown in RPMI1640 medium (CellGro) with 10% heat inactivated fetal bovine serum (FBS, Mediatech) and 1% penicillin/streptomycin solution (Life Technologies) at 37°C and 5% CO_2 in a humidified

environment. THP-1 cells were activated with 1 μM PMA (Sigma-Aldrich) for 24 hours and weaned to RPMI1640 medium with 10% FBS but without antibiotics for 24 hours.

Human primary macrophages were isolated from 40 ml of heparinized blood from consenting, healthy anonymous volunteers. Human macrophages were grown for 7 days in RPMI 1640 medium supplemented with 10% FBS, penicillin-streptomycin and 60 ng/mL M-CSF (PeproTech).

Alveolar macrophages were isolated from de-identified human bronchoalveolar lavage (BAL) fluid that would have otherwise been discarded (Columbia University IRB-AAAI5300). BAL was passed through a sterile cell strainer (Fisher Scientific) to remove mucus and treated with RBC lysis buffer. Cells were washed in PBS and suspended in 1640 RPMI medium supplemented with 10% FBS and maintained at 37°C and 5% CO_2 in a humidified environment.

Skin cells.

HaCaT and HEKn cells were grown to confluence in DMEM medium (Gibco) with 10% FBS and 1% penicillin and streptomycin at 37°C and 5% CO^2 in a humidified environment. Cells were maintained in DMEM with 10% FBS but no antibiotics for 24 hours before infection.

Necroptosis inhibition in vitro.

THP-1 cells and human primary macrophages were pretreated 1 hour before *S. aureus* infection with 200 μM necrostatin-1 stable (Nec-1s, Enzo Life Technologies), 10 μM necrosulfonamide (NSA, Calbiochem), DMSO control (v/v), 10 mM N-acetyl-L-cysteine (NAC, Sigma), 1 mM or 2.5 mM 100,000 MW dextran (Sigma) or 60 mM KCl (Sigma). THP-1 cells and human primary macrophages were stimulated with *S. aureus* and their isotype controls at MOI of 10 for 2 hours.

Alveolar macrophages were pretreated with 10 μM necrosulfonamide (NSA) or DMSO (v/v) for 1 hour. Alveolar macrophages were stimulated with *S. aureus* MOI of 100 for 2 hours. HaCaT and HEKn cells were pretreated 1 hour prior to infection with increasing concentration (0 - 200 μM) of necrostatin-1 stable (Nec-1s, Enzo Life Technologies), 10 μM necrosulfonamide (NSA, Calbiochem), 10 μM GSK'872 (Calbiochem), DMSO control (v/v). HaCaT and HEKn cells were stimulated with *S. aureus* MOI of 10 for 4 hours. Cytotoxicity was measured by lactate dehydrogenase (LDH) assay (Roche) as described below.

***S. aureus* uptake and killing assays.**

Peritoneal exudate cells (PECs). Mice were injected intraperitoneally with 10^7 CFU of heat-killed *S. aureus* 48 h and 24 h prior to peritoneal exudate cells (PECs). PECs were obtained by washing peritoneal cavity of the mice with 8 ml of PBS (113). Red blood cells were lysed and cells kept in ice. *S. aureus* MOI of 10 was coated for 30 mins with 50% normal mouse serum (NMS, Innovative Research) in RPMI 1640 medium (Gibco), washed in PBS and suspended in RPMI 1640 medium. Microtiter plates were coated with 20% NMS in RPMI for 60 min at 37°C, washed to remove residual serum and the plates chilled in ice. PECs were infected with opsonized *S. aureus* MOI of 1 in coated plates for 1 h and 24 h. PECs were lysed with 0.1% saponin and bacteria enumerated by serial dilutions on Luria Bertani (LB) agar plates at 37°C.

Gentamicin protection assays. HaCaT cells were stimulated for 2 hours and BMDMs for 20 minutes with *S. aureus* MOI of 100. Cells were washed and treated with 500 μg/ml of gentamicin for 1 h and 24 h. Cells were washed in PBS, lysed with 0.1% saponin and bacteria enumerated by serial dilution on agar plates.

siRNA knockdown. HaCaT and THP-1 cells grown in 24-well plates to confluence. Cells were transfected with 100 nM RIPK3, non-targeting siRNA (human ONTARGETplus siRNA pools of four oligos; Dharmacon) or MLKL (human MLKL siRNA pools of three targets, Santa Cruz Biotechnology) using Lipofectamine RNAiMAX (Life Technologies). After 3 days, cells were infected with *S. aureus* (MOI of 10) or PBS for 2 h (THP-1s) or 4 h (HaCaT). Knockdown was confirmed by immunoblotting of cell lysates and level of cytotoxicity determined in the cell supernatants as described below.

Cytotoxicity assays. Level of cytotoxicity in cells was measured using LDH kit (Roche) as per manufacturer's instructions or using 2µg/mL propidium iodide (Life Technologies) staining. Maximal death was achieved freezing and thawing cells multiple types to release maximal LDH or to achieve 100% PI staining. Cell culture medium alone used as a baseline. Fluorescence intensity was read on a Tecan Microplate Reader (Tecan Group). LDH assay was used in most assays except in the instance where the reagents (for example, NAC) interfered with the LDH reagents. Necrotic cells were imaged using a Zeiss Observer.Z1 microscope with AxioVision software (version 4.6.2.0; Zeiss).

Immunoblotting. HaCaT and THP-1 cells were lysed using RIPA buffer (20 mM Tris-Cl, 50 mM NaCl, 0.1% SDS, 1% Triton X-100, 10% glycerol, 2 mM EDTA, 0.5% sodium deoxycholate) containing 1X Halt protease and phosphatase inhibitor cocktail (Thermo Scientific). Proteins were separated on Bolt 4%–12% Bis-Tris Plus gels (Life Technologies), transferred using iBlot Dry Blotting System (Life Technologies), and blocked with 5% milk in

TBST (Tris-buffered saline plus Tween) (50 mM Tris, pH 7.5, 150 mM NaCl, 0.05% Tween) or 5% bovine serum albumin (BSA) in TBST for 1 hour at room temperature.

Secreted *S. aureus* toxin expression was determined in cultures grown overnight in LB to stationary phase and supernatant filtered. *pvl* and *pvl/pvl+* complemented mutant and their WT controls were grown to exponential phase in CCY media at 37°C and filter sterilized (114). Supernatants were ran on a gel and immunoblotted as described below.

Immuno-detection was performed using anti-MLKL (phospho S358) (Abcam), anti-MLKL (Abcam), RIPK3 (Santa Cruz Biotechnology Inc.), anti-caspase-1 (Santa Cruz Biotechnology Inc.), anti-Caspase-1 (p20) (Casper-1, Adipogen), β-actin (Sigma-Aldrich), Hla (a gift from Juliane Bubeck-Wardenburg) and LukF (IBT Bioservices) antibodies followed by secondary antibodies conjugated to horseradish peroxidase (Santa Cruz Biotechnology Inc.). Equal loading was confirmed by staining the gels with 0.1% Ponceau S (w/v) in 5% acetic acid (Sigma). Densitometry was determined by ImageJ (NIH).

Immunohistochemistry. 5 mm sections from paraffin blocks were mounted on glass slides. The sections were deparaffinalized in xylene alternative (Safe Clear, Protocol) and ethanol. Antigens were exposed using Tris-EDTA buffer (10mM Tris Base, 1mM EDTA Solution, 0.05% Tween 20, pH 9.0) at 70^{o}C overnight. Sections were permeabilized with Tween 20 0.5% for 10 minutes, hydrated with 0.3% H2O2 for 10 minutes, and stained with anti-MLKL (phospho S358, Abcam), anti-MLKL (Abcam), anti-DAPI (Santa Cruz Biotechnology) and anti-pan cytokeratin (Santa Cruz Biotechnology) followed by peroxidase staining using the Immunocruz ABC Staining kit (Santa Cruz Biotechnology Inc.). Control sections were stained with secondary antibodies only. Confocal microscopy was used to image to sections.

RNA analysis. RNA was isolated and analyzed as described previously (115). Sequences for mouse *Tnf, KC, Il6* and *actin* primers have been published elsewhere (115). Here is a list of primers used:

Human *actin*: 5'-GTGGGGCGCCCCAGGCACCA-3'; and 5'-CGGTTGGCCTTGGGGTTCAGGGGGG-3';

RIPK3 -- 5'-CTCTCTGCGAAAGGACCAAG-3' and 5'- CATCGTAGCCCCACTTCCTA-3';

MLKL -- 5'-CTCTTTCCCCACCATTTGAA-3' and 5'-TCATTCTCCAGCATGCTCAC-3'

IL15 -- 5'-GAAGTATTTCCATCCAGTGC-3', 5'-CTTCATTGCTGTTACTTTGC-3';

IL6 -- 5'-AAGAGTAACATGTGTGAAAGC-3', 5'-CTACTCTCAAATCTGTTCTGG-3';

CSF2 -- 5'-GAACCTGAGTAGAGACACTGC-3', 5'-AGGTGATAATCTGGGTTGC-3';

ACTB -- 5'-TCCTCCCTGGAGAAGAGCTAC-3', 5'-TAAAGCCATGCCAATCTCATC-3';

TNF -- 5'-GAGTGACAAGCCTGTAGCCCA-3', 5'-GAATGATAAAGTAGACCTGCC-3';

CCL20 -- 5'-GTGCTGTACCAAGAGTTTGC-3', 5'-CAAGTCTGTTTTGGATTTGC-3';

IL8 -- 5'-GTGCAGTTTTGCCAAGGAGT-3', 5'-CTCTGCACCCAGTTTTCCTT-3';

CXCL11 -- 5'-AGTCATAGCCACACTCAAGAATGG-3', 5'-GATGCAGGATTGAGGCAAGC-3';

CXCL10 -- 5'-TTCCTGCAAGCCAATTTTGT-3', 5'-TTCTTGATGGCCTTCGATTC-3';

IL23 -- 5'-GAGGGAGATGAAGAGACTAC-3', 5'-TTTAGGGACTCAGGGTTGCT-3';

CCL2 -- 5'-GCCTGAGTAACTGTGAAAGC-3', 5'-GAAAACTGGACATTGTTTGC-3';

IL1b -- 5'-ATGATGGCTTATTACAGTGGCAA-3', 5'-GTCGGAGATTCGTAGCTGGA-3';

IL17 -- 5'-GCTGTCGATATTGGGGCTTG-3', 5'-GGAAACGCGCTGGTTTTCAT-3';

CSF3 -- 5'-GAGCTGAGAACTACCGAACGG-3', 5'-GGCCTGAGGGTCTCCAAGA-3';

IL10 -- 5’-ATGAGCATTCAGACTGGGTAAAC-3’, 5’-TTTTAGGGGCTAAGAAACGCAT-3’;

CCL7 -- 5’-AGCTCTCCAGCCTCTGCTTA-3’, 5’-CTGCTTTCAGCCCCCAG-3’;

IL27 -- 5’-GCTGACTCTGAACTCCCTCC-3’, 5’-AGACGGCAGGCGACCTT-3’;

CSF1 -- 5’-TGGCGAGCAGGAGTATCAC-3’, 5’-AGGTCTCCATCTGACTGTCAAT-3’ and

TNFSF10 -- 5’- CTCTCTTCGTCATTGGGGTC-3’ and 5’-TGCAGTCTCTCTGTGTGGCT-3’.

All RNA expressions were normalized to actin.

Ethics statement. Animal work in this study was carried out in strict accordance with the recommendations in the Guide for the Care and Use of Laboratory Animals of the National Institutes of Health, the Animal Welfare Act and the U.S. federal law. The Institutional Animal Care and Use Committee (IACUC) of Columbia University approved the protocol (AC-AAAG9307, AC-AAAH2350 and AC-AAAG7408). Alveolar macrophages were isolated from de-identified human bronchoalveolar lavage fluid (Columbia University IRB-AAAI5300) that would have otherwise been discarded. All subjects enrolled provided voluntary informed written consent and signed a copy of the appropriate and stamped consent documents. Copies of the consent documents were given to the subjects for their record. Human primary macrophages were isolated from 40 ml of heparinized blood from consenting, healthy anonymous volunteers with informed oral consent (Columbia University IRB-AAAC5450). Columbia University Institutional Review Board approved a waiver for documentation of consent for blood collection because blood draws involve minimal risk.

Statistical Analysis. Samples with normal distribution were analyzed by two-tailed Student's *t* test. Data with multiple comparisons were analyzed using one-way ANOVA followed by Bonferroni corrections to correct for multiple comparisons. Mouse cytokines, bacterial counts, and immune cell numbers and other samples with non-normal distributions were analyzed using the nonparametric Mann-Whitney test. Outliers were determined by Grubb's test (GraphPad Software, Inc.) and removed. Differences in groups were considered significant if $p < 0.05$. Statistical analyses were performed using GraphPad Prism Version 4.00 (GraphPad Software, Inc.).

References

1. Otto M (2010) Basis of virulence in community-associated methicillin-resistant Staphylococcus aureus. *Annu Rev Microbiol* 64:143-162.
2. Klein E, Smith DL, & Laxminarayan R (2007) Hospitalizations and deaths caused by methicillin-resistant Staphylococcus aureus, United States, 1999-2005. *Emerg Infect Dis* 13(12):1840-1846.
3. Kollef MH*, et al.* (2005) Epidemiology and outcomes of health-care-associated pneumonia: results from a large US database of culture-positive pneumonia. *Chest* 128(6):3854-3862.
4. Lowy FD (1998) Staphylococcus aureus infections. *N Engl J Med* 339(8):520-532.
5. Maltezou HC & Giamarellou H (2006) Community-acquired methicillin-resistant Staphylococcus aureus infections. *Int J Antimicrob Agents* 27(2):87-96.
6. Otto M (2014) Staphylococcus aureus toxins. *Curr Opin Microbiol* 17:32-37.
7. DuMont AL & Torres VJ (2014) Cell targeting by the Staphylococcus aureus pore-forming toxins: it's not just about lipids. *Trends Microbiol* 22(1):21-27.
8. Soong G*, et al.* (2015) Methicillin-resistant Staphylococcus aureus adaptation to human keratinocytes. *MBio* 6(2).
9. Berube BJ & Bubeck Wardenburg J (2013) Staphylococcus aureus alpha-toxin: nearly a century of intrigue. *Toxins (Basel)* 5(6):1140-1166.
10. Song L*, et al.* (1996) Structure of staphylococcal alpha-hemolysin, a heptameric transmembrane pore. *Science* 274(5294):1859-1866.
11. Bubeck Wardenburg J & Schneewind O (2008) Vaccine protection against Staphylococcus aureus pneumonia. *J Exp Med* 205(2):287-294.
12. Craven RR*, et al.* (2009) Staphylococcus aureus alpha-hemolysin activates the NLRP3-inflammasome in human and mouse monocytic cells. *PLoS One* 4(10):e7446.
13. Kitur K*, et al.* (2015) Toxin-induced necroptosis is a major mechanism of Staphylococcus aureus lung damage. *PLoS Pathog* 11(4):e1004820.
14. Inoshima I*, et al.* (2011) A Staphylococcus aureus pore-forming toxin subverts the activity of ADAM10 to cause lethal infection in mice. *Nat Med* 17(10):1310-1314.
15. Spaan AN*, et al.* (2013) The staphylococcal toxin Panton-Valentine Leukocidin targets human C5a receptors. *Cell Host Microbe* 13(5):584-594.
16. DuMont AL*, et al.* (2013) Staphylococcus aureus LukAB cytotoxin kills human neutrophils by targeting the CD11b subunit of the integrin Mac-1. *Proc Natl Acad Sci U S A* 110(26):10794-10799.
17. Spaan AN*, et al.* (2014) The staphylococcal toxins gamma-haemolysin AB and CB differentially target phagocytes by employing specific chemokine receptors. *Nat Commun* 5:5438.
18. Fowler VG*, et al.* (2013) Effect of an investigational vaccine for preventing *Staphylococcus aureus* infections after cardiothoracic surgery: a randomized trial. *JAMA* 309(13):1368-1378.
19. Mestas J & Hughes CC (2004) Of mice and not men: differences between mouse and human immunology. *J Immunol* 172(5):2731-2738.

20. Takao K & Miyakawa T (2015) Genomic responses in mouse models greatly mimic human inflammatory diseases. *Proc Natl Acad Sci U S A* 112(4):1167-1172.
21. Shultz LD, Brehm MA, Garcia-Martinez JV, & Greiner DL (2012) Humanized mice for immune system investigation: progress, promise and challenges. *Nat Rev Immunol* 12(11):786-798.
22. Leung C*, et al.* (2013) Infectious diseases in humanized mice. *Eur J Immunol* 43(9):2246-2254.
23. Libby SJ*, et al.* (2010) Humanized nonobese diabetic-scid IL2rgammanull mice are susceptible to lethal Salmonella Typhi infection. *Proc Natl Acad Sci U S A* 107(35):15589-15594.
24. Tseng CW*, et al.* (2015) Increased Susceptibility of Humanized NSG Mice to Panton-Valentine Leukocidin and Staphylococcus aureus Skin Infection. *PLoS Pathog* 11(11):e1005292.
25. Knop J*, et al.* (2015) Staphylococcus aureus Infection in Humanized Mice: A New Model to Study Pathogenicity Associated With Human Immune Response. *J Infect Dis* 212(3):435-444.
26. Miller LS & Cho JS (2011) Immunity against Staphylococcus aureus cutaneous infections. *Nat Rev Immunol* 11(8):505-518.
27. Nestle FO, Di Meglio P, Qin JZ, & Nickoloff BJ (2009) Skin immune sentinels in health and disease. *Nat Rev Immunol* 9(10):679-691.
28. Choi SM*, et al.* (2013) Innate Stat3-mediated induction of the antimicrobial protein Reg3gamma is required for host defense against MRSA pneumonia. *J Exp Med* 210(3):551-561.
29. Urban CF*, et al.* (2009) Neutrophil extracellular traps contain calprotectin, a cytosolic protein complex involved in host defense against Candida albicans. *PLoS Pathog* 5(10):e1000639.
30. Thammavongsa V, Missiakas DM, & Schneewind O (2013) Staphylococcus aureus degrades neutrophil extracellular traps to promote immune cell death. *Science* 342(6160):863-866.
31. Heyworth PG, Cross AR, & Curnutte JT (2003) Chronic granulomatous disease. *Curr Opin Immunol* 15(5):578-584.
32. Kolaczkowska E & Kubes P (2013) Neutrophil recruitment and function in health and inflammation. *Nat Rev Immunol* 13(3):159-175.
33. Muller S*, et al.* (2015) Poorly Cross-Linked Peptidoglycan in MRSA Due to mecA Induction Activates the Inflammasome and Exacerbates Immunopathology. *Cell Host Microbe* 18(5):604-612.
34. McLoughlin RM*, et al.* (2006) CD4+ T cells and CXC chemokines modulate the pathogenesis of Staphylococcus aureus wound infections. *Proc Natl Acad Sci U S A* 103(27):10408-10413.
35. Martin CJ, Peters KN, & Behar SM (2014) Macrophages clean up: efferocytosis and microbial control. *Curr Opin Microbiol* 17:17-23.

36. Martin FJ, Parker D, Harfenist BS, Soong G, & Prince A (2011) Participation of CD11c(+) leukocytes in methicillin-resistant Staphylococcus aureus clearance from the lung. *Infect Immun* 79(5):1898-1904.
37. Abtin A*, et al.* (2014) Perivascular macrophages mediate neutrophil recruitment during bacterial skin infection. *Nat Immunol* 15(1):45-53.
38. Gordon S (2003) Alternative activation of macrophages. *Nat Rev Immunol* 3(1):23-35.
39. Hussell T & Bell TJ (2014) Alveolar macrophages: plasticity in a tissue-specific context. *Nat Rev Immunol* 14(2):81-93.
40. Hao NB*, et al.* (2012) Macrophages in tumor microenvironments and the progression of tumors. *Clin Dev Immunol* 2012:948098.
41. Ashkenazi A & Salvesen G (2014) Regulated cell death: signaling and mechanisms. *Annu Rev Cell Dev Biol* 30:337-356.
42. Fink SL & Cookson BT (2005) Apoptosis, pyroptosis, and necrosis: mechanistic description of dead and dying eukaryotic cells. *Infect Immun* 73(4):1907-1916.
43. Pasparakis M & Vandenabeele P (2015) Necroptosis and its role in inflammation. *Nature* 517(7534):311-320.
44. Frisch SM & Francis H (1994) Disruption of epithelial cell-matrix interactions induces apoptosis. *J Cell Biol* 124(4):619-626.
45. Paoli P, Giannoni E, & Chiarugi P (2013) Anoikis molecular pathways and its role in cancer progression. *Biochim Biophys Acta* 1833(12):3481-3498.
46. Guo H, Callaway JB, & Ting JP (2015) Inflammasomes: mechanism of action, role in disease, and therapeutics. *Nat Med* 21(7):677-687.
47. Man SM & Kanneganti TD (2015) Gasdermin D: the long-awaited executioner of pyroptosis. *Cell Res* 25(11):1183-1184.
48. Jorgensen I & Miao EA (2015) Pyroptotic cell death defends against intracellular pathogens. *Immunol Rev* 265(1):130-142.
49. Dockrell DH*, et al.* (2003) Alveolar macrophage apoptosis contributes to pneumococcal clearance in a resolving model of pulmonary infection. *J Immunol* 171(10):5380-5388.
50. Kebaier C*, et al.* (2012) Staphylococcus aureus alpha-hemolysin mediates virulence in a murine model of severe pneumonia through activation of the NLRP3 inflammasome. *J Infect Dis* 205(5):807-817.
51. Vandenesch F, Lina G, & Henry T (2012) Staphylococcus aureus hemolysins, bi-component leukocidins, and cytolytic peptides: a redundant arsenal of membrane-damaging virulence factors? *Front Cell Infect Microbiol* 2:12.
52. Wallach D, Kang TB, Dillon CP, & Green DR (2016) Programmed necrosis in inflammation: Toward identification of the effector molecules. *Science* 352(6281):aaf2154.
53. Kaczmarek A, Vandenabeele P, & Krysko DV (2013) Necroptosis: the release of damage-associated molecular patterns and its physiological relevance. *Immunity* 38(2):209-223.
54. Declercq W, Vanden Berghe T, & Vandenabeele P (2009) RIP kinases at the crossroads of cell death and survival. *Cell* 138(2):229-232.
55. Chan FK, Luz NF, & Moriwaki K (2015) Programmed necrosis in the cross talk of cell death and inflammation. *Annu Rev Immunol* 33:79-106.

56. Su L*, et al.* (2014) A plug release mechanism for membrane permeation by MLKL. *Structure* 22(10):1489-1500.
57. Cai Z*, et al.* (2014) Plasma membrane translocation of trimerized MLKL protein is required for TNF-induced necroptosis. *Nat Cell Biol* 16(1):55-65.
58. Chen X*, et al.* (2014) Translocation of mixed lineage kinase domain-like protein to plasma membrane leads to necrotic cell death. *Cell Res* 24(1):105-121.
59. Xia B*, et al.* (2016) MLKL forms cation channels. *Cell Res*.
60. Weinlich R & Green DR (2014) The Two Faces of Receptor Interacting Protein Kinase-1. *Mol Cell* 56(4):469-480.
61. Dannappel M*, et al.* (2014) RIPK1 maintains epithelial homeostasis by inhibiting apoptosis and necroptosis. *Nature* 513(7516):90-94.
62. Sridharan H & Upton JW (2014) Programmed necrosis in microbial pathogenesis. *Trends Microbiol* 22(4):199-207.
63. Dobbelstein M & Shenk T (1996) Protection against apoptosis by the vaccinia virus SPI-2 (B13R) gene product. *J Virol* 70(9):6479-6485.
64. Li M & Beg AA (2000) Induction of necrotic-like cell death by tumor necrosis factor alpha and caspase inhibitors: novel mechanism for killing virus-infected cells. *J Virol* 74(16):7470-7477.
65. Cho YS*, et al.* (2009) Phosphorylation-driven assembly of the RIP1-RIP3 complex regulates programmed necrosis and virus-induced inflammation. *Cell* 137(6):1112-1123.
66. Upton JW, Kaiser WJ, & Mocarski ES (2010) Virus inhibition of RIP3-dependent necrosis. *Cell Host Microbe* 7(4):302-313.
67. Rodrigue-Gervais IG*, et al.* (2014) Cellular inhibitor of apoptosis protein cIAP2 protects against pulmonary tissue necrosis during influenza virus infection to promote host survival. *Cell Host Microbe* 15(1):23-35.
68. Robinson N*, et al.* (2012) Type I interferon induces necroptosis in macrophages during infection with Salmonella enterica serovar Typhimurium. *Nat Immunol* 13(10):954-962.
69. Roca FJ & Ramakrishnan L (2013) TNF dually mediates resistance and susceptibility to mycobacteria via mitochondrial reactive oxygen species. *Cell* 153(3):521-534.
70. Weng D*, et al.* (2014) Caspase-8 and RIP kinases regulate bacteria-induced innate immune responses and cell death. *Proc Natl Acad Sci U S A* 111(20):7391-7396.
71. Philip NH*, et al.* (2014) Caspase-8 mediates caspase-1 processing and innate immune defense in response to bacterial blockade of NF-kappaB and MAPK signaling. *Proc Natl Acad Sci U S A* 111(20):7385-7390.
72. Kang TB, Yang SH, Toth B, Kovalenko A, & Wallach D (2013) Caspase-8 blocks kinase RIPK3-mediated activation of the NLRP3 inflammasome. *Immunity* 38(1):27-40.
73. Lawlor KE*, et al.* (2015) RIPK3 promotes cell death and NLRP3 inflammasome activation in the absence of MLKL. *Nat Commun* 6:6282.
74. Wang X*, et al.* (2014) RNA viruses promote activation of the NLRP3 inflammasome through a RIP1-RIP3-DRP1 signaling pathway. *Nat Immunol* 15(12):1126-1133.
75. Moriwaki K*, et al.* (2014) The necroptosis adaptor RIPK3 promotes injury-induced cytokine expression and tissue repair. *Immunity* 41(4):567-578.

76. Kearney CJ*, et al.* (2015) Necroptosis suppresses inflammation via termination of TNF- or LPS-induced cytokine and chemokine production. *Cell Death Differ* 22(8):1313-1327.
77. Stephenson HN, Herzig A, & Zychlinsky A (2015) Beyond the grave: When is cell death critical for immunity to infection? *Curr Opin Immunol* 38:59-66.
78. Klevens RM*, et al.* (2007) Invasive methicillin-resistant Staphylococcus aureus infections in the United States. *JAMA* 298(15):1763-1771.
79. Brundage JF (2006) Interactions between influenza and bacterial respiratory pathogens: implications for pandemic preparedness. *Lancet Infect Dis* 6(5):303-312.
80. Sun K & Metzger DW (2008) Inhibition of pulmonary antibacterial defense by interferon-gamma during recovery from influenza infection. *Nat Med* 14(5):558-564.
81. Murray PJ & Wynn TA (2011) Protective and pathogenic functions of macrophage subsets. *Nat Rev Immunol* 11(11):723-737.
82. Munoz-Planillo R*, et al.* (2013) K(+) efflux is the common trigger of NLRP3 inflammasome activation by bacterial toxins and particulate matter. *Immunity* 38(6):1142-1153.
83. Degterev A, Maki JL, & Yuan J (2013) Activity and specificity of necrostatin-1, small-molecule inhibitor of RIP1 kinase. *Cell Death Differ* 20(2):366.
84. Greenlee-Wacker MC*, et al.* (2014) Phagocytosis of Staphylococcus aureus by human neutrophils prevents macrophage efferocytosis and induces programmed necrosis. *J Immunol* 192(10):4709-4717.
85. Diep BA*, et al.* (2010) Polymorphonuclear leukocytes mediate *Staphylococcus aureus* Panton-Valentine leukocidin-induced lung inflammation and injury. *Proc Natl Acad Sci U S A* 107(12):5587-5592.
86. Gillet Y*, et al.* (2002) Association between *Staphylococcus aureus* strains carrying gene for Panton-Valentine leukocidin and highly lethal necrotising pneumonia in young immunocompetent patients. *Lancet* 359(9308):753-759.
87. Labandeira-Rey M*, et al.* (2007) *Staphylococcus aureus* Panton-Valentine leukocidin causes necrotizing pneumonia. *Science* 315(5815):1130-1133.
88. Shallcross LJ, Fragaszy E, Johnson AM, & Hayward AC (2013) The role of the Panton-Valentine leucocidin toxin in staphylococcal disease: a systematic review and meta-analysis. *Lancet Infect Dis* 13(1):43-54.
89. Shallcross LJ*, et al.* (2010) Panton-Valentine leukocidin associated staphylococcal disease: a cross-sectional study at a London hospital, England. *Clin Microbiol Infect* 16(11):1644-1648.
90. Bubeck Wardenburg J, Bae T, Otto M, Deleo FR, & Schneewind O (2007) Poring over pores: alpha-hemolysin and Panton-Valentine leukocidin in *Staphylococcus aureus* pneumonia. *Nat Med* 13(12):1405-1406.
91. Villaruz AE*, et al.* (2009) A point mutation in the agr locus rather than expression of the Panton-Valentine leukocidin caused previously reported phenotypes in *Staphylococcus aureus* pneumonia and gene regulation. *J Infect Dis* 200(5):724-734.
92. Naber CK (2009) Staphylococcus aureus bacteremia: epidemiology, pathophysiology, and management strategies. *Clin Infect Dis* 48 Suppl 4:S231-237.
93. Kovalenko A*, et al.* (2009) Caspase-8 deficiency in epidermal keratinocytes triggers an inflammatory skin disease. *J Exp Med* 206(10):2161-2177.

94. Christofferson DE, Li Y, & Yuan J (2014) Control of life-or-death decisions by RIP1 kinase. *Annu Rev Physiol* 76:129-150.
95. Vanden Berghe T, Linkermann A, Jouan-Lanhouet S, Walczak H, & Vandenabeele P (2014) Regulated necrosis: the expanding network of non-apoptotic cell death pathways. *Nat Rev Mol Cell Biol* 15(2):135-147.
96. Wong WW*, et al.* (2014) cIAPs and XIAP regulate myelopoiesis through cytokine production in an RIPK1- and RIPK3-dependent manner. *Blood* 123(16):2562-2572.
97. Zhang T*, et al.* (2016) CaMKII is a RIP3 substrate mediating ischemia- and oxidative stress-induced myocardial necroptosis. *Nat Med*.
98. Sun X*, et al.* (1999) RIP3, a novel apoptosis-inducing kinase. *J Biol Chem* 274(24):16871-16875.
99. Pazdernik NJ, Donner DB, Goebl MG, & Harrington MA (1999) Mouse receptor interacting protein 3 does not contain a caspase-recruiting or a death domain but induces apoptosis and activates NF-kappaB. *Mol Cell Biol* 19(10):6500-6508.
100. Mandal P*, et al.* (2014) RIP3 induces apoptosis independent of pronecrotic kinase activity. *Mol Cell* 56(4):481-495.
101. Kasof GM, Prosser JC, Liu D, Lorenzi MV, & Gomes BC (2000) The RIP-like kinase, RIP3, induces apoptosis and NF-kappaB nuclear translocation and localizes to mitochondria. *FEBS Lett* 473(3):285-291.
102. Yu PW*, et al.* (1999) Identification of RIP3, a RIP-like kinase that activates apoptosis and NFkappaB. *Curr Biol* 9(10):539-542.
103. Sokolovska A*, et al.* (2013) Activation of caspase-1 by the NLRP3 inflammasome regulates the NADPH oxidase NOX2 to control phagosome function. *Nat Immunol* 14(6):543-553.
104. Gonzalez-Juarbe N*, et al.* (2015) Pore-Forming Toxins Induce Macrophage Necroptosis during Acute Bacterial Pneumonia. *PLoS Pathog* 11(12):e1005337.
105. Newton K & Manning G (2016) Necroptosis and Inflammation. *Annu Rev Biochem*.
106. Cohen TS & Prince AS (2013) Bacterial pathogens activate a common inflammatory pathway through IFNlambda regulation of PDCD4. *PLoS Pathog* 9(10):e1003682.
107. Powers ME, Becker RE, Sailer A, Turner JR, & Bubeck Wardenburg J (2015) Synergistic Action of Staphylococcus aureus alpha-Toxin on Platelets and Myeloid Lineage Cells Contributes to Lethal Sepsis. *Cell Host Microbe* 17(6):775-787.
108. Kuida K*, et al.* (1995) Altered cytokine export and apoptosis in mice deficient in interleukin-1 beta converting enzyme. *Science* 267(5206):2000-2003.
109. Newton K, Sun X, & Dixit VM (2004) Kinase RIP3 is dispensable for normal NF-kappa Bs, signaling by the B-cell and T-cell receptors, tumor necrosis factor receptor 1, and Toll-like receptors 2 and 4. *Mol Cell Biol* 24(4):1464-1469.
110. Murphy JM*, et al.* (2013) The pseudokinase MLKL mediates necroptosis via a molecular switch mechanism. *Immunity* 39(3):443-453.
111. Parker D, Planet PJ, Soong G, Narechania A, & Prince A (2014) Induction of type I interferon signaling determines the relative pathogenicity of Staphylococcus aureus strains. *PLoS Pathog* 10(2):e1003951.

112. Pearson T, Greiner DL, & Shultz LD (2008) Humanized SCID mouse models for biomedical research. *Curr Top Microbiol Immunol* 324:25-51.
113. Reyes-Robles T*, et al.* (2013) Staphylococcus aureus leukotoxin ED targets the chemokine receptors CXCR1 and CXCR2 to kill leukocytes and promote infection. *Cell Host Microbe* 14(4):453-459.
114. Graves SF*, et al.* (2010) Relative contribution of Panton-Valentine leukocidin to PMN plasma membrane permeability and lysis caused by USA300 and USA400 culture supernatants. *Microbes Infect* 12(6):446-456.
115. Parker D & Prince A (2012) Staphylococcus aureus induces type I IFN signaling in dendritic cells via TLR9. *J Immunol* 189(8):4040-4046.